STRUCTURAL-STRATIGRAPHIC CONTROLS ON CARBON AND RELATED MINERALIZATION IN THE WITWATERSRAND BASIN

by

ARNOLDUS JACOBUS JOUBERT

Thesis submitted in fulfillment of the requirements for the degree of

MASTER OF SCIENCE

In the Faculty of Natural and Agricultural Sciences
Department of Geology
University of the Free State
BLOEMFONTEIN
South Africa

Supervisor: Prof Wayne P Colliston

February 2012

Verklaring

Ek Arnoldus Jacobus Joubert doen afstand van my outeursreg in die proefskrif /verhandeling ten gunste van die Universiteit van die Vrystaat.

AJ Joubert

1st July 2012

Declaration

I, declare that this thesis is my own unaided work. It is being submitted for the Degree of Master of Science in the Faculty of Natural and Agricultural Sciences, University of the Free State, Bloemfontein, South Africa.

Arnoldus Jacobus Joubert

Bloemfontein, the 1st July 2012

ABSTRACT

The Witwatersrand basin is loaded with carbon. The carbon deposits locations are not site specific. Many localities where deposits occur are related to the structure and the sedimentology of the particular area. The purpose of this thesis is to document and describe the distribution of carbon in the Witwatersrand basin and to establish the mechanisms controlling emplacement. The approach used was a multidisciplinary one incorporating aspects of sedimentology and macro to mesoscopic tectonic structures and their relationships with carbon distribution patterns to establish the controls on carbon emplacement. One of the major controls on carbon deposition is structural geology. Bedding parallel fractures that cut pebbles with carbon fill is indicative of the influence of bigger and more forceful movements within the ore body. The thesis begins with a back ground study of all the major theories and ends with a possible explanation for the influence of structure and sedimentology on the deposition of carbon, and a new catalyst for the dehydration reaction that could lead to the deposition of carbon.

The various types of carbon have been classified and grouped to specific sedimentological and tectonic structures. These types are deposited in lithofacies horizons that are not related in space to one another. They also differ in texture. Type A is observed in reefs and bedding planes, bedding parallel fractures and on fault planes. Type B consists of massive carbon and vug type carbon.

Carbon on the reef contacts in most cases is developed on intersections with fluid pathways (phylonites or shear zones) which are characterised by the alignment of the minerals within the pathway. Carbon precipitation is controlled by the type of footwall and the amount of fluid pathways. The higher the occurrence of bedding parallel fractures the more consistent the emplacement of carbon. Phylonites are classified as follows: Type 1 exhibits a low degree of deformation and the minerals show a low degree of orientation. Type 2 exhibits a medium degree of deformation and the minerals show a larger degree of

orientation. Type 3 phylonite is where all the original sedimentary character of the original rock has been sheared and the deformation gives rise to a foliated rock with a distinctive foliation.

It is suggested that the large extensional faults in the Free State Gold Fields and the Master Bedding plane fault in the West Rand Gold Fields are conduits for the fluids into the Basin. The in-flow of fluids is from below the reef horizons. It is further speculated that in the Free State, the fluids had a north-easterly transport direction.

The SEM analyses showed new mineral associations. The mineral phases are shown in three dimensions and the order of precipitation can be deduced. The element tantalum was prominent in one of the high grade samples. The most prominent mineral in the fluid pathways within the matrix of the various reefs is pyrophyllite. The carbon is emplaced within the pyrophyllite within a fluid pathway and this is indicative of the sequence of mineralization. The uranium replaced the pyrophyllite and the pyrite crystallized in a fracture within the pyrophyllite. It is concluded that the three main minerals: carbon, uranium and gold all came in at the same time into the basin.

A hydrothermal origin for carbon and associated minerals is supported by the study. The proposed hypothesis to explain the timing and origin of carbon and gold into the Witwatersrand Basin is that of the 2.02 Ga Vredefort Impact event. Gold and uranium are inferred to have been transported by the carbon plasma that originates from the mantle during the Vredefort Impact event.

ACKNOWLEDGEMENTS

I would like to express my appreciation to Prof Wayne Colliston from the Department of Geology, UFS, Bloemfontein, for providing dedicated and stimulating supervision throughout my work. Prof Willem van der Westhuizen is thanked for the worthy comments on the research subject. I would also like to thank the laboratory personnel of the Department of Geology for preparing my polished thin sections and (SEM) disks. The personnel from centre of microscopy (UFS) will be thanked for the assistance during the SEM analyses.

I am grateful to the geology staff of Anglo American SA, Ghana, AngloGold, Goldfields SA and DRC, Gold One, for the hospitality, support and provision of logistics and data.

I am grateful to all scientists and departments that contributed to my work providing not only data but also knowledge and inspiration. I would like to thank Mr Peet Roodt and Mrs Petro Swart and Mr Andries Felix for technical assistance during the last 4 years and the personnel that assisted me in the laboratory.

Lastly I would like to dedicate this thesis to my dad, Ds. P.J.W. Joubert for the philosophy behind my thought process.

CONTENTS

CHAPTER 2

CHAPTER 3

DETAILED MICROSCOPIC STUDY OF CARBON AND RELATED MINERALS AND ELEMENTS 42

CHAPTER 4

CHAPTER 5

LIST OF FIGURES

LIST OF TABLES

CHAPTER 1

INTRODUCTION

1.1 The Objectives of this Thesis

The aim of this thesis is to investigate, document and describe the occurrence of carbon as preserved within the strata in the Witwatersrand basin and to establish the mechanisms controlling its emplacement.

There are numerous occurrences of carbon deposits within the structural framework of the Witwatersrand basin and it is in this structural framework that the author has selected individual samples from various stratigraphic horizons. The macroscale and mesoscale observations are tested under the microscope to see if gold is in fact only on the spindles and not in the carbon mass. Where is carbon emplaced? Is it only in fractures and in veins along contacts? What is associated with carbon veins and is the uraninite specifically associated with carbon or not?

The approach to the thesis was a multidisciplinary one incorporating aspects of sedimentology and structure (major & minor). These were used to establish carbon distribution patterns and to establish the controls on carbon emplacement.

1.2 The locality of different study areas

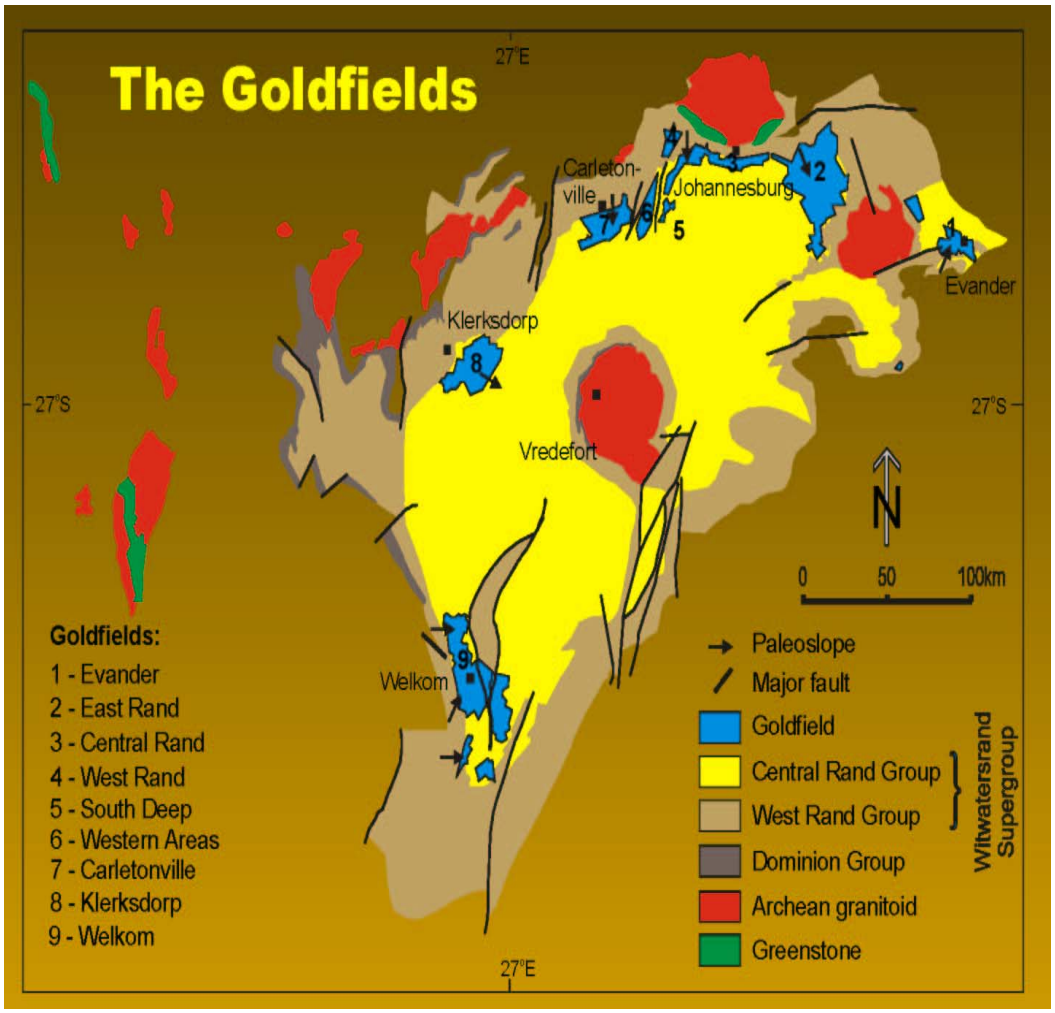

Fig. 1.1 The various goldfields in the Witwatersrand basin (Internal mine departmental Report, Gencor)

The various study areas are situated within the following gold fields: No 4 to No 9. (Fig. 1.1)

The following mines within these study areas were visited underground or were extensively mapped as an employee of the specific mining house (Fig. 1.2 and 1.3)

1. **Gold One** (Cooke mine; Cooke 2# and Cooke 3#): The reefs studied were: K9, K7, E8, UE1A, E9GB, UE7 and VCR.

2. **Goldfields** (South deep mine): Studied the core from the ultra deep drilling project on mainly upper Elsburgs' reefs.
3. **Goldfields** (Driefontein mine; 1#, 2#, 4#, 5# ,8# and 10#): Studied the Carbon leader reef, the VCR and Middelvlei reef.
4. **Anglo gold Ashanti** (Vaal Reefs mine; 1#, 8# and 9#): Studied the Vaal reef.
5. **Anglo Gold Ashanti** (Western Holdings mine; 1# and 2#): The reefs studied were the Basal reef, Steyn Reef.
6. **Gencor** (St Helena Gold mine; 2#, 4# and 8#): The Basal reef, Leader reef and Intermediate reef.
7. **DRD** (Blyvooruitzicht mine; 2# and 4#): Middelvlei reef.
8. **Anglo Gold Ashanti**: (Joel mine; Taung North Shaft and Taung South Shaft): Beatrix reef.
9. **Goldfields South Africa**: (Beatrix mine): Beatrix reef at 2# and Kalkoenkrans reef at Beatrix 4# respectively.

The shaft names of the mines are used as known at the time when the author was working at these shafts. Most geologists are unfamiliar with current naming.

This study was done in 26 years of underground geological mapping and structural analysis of numerous panels and development ends, which totals to 4500 underground visits.

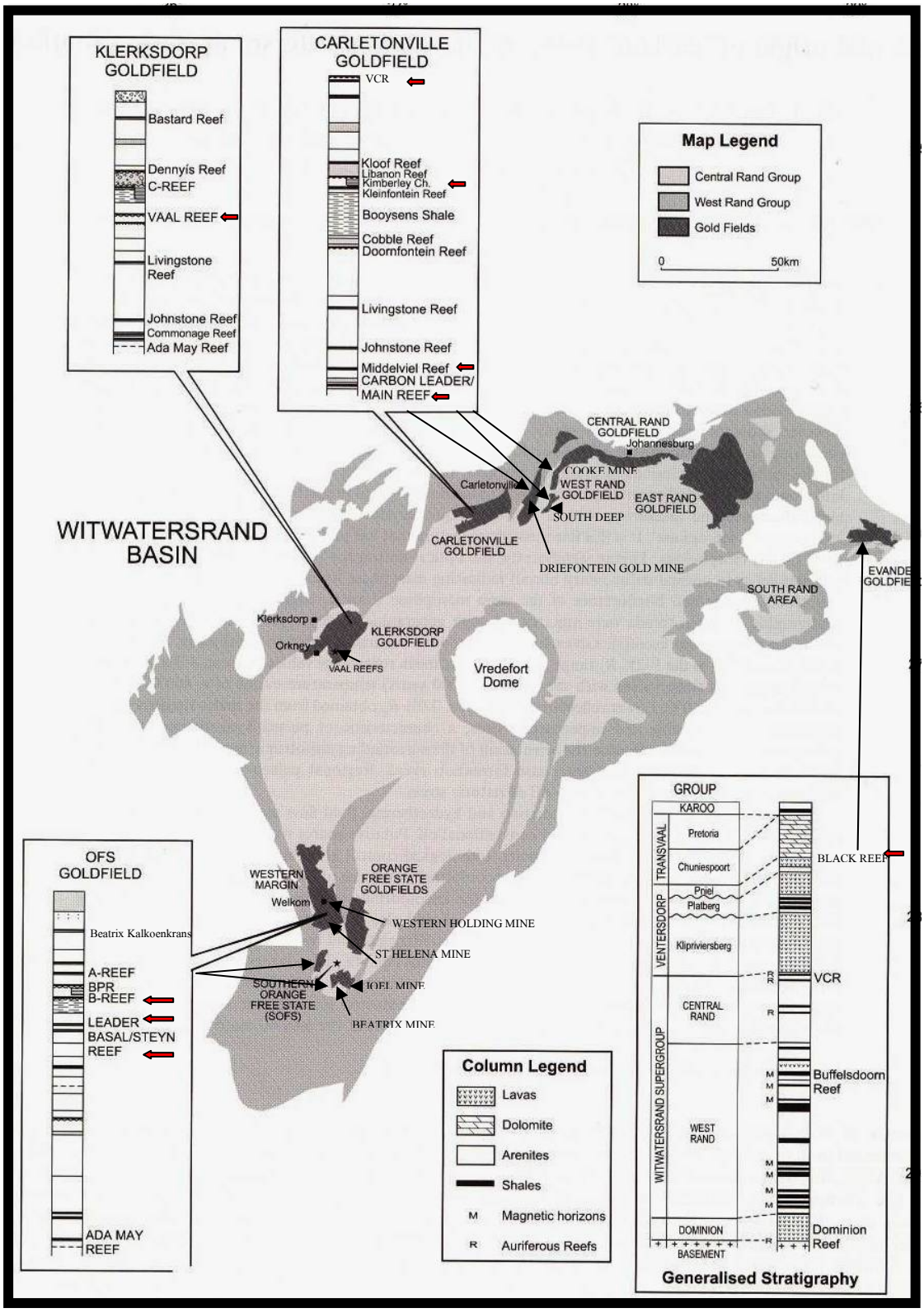

Fig. 1.2 The study areas in detail after Gray et al.,(1998).The red arrows indicate the reef studied in that particular goldfield.

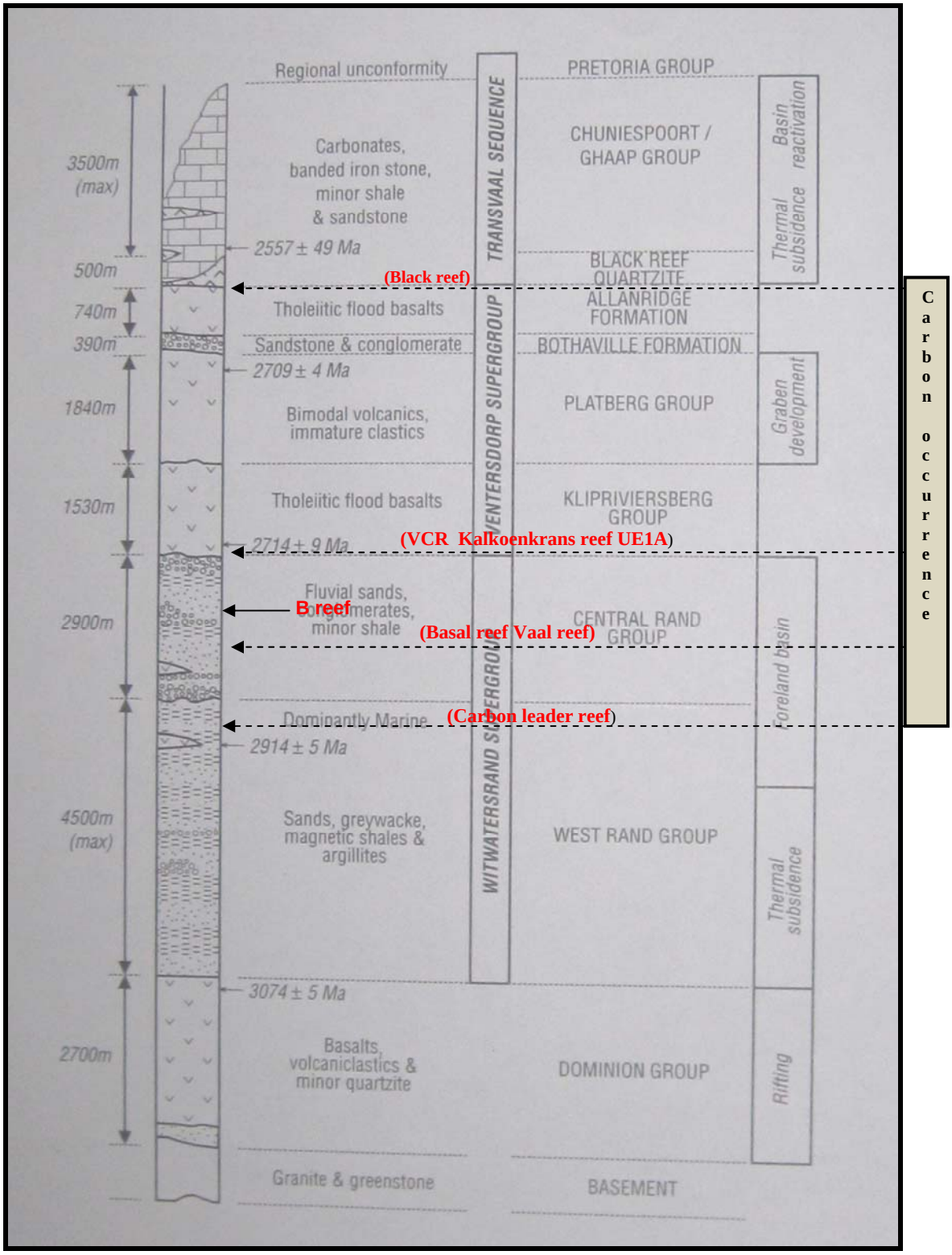

Fig. 1.3 General Lithostratigraphic column for the Witwatersrand Basin showing the reef positions in more detail after (Internal mine departmental Report, Gencor)

More detail on Vaal reef and Kalkoenkrans reef package will follow in chapter 4.

1.3 A review of the geology and the evolution of the Witwatersrand Basin

1.3.1 Kaapvaal Craton

The mantle forms a 250-300 km thick anisotropic body below the very old cratonic areas (James et al., 2001). The Kaapvaal Craton is one of the most studied areas of all the continental plates in the world. The Kaapvaal consist of two major blocks, one block to the south east, Mid Archaean Kaapvaal shield (3.0 – 3.7 Ga) and another block in the west to northwest, Late Archean Margin to the Kaapvaal shield (2.5 – 3.0 Ga), as indicated on the map shown in Fig. 1.4.

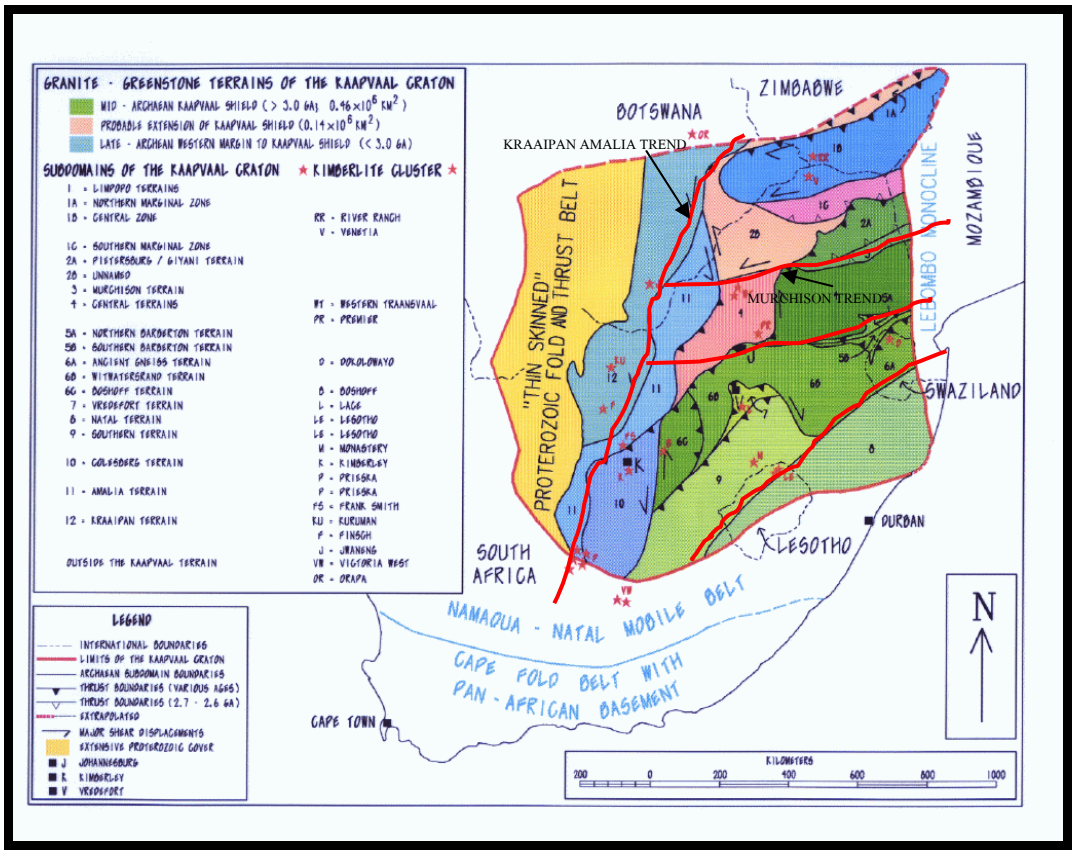

Fig. 1.4 Tectonic blocks of the Kaapvaal Craton showing variation in ages. De Wit et al., (1992).

The Kaapvaal Craton can be vertically divided into two geological zones. (Table 1.1)

A granitic zone or base with metamorphic belts or greenstone belts, secondly which is overlain by layered sedimentary and volcanic packages. Pretorius (1964) gave the name Kaapvaal Craton to the oldest nucleus of the southern African continental plate; Leube (1962), used the term “Paleoafrizidic region”.

The Kaapvaal Craton basement rocks form a granitic shield underlying the Witwatersrand basin (Leube and Cissarz, 1966). The Archaean Zimbabwean sialic plate is in fixed position to this craton and faults cutting through the granitic shield, divided the granitic shield into various blocks (Fig. 1.4). It is from the spatial orientation of these blocks that the depositional style has been derived. The geometry of these blocks and the subsequent mode of sedimentation lead many geologists to recognize fan deltas, slump patterns and various other depositional environments within the basin as well as on its margins.

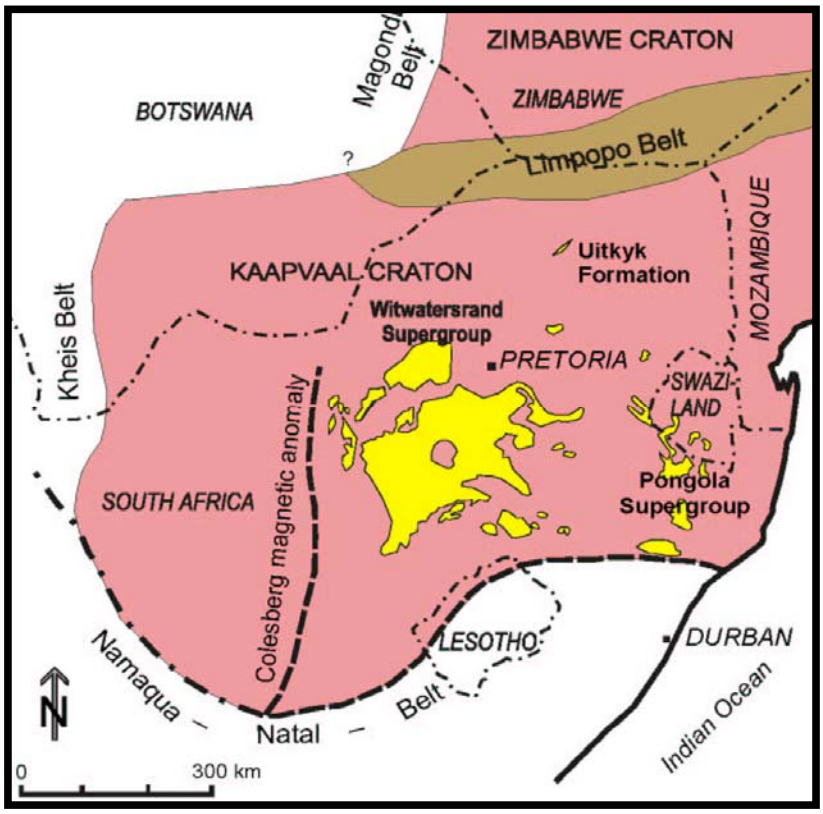

Fig. 1.5a The distribution of the Kaapvaal Craton (pink) and the Witwatersrand and Pongola Supergroups in yellow (Internal mine departmental Report, Gencor).

Tectonism occurred within the craton boundaries during sedimentation of the basin as well as after the basin was filled (Table1.1). There are various overturns along the western edge of the basin mainly in the upper portion of the Witwatersrand ore body namely the Central Rand Group (CRG). Tectonism caused duplication of various reef horizons of the CRG.

Table 1.1 Archaean-Precambrian Stratigraphy of the Kaapvaal Craton *(Internal mine departmental Report, Gencor)*

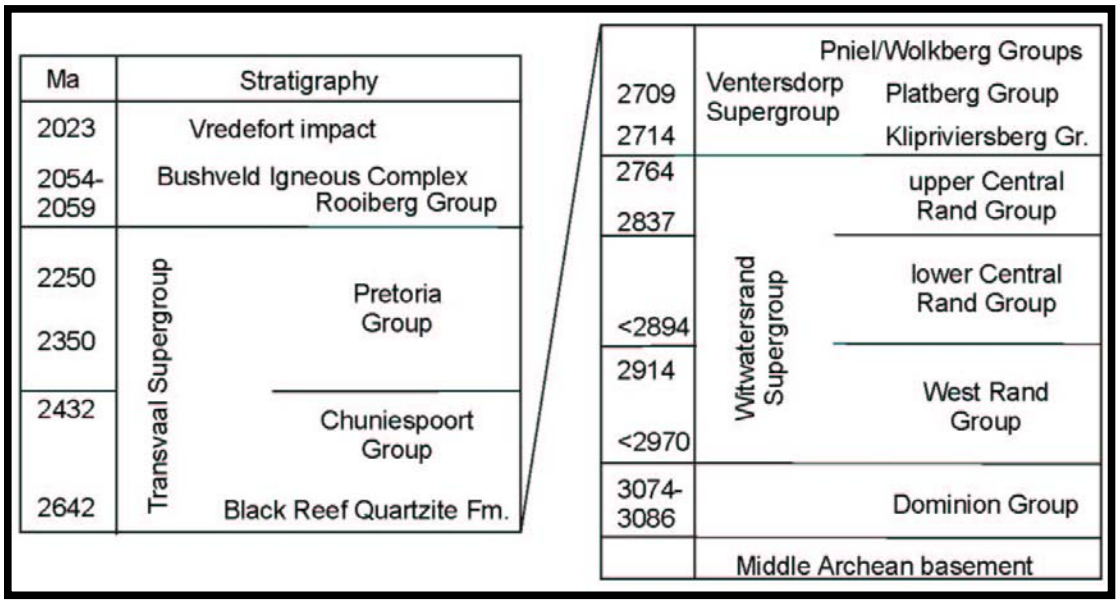

1.4 The Geological Setting of the Witwatersrand Basin

1.4.1 The tectonic evolution of the Witwatersrand Basin

The perceptions on the tectonic environment for the Witwatersrand changed after the global plate tectonic theory was applied to the Witwatersrand basin (Robb and Meyer, 1994). Pretorius (1964) studied the development of domes, depressions and geometry of the basin, linking it to interference folding.

The deformation of the Witwatersrand Basin is controlled by the collision of the Kaapvaal and Zimbabwe Cratons at ca. 2.7Ga. (Fig. 1.5a) The old fault planes of the pre 3.1 Ga basement rocks were reactivated during the

development of the Witwatersrand basin (Fig. 1.5b; Stanistreet and McCarthy, 1991). Two sets of lineaments are evident in the basement, an east-northeast lineament along the greenstone belts of Murchison, Barberton and Pietersburg and the second set, a north-northwest lineament along the Kraaipan and the Amalia greenstone belts (Fig. 1.5b). Faults striking parallel to these lineaments or zones of weakness gave rise to the syn-sedimentary fault zones that played a major role in the evolution of the basin (Robb and Meyer 1994).

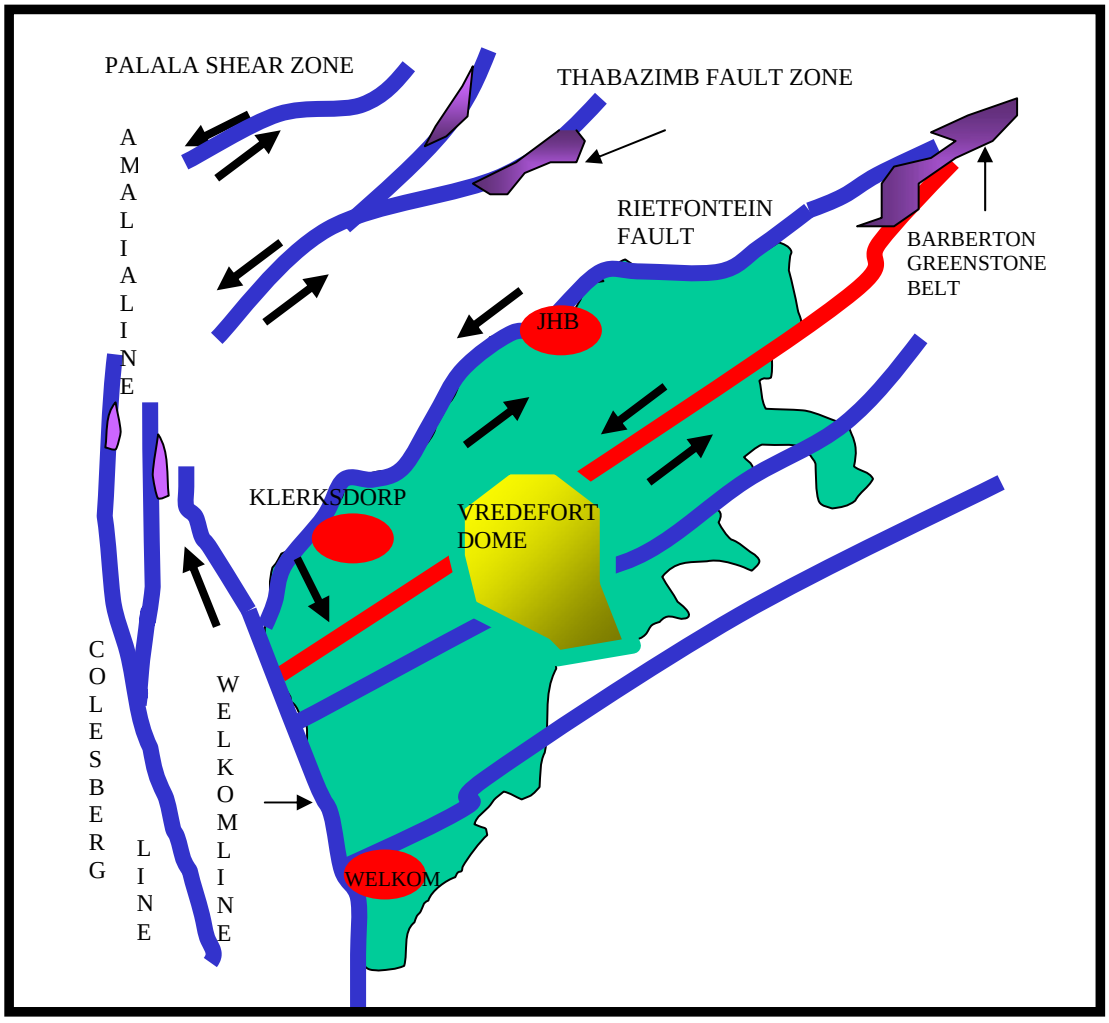

Fig. 1.5b Syn-sedimentary faults after Stanistreet & McCarthy (1991).

1.5 The Four Deformational Phases

The extensional phase (Fig. 1.6A)

The extensional rift period started at 3100 Ma years ago, lasted 90 Ma years and ended 3010 Ma years ago, giving rise to the deposition of the Dominion volcano-sedimentary sequence in a low-lying part of the basin. Numerous faults occurred in the basement during this extensional stage. At the same time plutons such as Westerdam and Coligny, and also hidden plutons recorded by the detrital zircon population were emplaced. (Robb and Meyer, 1994).

The Foreland basin phase (Fig. 1. 6B)

The next stage is the foreland basin stage. The duration was 80 Ma years; starting at 2980 Ma years ago ending at 2900 Ma years ago. During this stage the West Rand and the lower Central Rand Groups were deposited as well as S-type granites produced from the upper crust, which are exposed in the Barberton region (Robb and Meyer, 1994).

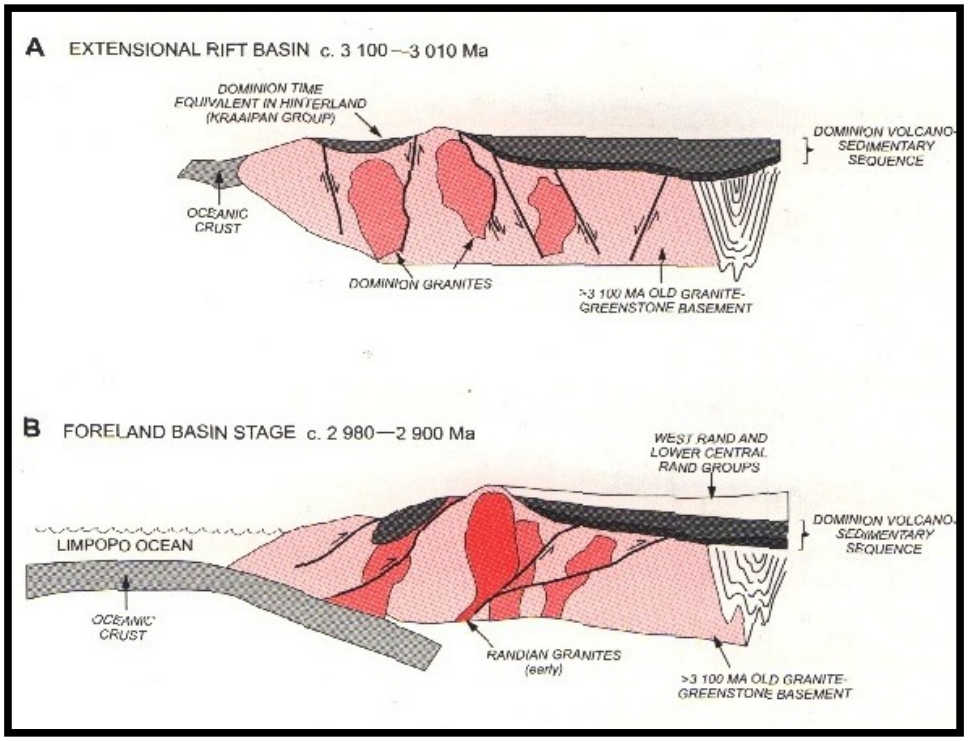

Fig. 1.6(A&B) The first two stages of deformation and sedimentation A&B and the two distinct zones illustrate basement granite and the Witwatersrand sediment after Robb and Meyer, (1994).

The Indentation phase (Fig. 1.6C) (Upper Central Rand and Klipriviersberg Groups)

The third phase represents the collision of the Kaapvaal and the Zimbabwe cratons. This event started 2840 Ma years ago and lasted 80 Ma years and ended at 2720 Ma years ago. In this phase three events took place; the Gaborone-Kanye event (emplacement of granite, anorthosite and rhyolite); the Schweizer-Reneke granite emplacement and the hydrothermally altered granite emplacement west of Welkom (Robb and Meyer, 1994).

The Impactogenal phase (Fig. 1.6D) (Platberg Group)

The last event was the impactogenal rift event with the emplacement of I-Type granites of deep mantle origin, on the northern and western perimeter of the craton. This event started 2700Ma years ago (Robb and Meyer, 1994).

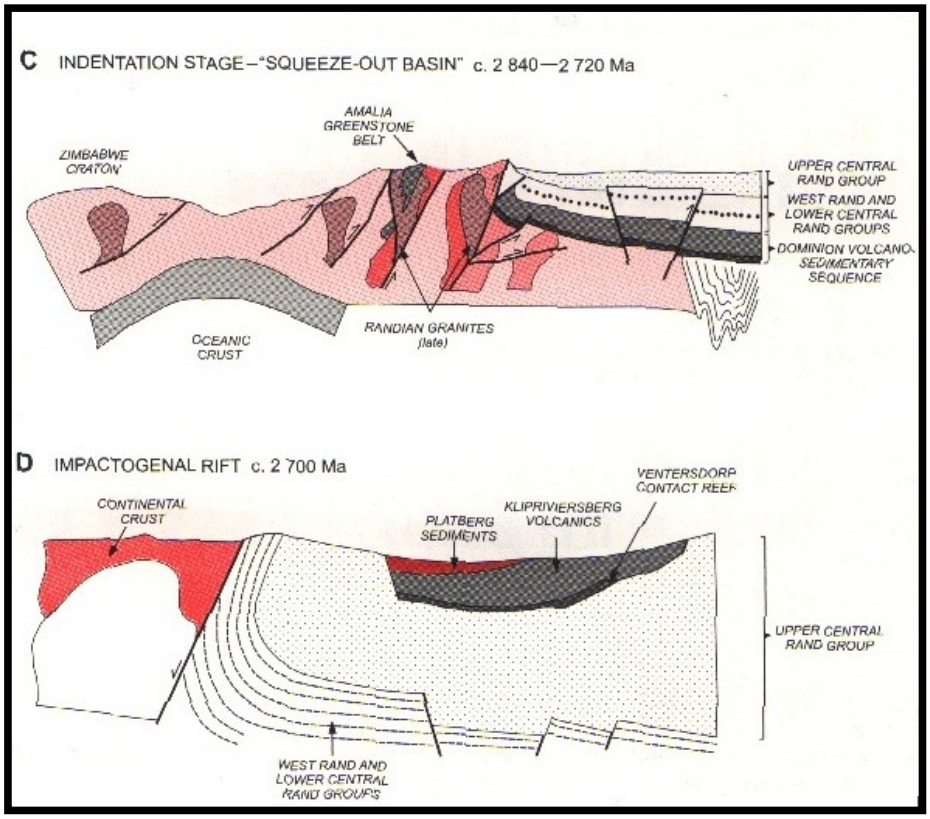

Fig. 1.6(C,D) The last two stages of deformation and sedimentation C&D and the two distinct zones illustrate basement granite and the Witwatersrand sediment after Robb and Meyer (1994).

1.6 Other important related events in the Witwatersrand Basin

1.6.1 The Metamorphic aspects of the Witwatersrand Basin

The entire rock assemblage of the Witwatersrand Super Group was regionally metamorphosed to at least the greenschist facies. The process produced mineral assemblages that include pyrophyllite and chloritoid (Phillips, 1987). The regional extent of the two minerals has been confirmed across the entire basin.

The question unanswered to date is the timing of metamorphism in the Wits basin and some inferred timing is possible from two chosen observations within the Wits Basin. Neither the Transvaal nor the upper part of the Ventersdorp Supergroup have any pyrophyllite or chloritoid assemblages, but pyrophyllite is present in the base of the Ventersdorp Supergroup and in the metabasalts of the Klipriviersberg (Palmer, 1986). To the north of Johannesburg, the pyrophyllite-kyanite-quartz isograd has been mapped within the Witwatersrand Supergroup, but it is truncated by the Black Reef Formation of the Transvaal Sequence and provides some confirmation on the timing of metamorphism. In this case the metamorphism predates the Transvaal Sequence (Coetzee et al., 1995). The pyrophyllite-chloritoid-chlorite-muscovite-quartz-pyrite metamorphic assemblage is present in the reefs and in quartzites and in the alteration zones within the basalts and the dykes (Phillips et al., 1987). It is deduced that the regional metamorphic event in the Witwatersrand Basin was associated with the Indentation Phase of deformation on the Kaapvaal Craton (Fig. 1.6D). The interpretation of the metamorphic data will follow in Chapter 5.

1.6.2 Occurrence and origin of carbon

The distribution of carbon seams on sedimentary surfaces led previous researchers to suspect that they were algae matter. However this interpretation is no longer tenable as many workers since have recognised the association of hydrocarbon with fracturing (Jolley et al., 2004) and that all forms of hydrocarbons are hydrothermal pyrobitumen (Gray et al., 1998).

Macroscopic mapping has demonstrated the anastomosing nature of carbon over mine-wide areas. The areal extent of carbon is from the northeast to the south west all along the basin edge approximately 250 km in an east west direction all along the north to northwest basin edge and then approximately 150 km all along the west to southwest basin edge. The vertical distribution is over 2000 meters in the various conglomerates and faults. Mesoscopic observations prove that vein-like carbon seams are cross-cutting structural and sedimentary features. The carbon fills an anastomosing set of bed-parallel fractures and ramps within the sediment below and above the reef. (Gray et al.,1998).

Microscopic observations show a globular form for the carbon and inclusions of uraninite particles. In seam carbon the globules are generally modified into elongated 'spindles' orientated perpendicular to bedding. Optical properties are dominated by generally high reflectance and anisotropy with a 'swirling' liquid crystal structure, classifying seam carbon as `carbonaceous mesophase'. It is this fine mesophase texture that has previously been wrongly attributed to plant (algal) morphology (Gray et al., 1998).

There are three current models for the origin of carbonaceous matter within the Witwatersrand Basin, which occurs as stratiform seams and spherical nodules.

The first model is addressing the organic origin for carbon. There are two interpretations for the organic origin. The one sees carbon as algae associated with sedimentary processes during Central Rand deposition (Hallbauer, 1975). The algal mats were formed on the depositional surface

before deposition of the conglomerates and during the depositional process, the gold was trapped in the algal mats. The second interpretation sees carbon as a syngenetic deposit and is remnants of prokaryote microbial mats which acted as a mechanical trap for gold (Robb et al., 1989).

The second model sees carbon as a hydrothermal fluid deposited in areas with less resistance like the contacts of various reefs, fault planes and bedding parallel fractures. Parnell (1999) observed that carbon also occurs along sets of bedding-parallel micro fractures through individual quartz pebbles in mineralized conglomerates. A plane of fluid inclusions parallel to the micro fractures in pebbles is indicative of the importance of bedding-parallel fluid flow (Frimmel et al., 2005).

The third model sees the Witwatersrand deposit as a modified placer. In this model carbon is seen as an oil migrating in fractures in the upper zones of the Central Rand Group and Barnicoat et al., (1998) made the following statement: "We find that the gold precipitated as a consequence of interactions of the fluid with shale-derived hydrocarbons present within the basin." The Booysens shale is the suggested source for hydrocarbons.

1.6.3 Origin of gold

Four theories have been advanced to explain the origin of the gold (Park and MacDiarmaid, 1975). The ultimate timing of the gold deposition and the source are a difficult issue (Kirk et al., 2001). The timing of the gold deposits is indirect in nature and the nature of events is not certain.

Most mine geologists accept that the ores are placers. These supporters of the theory claim that the gold is no longer placer grains but has been recrystallized during metamorphism of the surrounding rocks (Ramdohr, 1958). Comparative studies done on the lead isotopes of the sulfides in the gold deposits of the eastern Transvaal and the lead isotopes of the Wits gold deposits concluded that the isotopic evidence supported the belief that

detritus originated from the greenstone belt in the Eastern Transvaal (Koppel and Saager, 1974; Hallbauer and Utter, 1977).

A second theory on the origin of gold originates as far back as 1888. This group of geologists says the mineralizations of ores are syngenetic. They see the deposition of gold as a chemical precipitation and not a mechanical deposition of placer grains (Penning, 1888). A modification of this theory argues that the gold is a diagenetic addition to the minerals syngenetic uranium-carbon deposits (Miholic, 1954). This theory expresses a reorganization of the ores during metamorphism (Frimmel and Gartz, 1997; Minter, 1999).

The third group of geologists from the late to mid 20th century argues that gold originates from an underlying magmatic source. Hydrothermal fluids originating from the magmatic source deposited the gold in the conglomerate layers (Maclaren, 1908; Hatch and Corstrophine, 1909; Davidson 1953, 1957; Phillips and Law, 1994; Barnicoat et al., 1997).

The fourth group of geologist considered the gold to be from the overlying volcanic and that the gold permeated into the layers along unconformities and open conglomerate layers. They deposited their metallic loads to outer cooler portions of the basin (Davidson, 1964-65). See appendices for further discussion on the origin of gold.

Data is needed to prove the mode of deposition or emplacement. Thus the aim of this thesis is to investigate, document and describe the occurrence of carbon as preserved within the strata in the Witwatersrand basin and to establish the mechanisms controlling its emplacement.

CHAPTER 2

MACROSCOPIC AND MESOSCOPIC CHARACTER OF CARBON

2.1 Introduction

Carbon occurs in several morphological varieties and several geological unique settings within the Witwatersrand basin. The key to the genesis of the carbon is still not determined.

The data collected will be shown on maps, face mapping sections and representative stratigraphic columns and photographic records of the best samples collected from selected localities in the Witwatersrand Basin. This chapter will cover the macroscopic and mesoscopic scale of observations.

2.2 The occurrence of carbon on the macroscopic scale

The macroscopic observations demonstrate the vast subsurface development of carbon deposits within the Witwatersrand Basin. The examples for the macroscopic scale make use of interpretative diagrams together with the representative samples on the mesoscopic scale. The mesoscopic scale consists of a study done on the drilling cores of selected areas to investigate bedding parallel fracturing and fluid pathways and includes petrographical analysis for investigation of fracturing and fluid pathways. The mesoscopic observations indicate that there are not one but two types of carbon present in the ore body.

The selected photographs of different types of carbon occurrences are shown in the following Figures 2.1 to 2.14.

It is intended to classify the carbon into two groups from several different unique occurrences in the last part of this chapter.

The photo below is unique to its depositional position within the Ventersdorp Conglomerate. In this photo one can observe the carbon seam crossing the fault. This carbon seam is a spindle type carbon on the contact. The carbon is the host of the gold in this conglomerate. The conglomerate consists of small scattered pebbles along the contact.

Fig. 2.1 Internal VCR quartzite (Cooke 2 Shaft) carbon seam, at 9.5cm mark, cutting across the small extensional fault of Platberg age

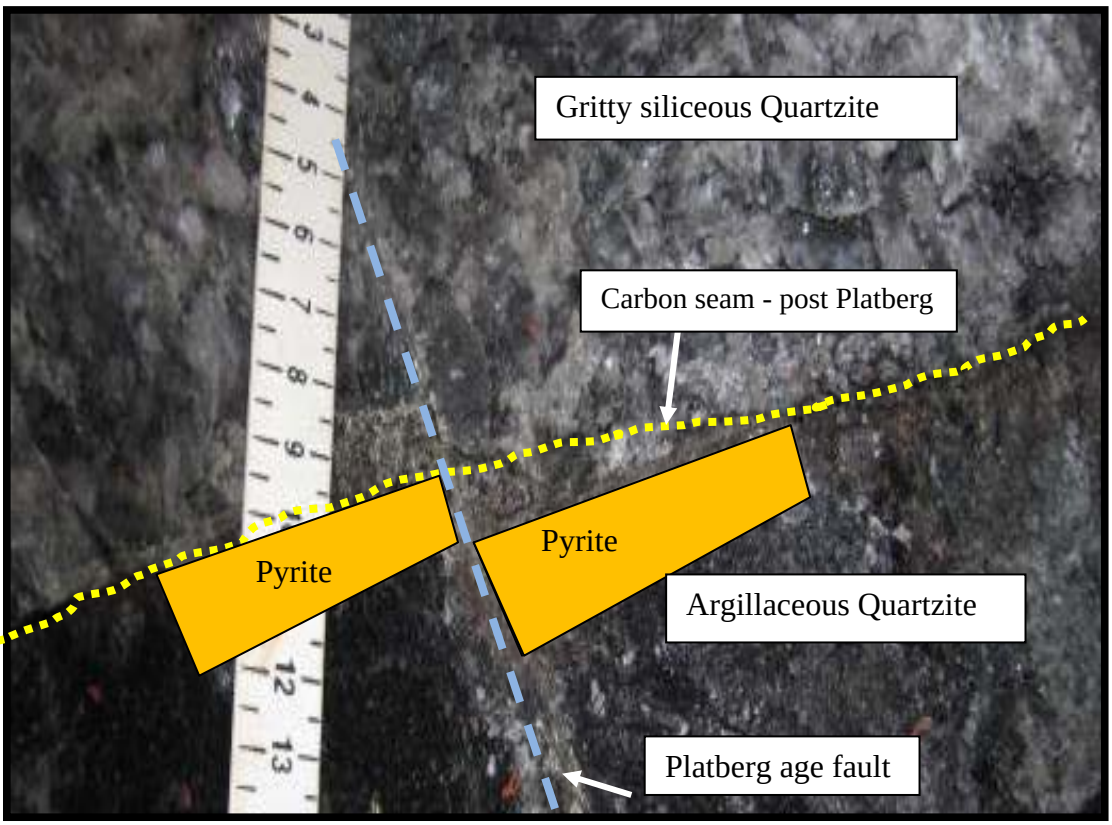

Fig.2.2: Note the carbon seam in yellow cutting across the small fault of Platberg age, which displaces an early pyrite phase.

In the photo below carbon is present in association with pyrite along the bedding parallel fracture within the quartz pebble. The carbon is massive and one cannot distinguish any spindles of carbon.

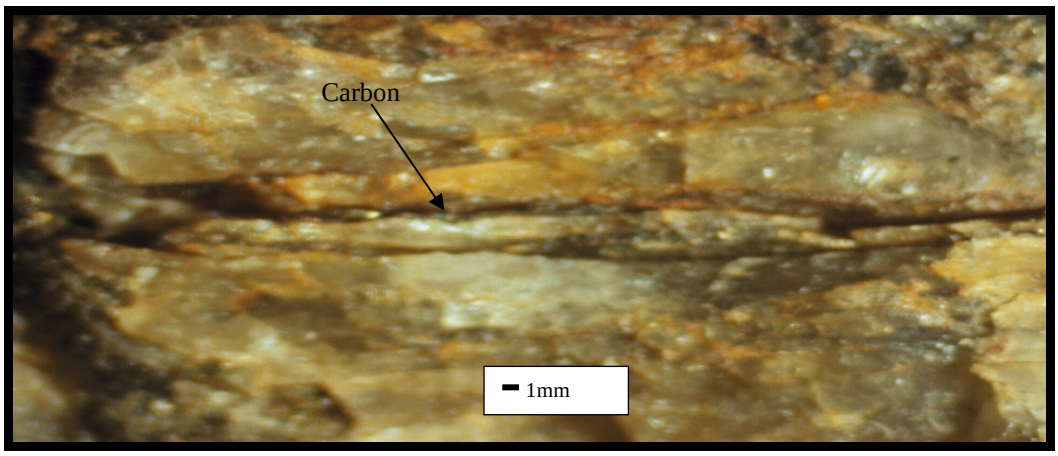

Fig. 2.3: Pebble with a 2 cm long bedding parallel fracture filled with carbon and pyrite. This indicates brittle fracturing (Western Holdings Gold Mine)

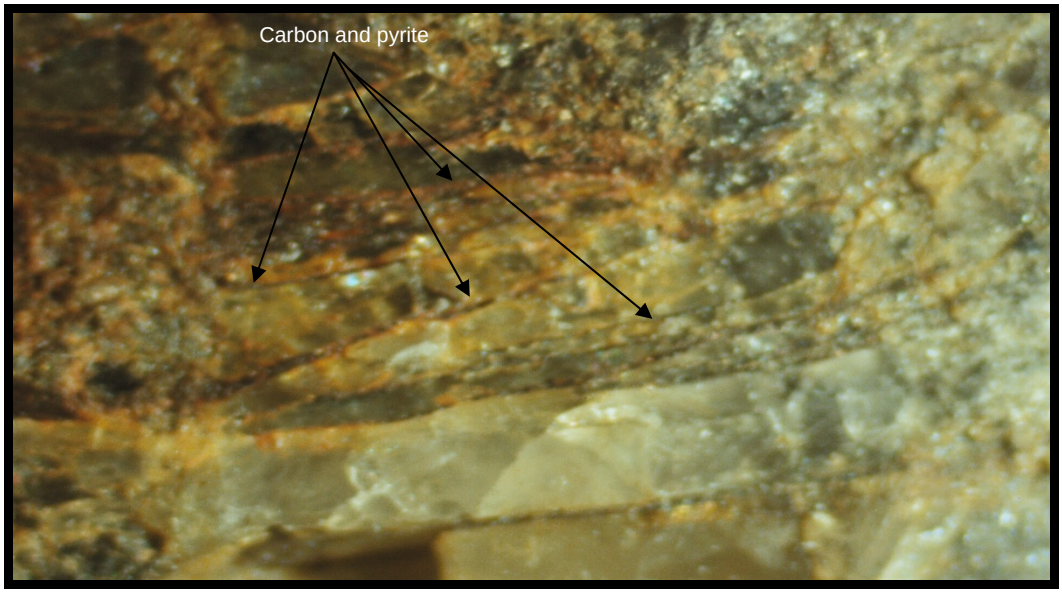

Fig. 2.4: Pebble with bedding parallel fractures filled with carbon and pyrite. Fracture is 1 centimeter long. (Western Holdings Gold Mine)

The carbon and gold in Fig.2.5 is rotated due to external stresses. The gold is plated onto the carbon and footwall quartzite.

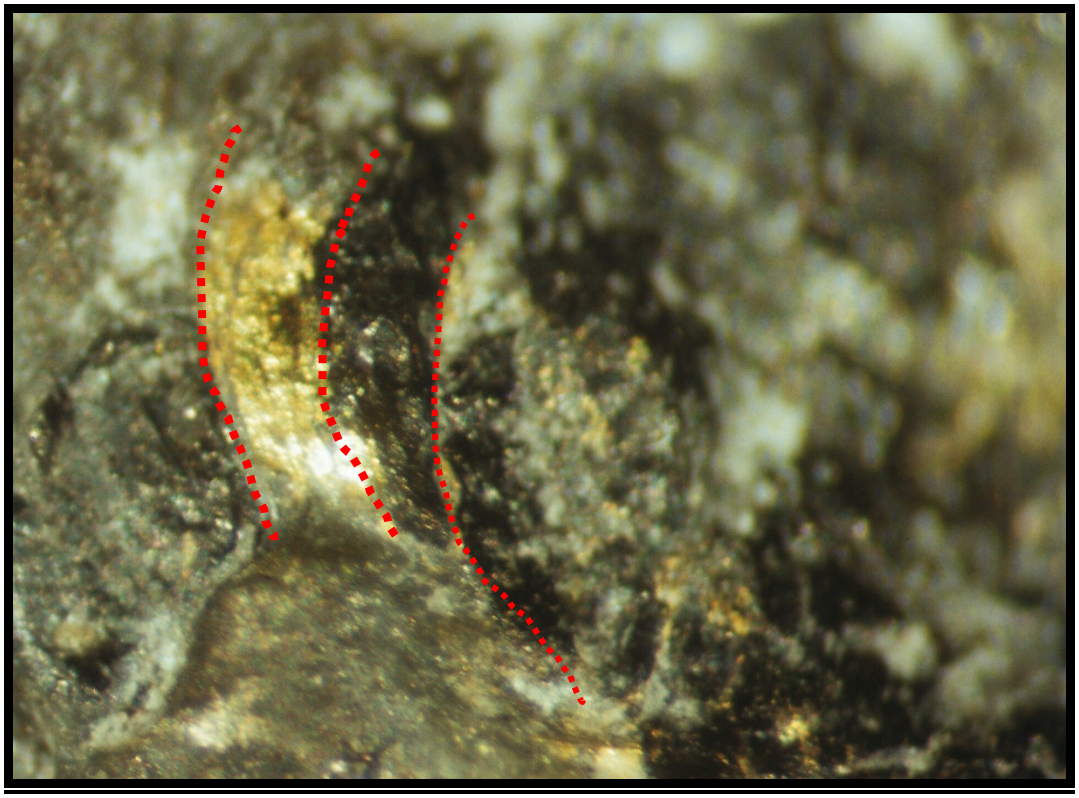

Fig. 2.5: This photo shows the rotation of carbon spindles on the contact of the B reef at Tshepong gold mine, after the emplacement was completed.

In Fig. 2.6 one can observe the top and bottom contact of the VCR conglomerate. The bottom contact has got carbon between the footwall quartzite and the conglomerate of the VCR.

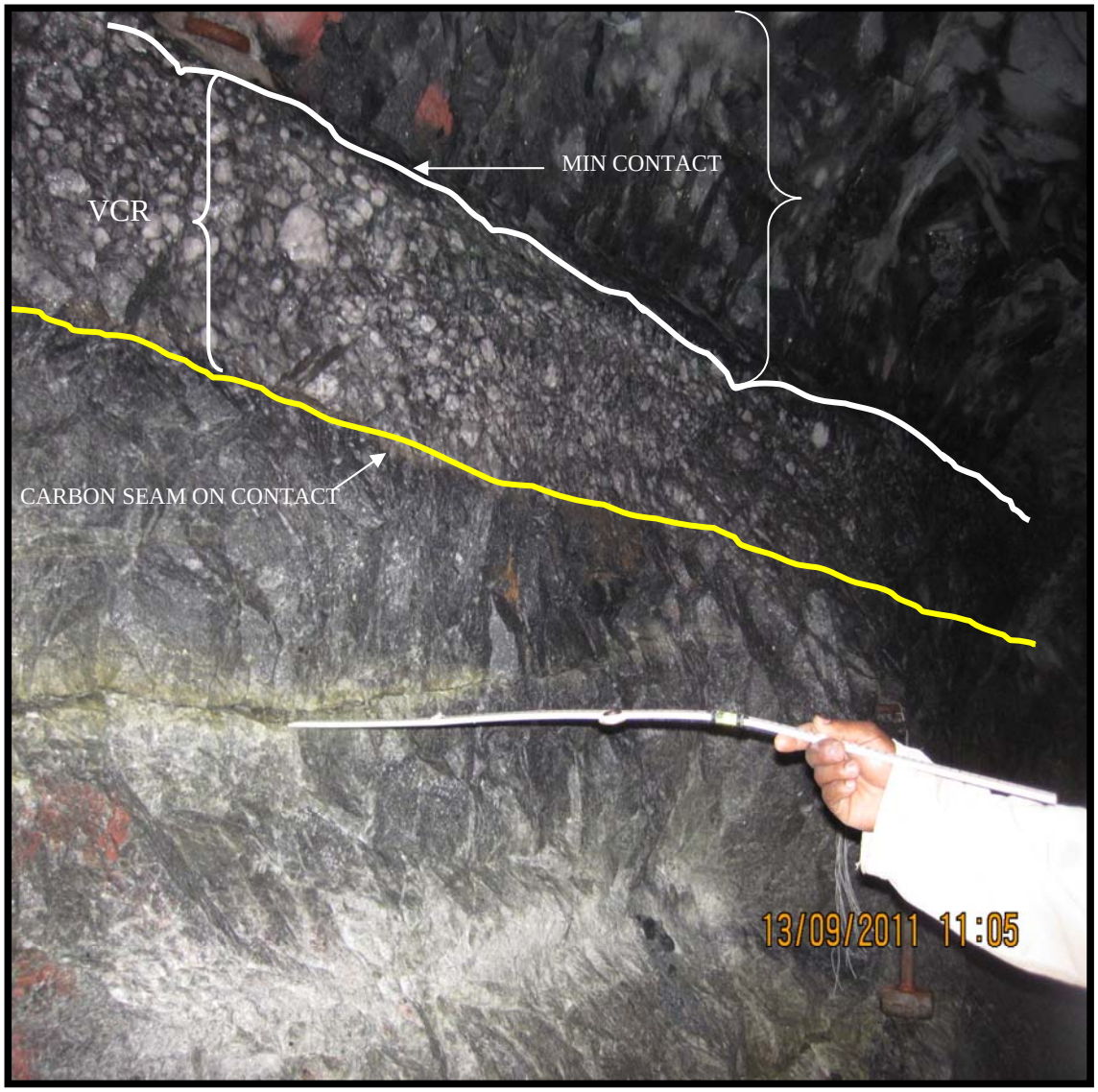

Fig. 2.6 The mineralized fluid pathway (phylonite) intersects the VCR above my assistant's hand. (Cooke Gold Mine)

The top contact in Fig.2.6 is well mineralized with pyrite on the contact. The fluid pathway is also mineralized with pyrite. The fluid pathway at the point of the ruler is well mineralized and consists of visible pyrite.

In Fig.2.7 one can see the carbon on the contact with the naked eye. This carbon is the spindle type associated with gold and sulfides. The shear zone is 25cm wide and consists of several shear planes. The movement along the

shear is from the northwest on the upper boundary and from the southeast on the lower boundary of the shear.

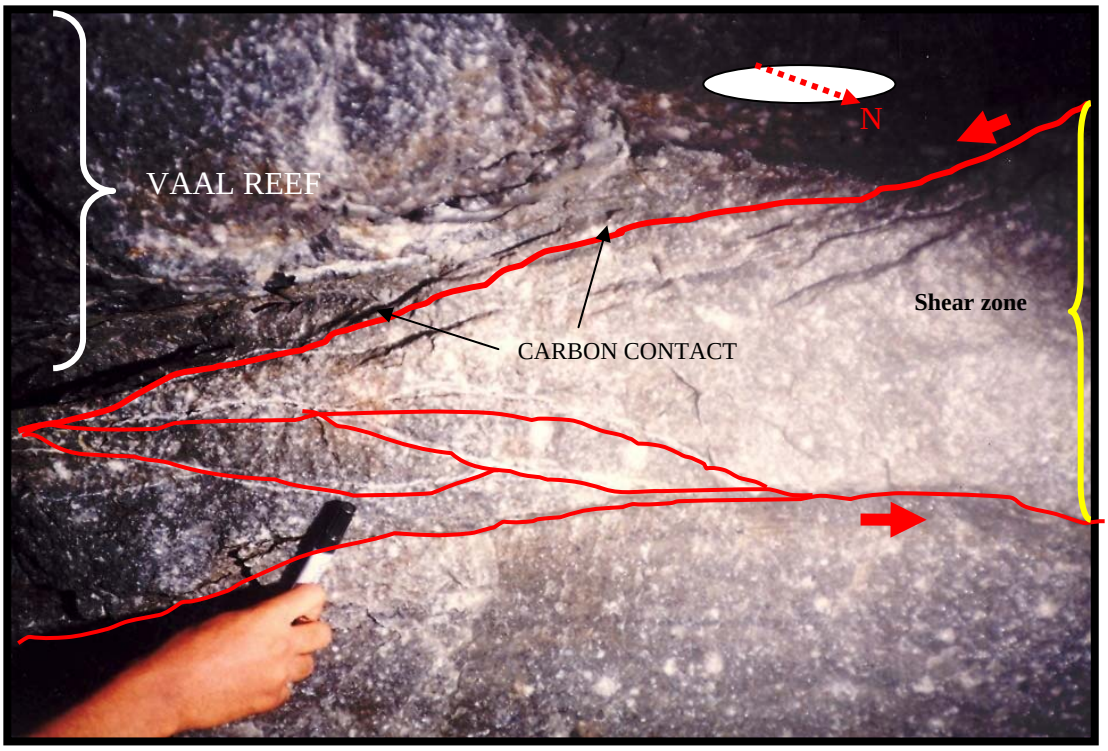

Fig. 2.7 Shear zone within the Vaal Reef with carbon along shear planes (Platberg extensional age). Carbon only visible on the contact but microscopic carbon present on the fluid pathways in red.

Carbon is present on the fault plane in Fig. 2.8. The 2 listric faults become one fault to the north. No visible carbon was observed within the fluid pathway. The fluid pathways on top of the VCR are enriched in sulfides and pyrite has replaced the lava in the middle of Fig. 2.9 and Fig. 2.10. The carbon is disseminated in the VCR below the mineralized zone Fig. 2.10.

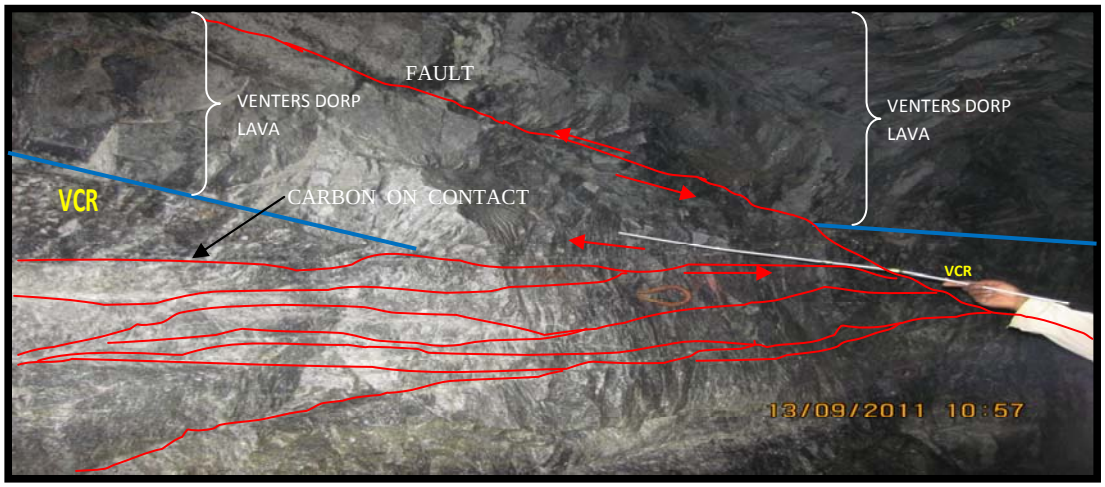

Fig. 2.8 Listric faulting and fluid pathways below the VCR at Cooke 2#.

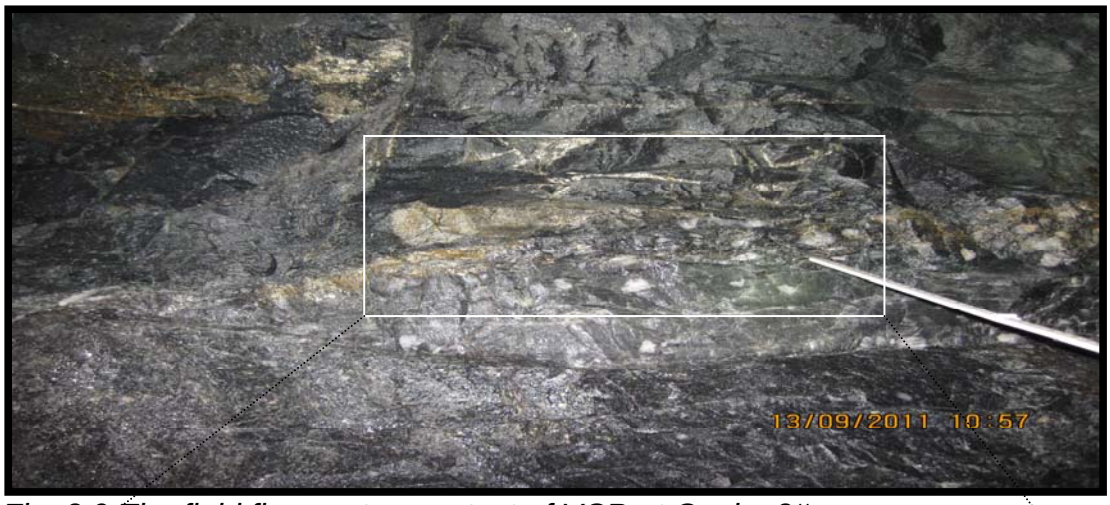

Fig. 2.9 The fluid flow on top contact of VCR at Cooke 2#.

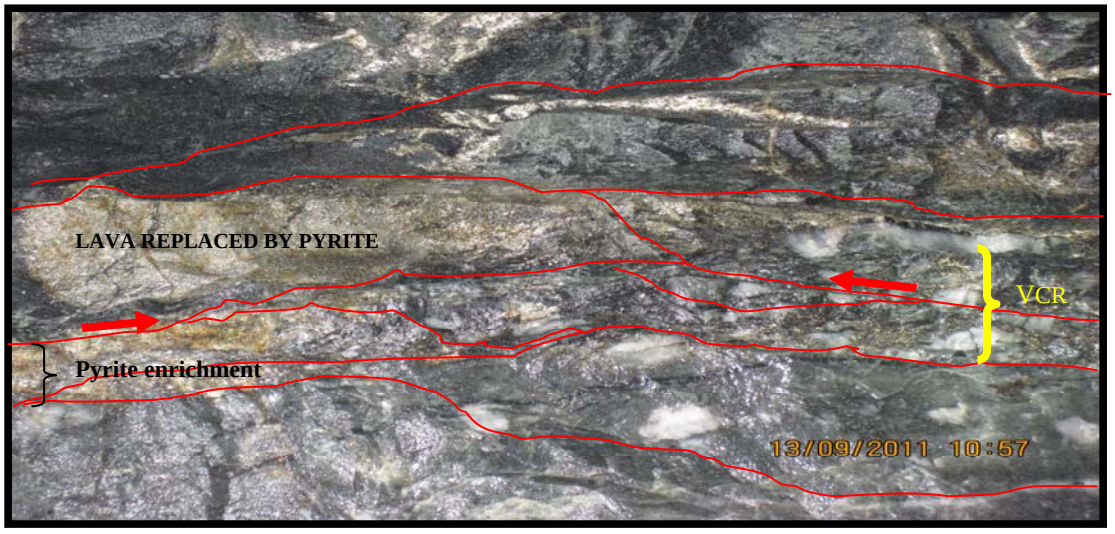

Fig. 2.10 This photograph is opposite Fig. 2.8 and the carbon is disseminated in the matrix of the VCR.

Fig.2.11 A ductile shear zone below the UE7 conglomerate. Microscopic carbon nodules are present within this phylonite.

This shear zone is 1.2m below the VCR conglomerate and is connected to the VCR along the strike into the VCR reef. The shear fabric is visible on the middle left part of the photo.

The carbon shown in Fig. 2.12 is 2cm thick and the pebbles are above and below the carbon seam. The carbon filaments are partly visible. The interesting observation is that the carbon is very soft. Take note of the fluid pathway on the right top stemming from the lava to above the carbon seam and below the quartz pebble.

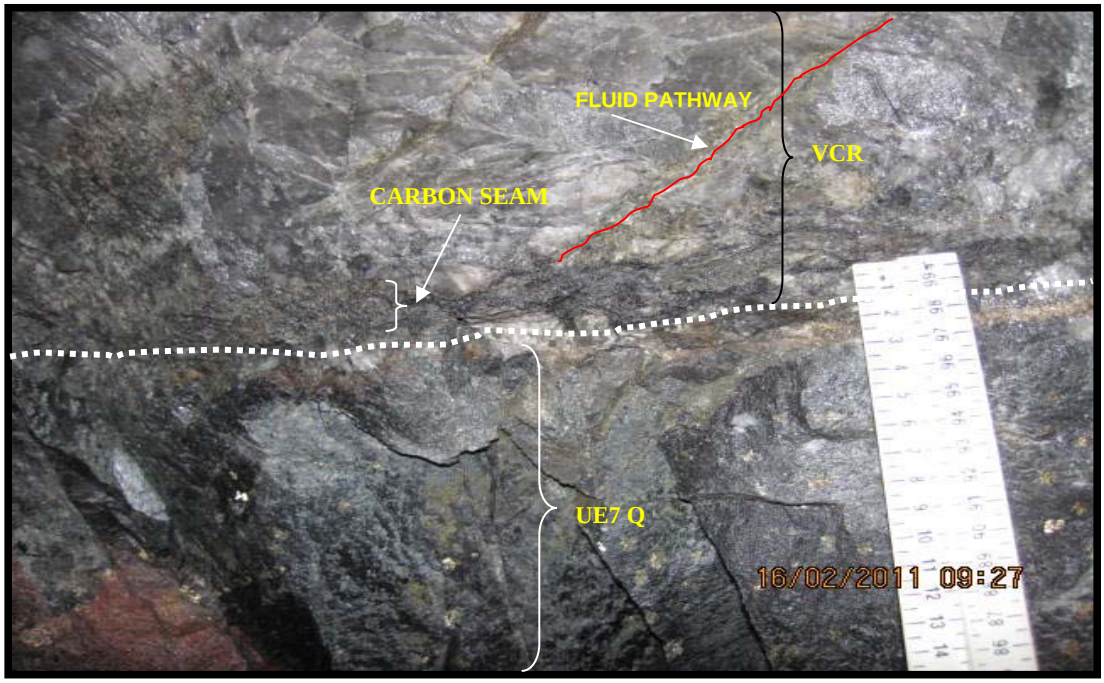

Fig. 2.12 Carbon on the VCR contact Cooke 2# (carbon 5-10mm thick).

The gold in Fig.2.13 is embedded in chlorite. Pyrite and carbon is in close proximity to the gold. This particular sample, sampled at just over a kilogram per ton.

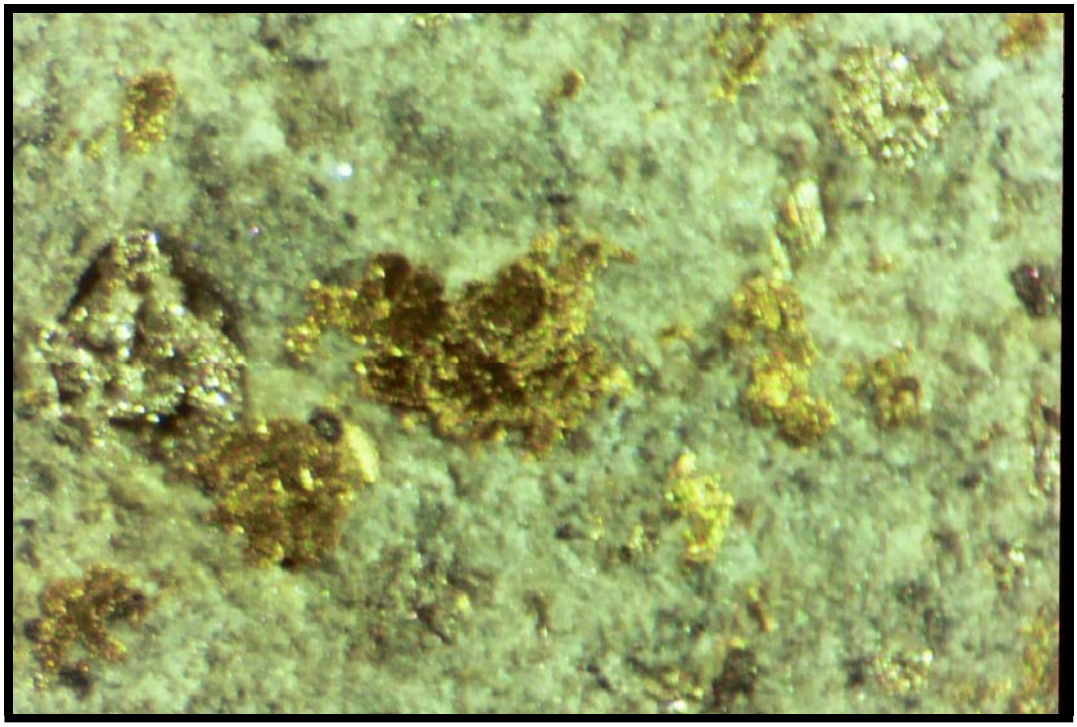

Fig. 2.13 Gold nuggets imbedded in chlorite VCR contact DGM 2#, with carbon nodules in the matrix.

The observation on carbon in Fig. 2.14 is 2-4cm thick and the carbon filaments are partly visible, but a more massive carbon contact has been observed further up-dip along the raise. The carbon stretches the entire length of the raise. The raise length was 55m.

The carbon seams are the thickets at the intersection point of the sub vertical fractures and the contact at point (A) as shown in Fig. 2.14. All the fractures below the Vaal Reef contact form part of a thrust zone.

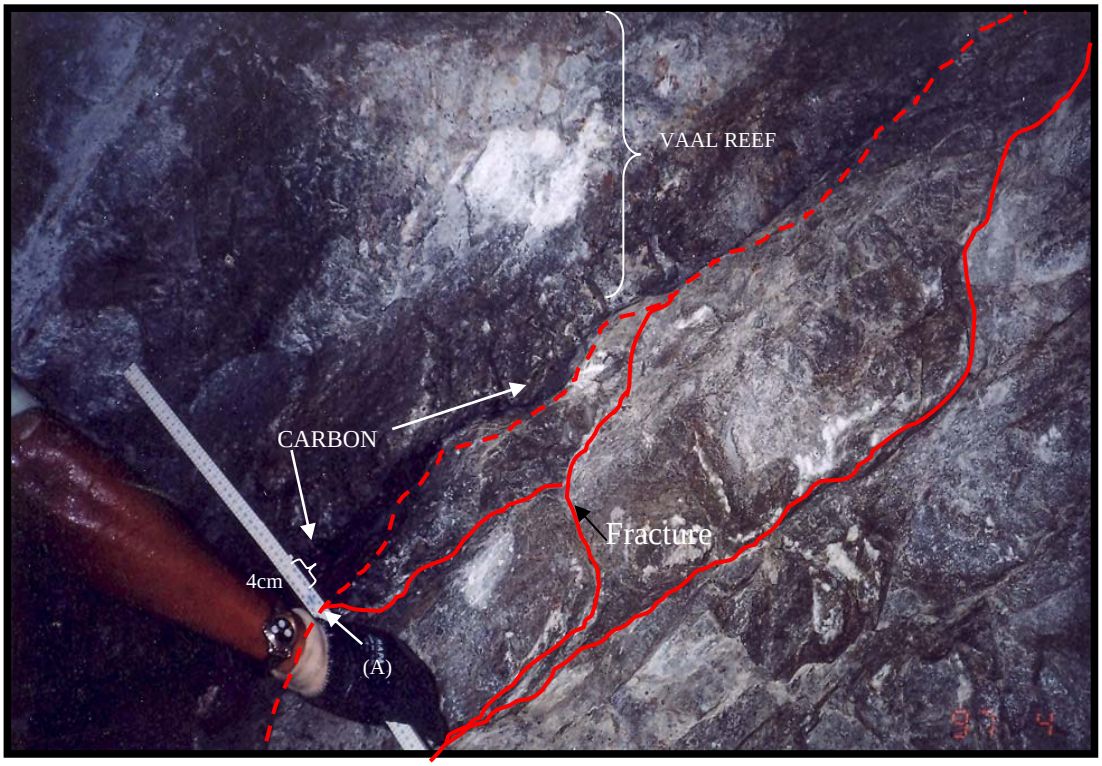

Fig. 2.14 Carbon exposure on the Vaal Reef contact Vaal Reefs Mine, Kopanang shaft or 9 #.

2.3 Carbon distribution in the Wits Basin

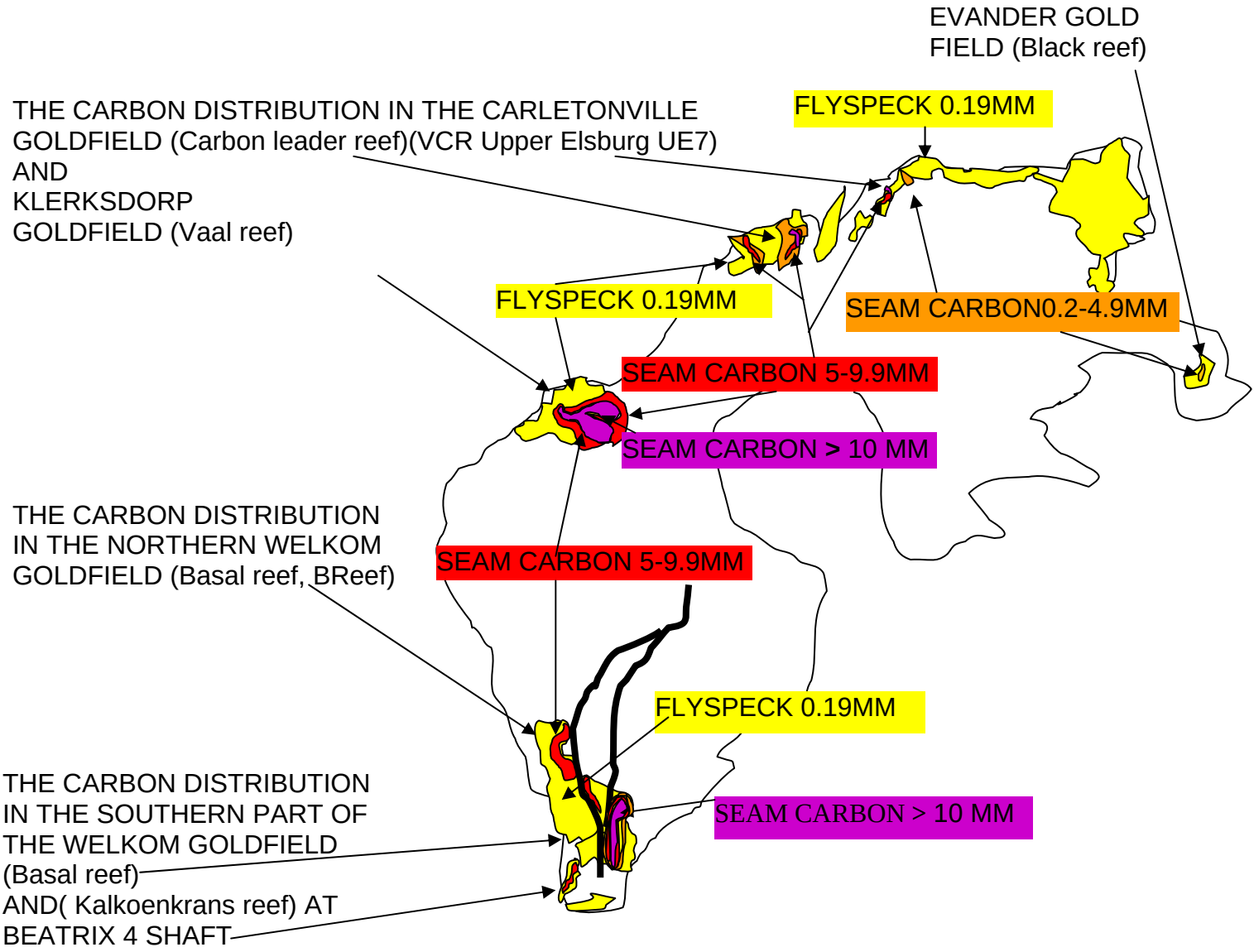

Fig.2. 15: The carbon thickness distribution plot.

The thickness and distribution of the carbon in various goldfields with the main carrier of carbon is shown in Fig. 2.15. The distribution of carbon in the stratigraphic record is basin wide in all the reefs as indicated in Fig. 1.3. It is also important to note the percentage carbon per reef type is increasing with depth below surface. Thus the deeper the reef the more carbon has been mapped and recorded basin wide. The carbon distribution on the Basal reef increases with depth from the west to the east on the old Western Holdings

mine. In the west the average thickness at two shafts Western Holdings Mine is 1cm and in the east it is 7cm.

The area that has the most and thickest carbon seams in the Witwatersrand Basin is Western Holdings Mine in the Free State where the carbon seams are in places over 10cm thick. The goldfield with the least carbon is Klerksdorp gold field.

Fig. 2.16 is a specimen from the carbon leader reef in the Carletonville goldfield. In this sample, two seams of carbon are structurally emplaced along two bedding parallel fractures.

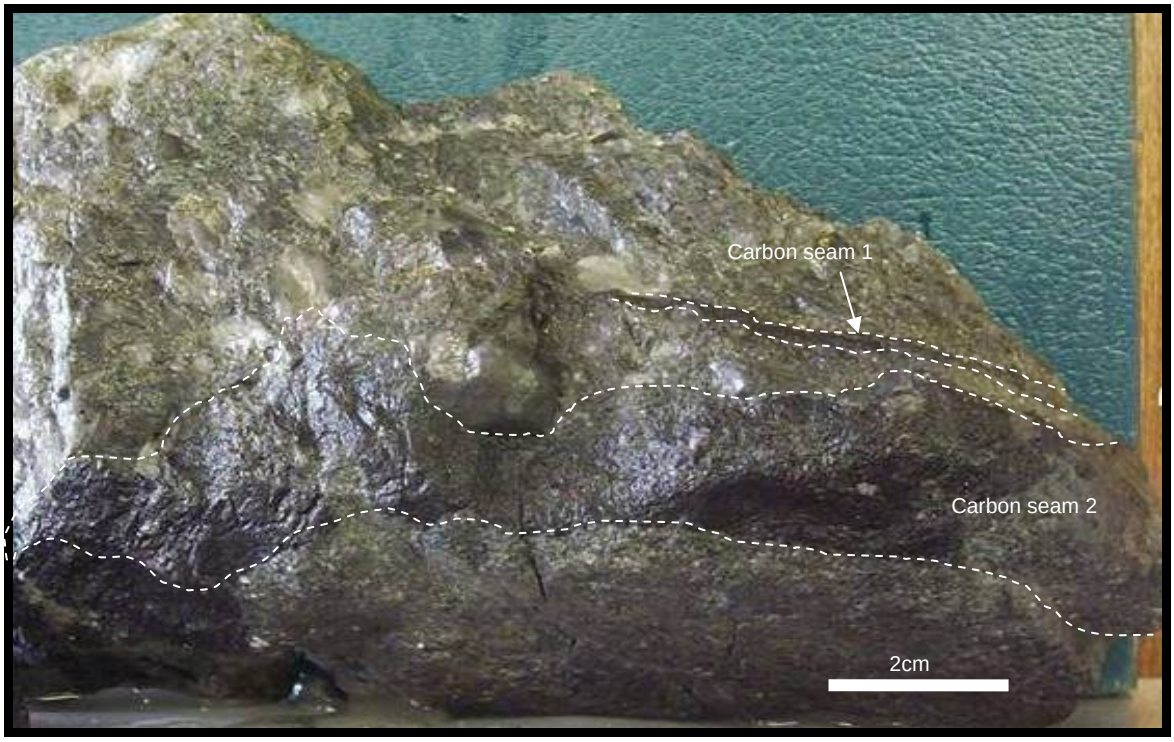

Fig. 2.16 Carbon seam on the contact of the Carbon Leader Reef at Driefontein Gold Mine. Seams occur within bedding-parallel fractures.

2.4 Underground classification of carbon.

2.4.1 Classification on the types of carbon

The occurrence of carbon mapped in the mesoscopic scale varies from 10 cm thick carbon seams or proto-graphitic form, called the mesophase (Barnicoat et al, 1997) to nodular (flyspeck carbon) which is referred to as Type A. The observed massive carbon with no internal texture to flaky carbon is referred to as Type B. This exhibits a dull appearance compared to the graphitic type having a shiny appearance for Type A carbon. It is possible to distinguish these two different types of carbon underground.

These types are deposited in lithofacies horizons that are not related in space to one another. They also differ in texture. Type A is observed in reefs and bedding planes, bedding parallel fractures and on fault planes.

Type A consists of spindle carbon, filamentous and nodular or flyspeck carbon.

Type B consists of massive carbon and vug type carbon.

Type B was observed:

1. 70m below the Vaal Reef.
2. Above the Basal Reef in quartz crystal pocket.
3. Type B carbon observed inside a vug within a quartz vein and in the shale layer above the Basal Reef.

2.4.2 Type A Carbon

Type A carbon consists of various forms of carbon.

1. The *spindle* carbon type are long elongated strings of carbon and is the main type of occurrence that was observed underground on reef contacts, inside reef packages, on bedding planes and on fault planes.(Fig. 2.17 and Fig. 2.18).

2. The *filamentous* carbon type has only been observed on the reef contact of the B reef at Tshepong mine.(Fig. 2.19).

3. The *nodular* carbon type has been mapped on the contacts only. (Fig. 2.20 and Fig. 2.21).

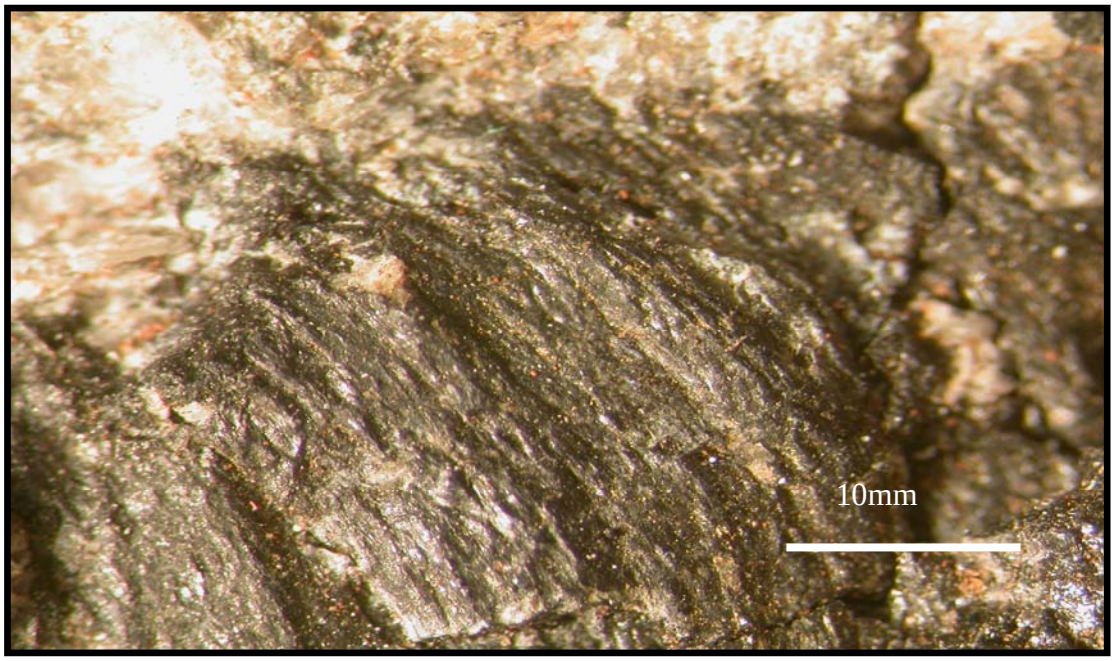

Fig.2.17 Spindle carbon from the Basal Reef (Western Holdings Gold Mine)

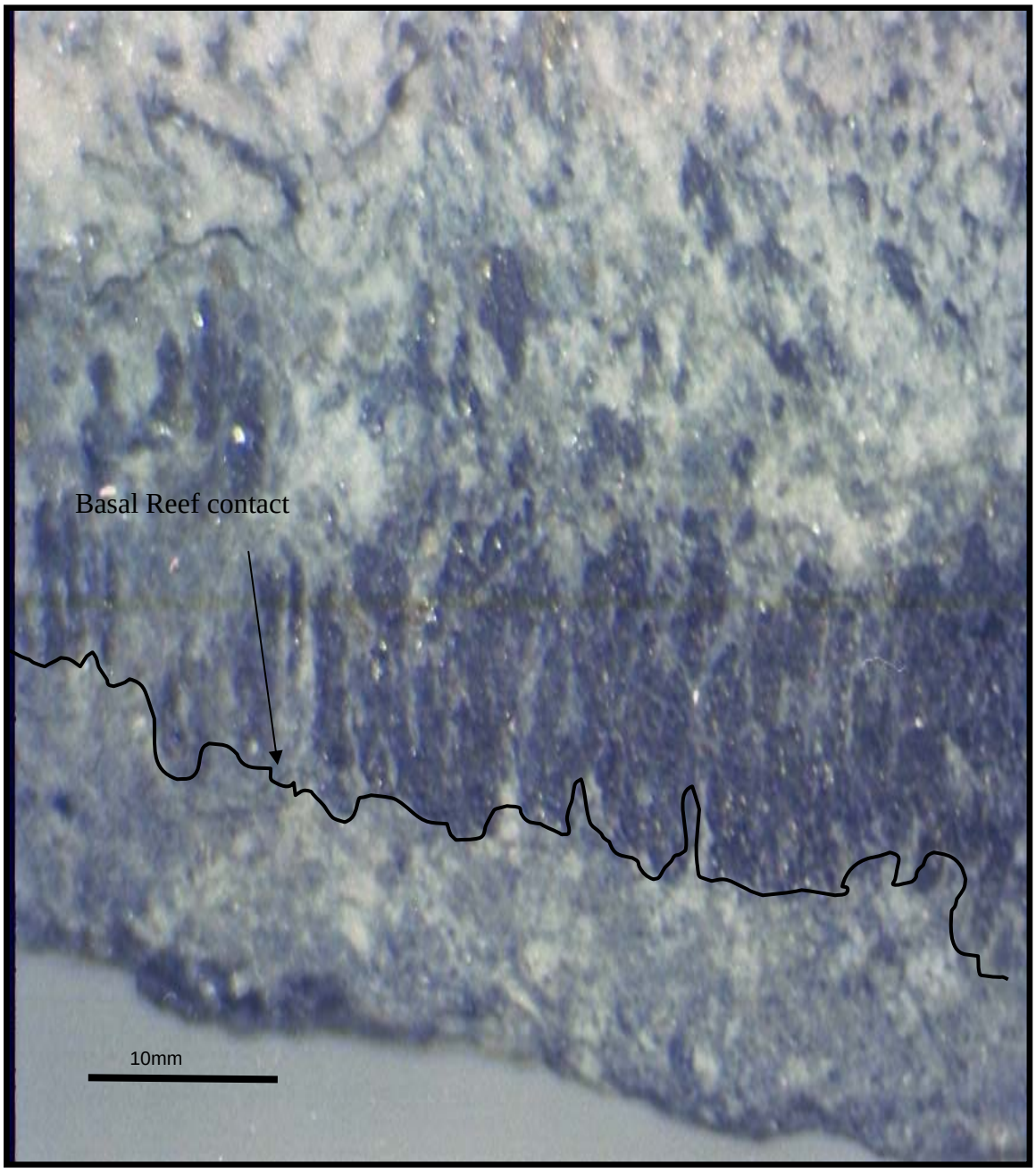

Fig. 2.18 Type A Spindle carbon on Basal Reef contact (Western Holdings Gold Mine)

Type A carbon shown in Fig. 2.19 with gold on the filaments and on top of the carbon.

Fig. 2.19 Filamentous carbon from the B reef with gold at Tshepong Mine.

The nodular type is hosted by the spindle type clearly visible in Fig. 2.20. The nodular carbon has the appearance of drops of carbon that were enclosed by the filaments (Fig. 2.20 and 2.21).

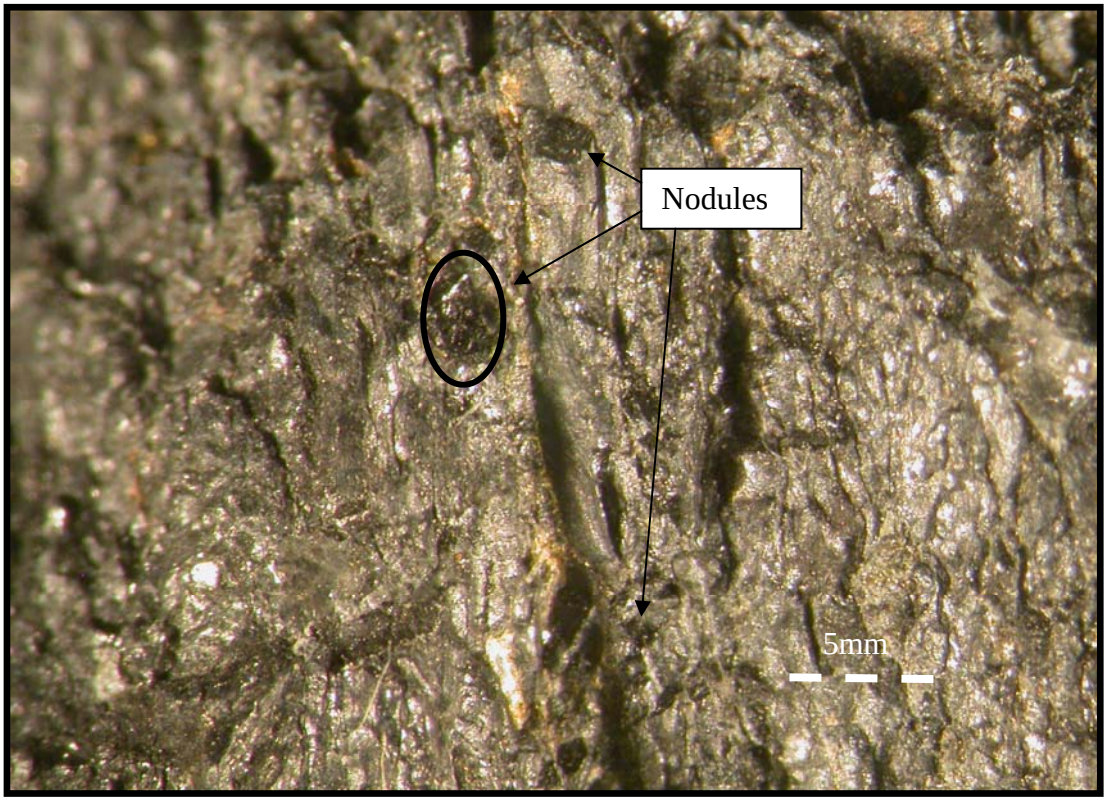

Fig. *2.20 Carbon nodules imbedded in carbon spindle.*

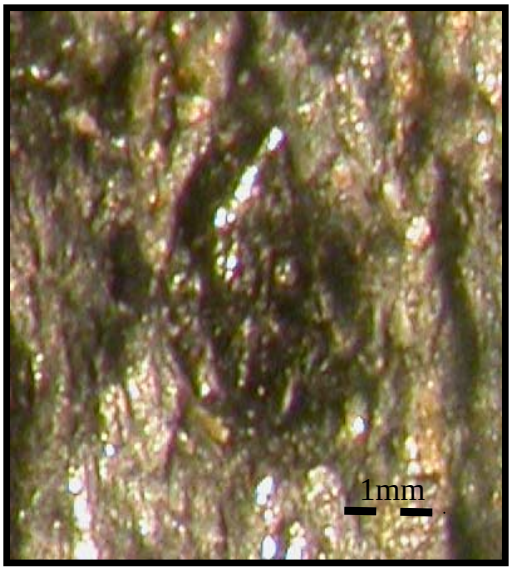

Fig. 2.21 Single carbon nodule having an elliptical shape. (Western Holdings mine)

Type A carbon is host to major amounts of the gold mined in the Witwatersrand Basin. The occurrence and mode of deposition of carbon have been investigated in detail and the photographs and maps of the faces and raises underground are the best examples chosen from the areas visited over the past 30 years. Fig. 2.22 depicts the edge of a filament within the carbon seam of the B reef at Tshepong mine. The gold forms filaments between carbon filaments and also plates on carbon filaments. The gold in the centre of the photo is very finely textured crystalline gold.

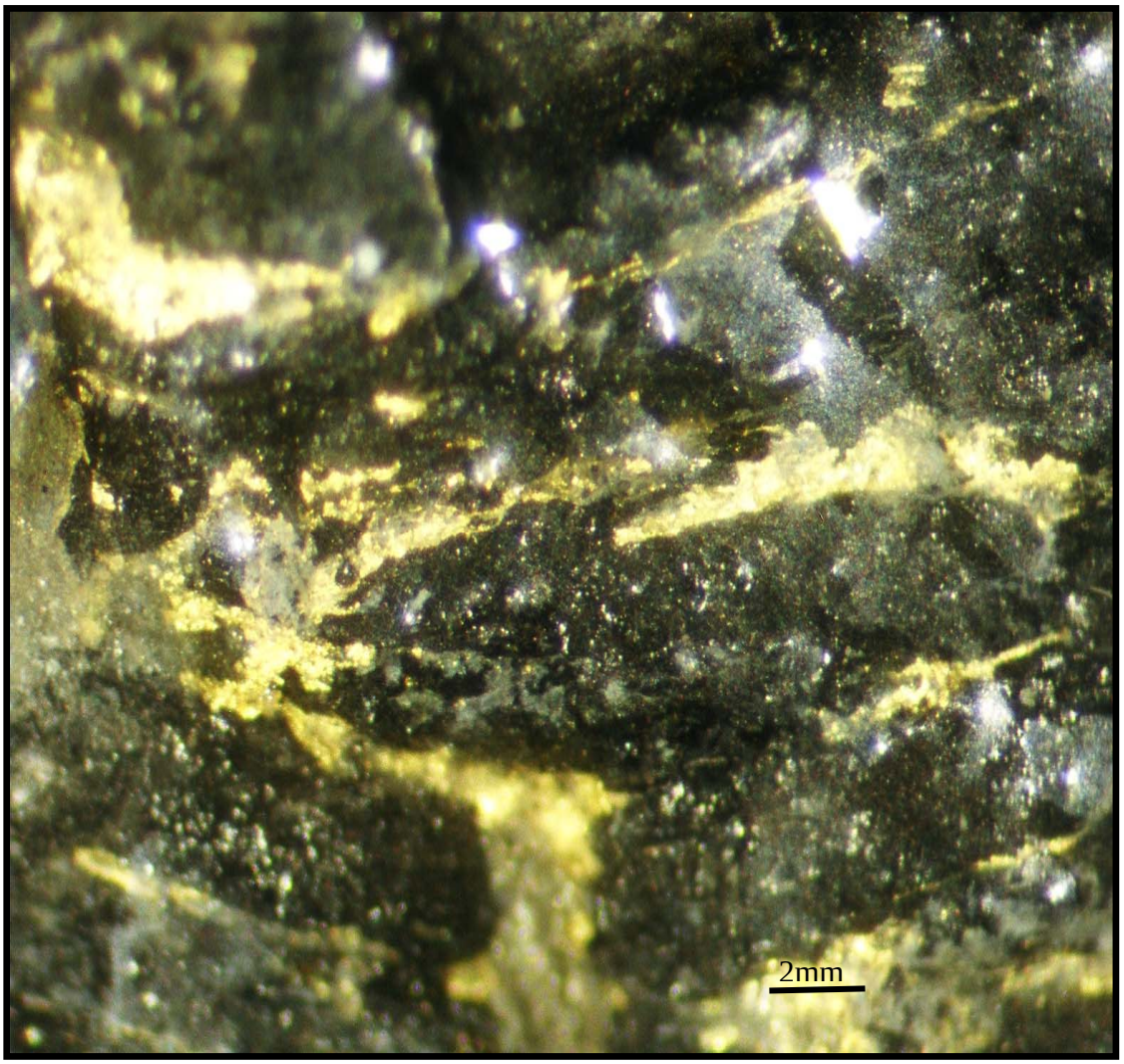

Fig. 2.22 Carbon filaments (Type A) and gold. The gold forms filaments in between the carbon filaments B Reef, Tshepong mine.

2.4.3 The Type B Carbon Observed Underground Type B is observed in Fig.2.23 70m below the Vaal reef contact in the footwall quartzite to the Vaal Reef. This occurrence is rare and has only been observed in this form and in this setting at Vaal reefs mine in 1989. The carbon is massive and does not show any texture. The hardness is that of graphite. It is situated within a fracture that is 5m away from a major extensional fault. .

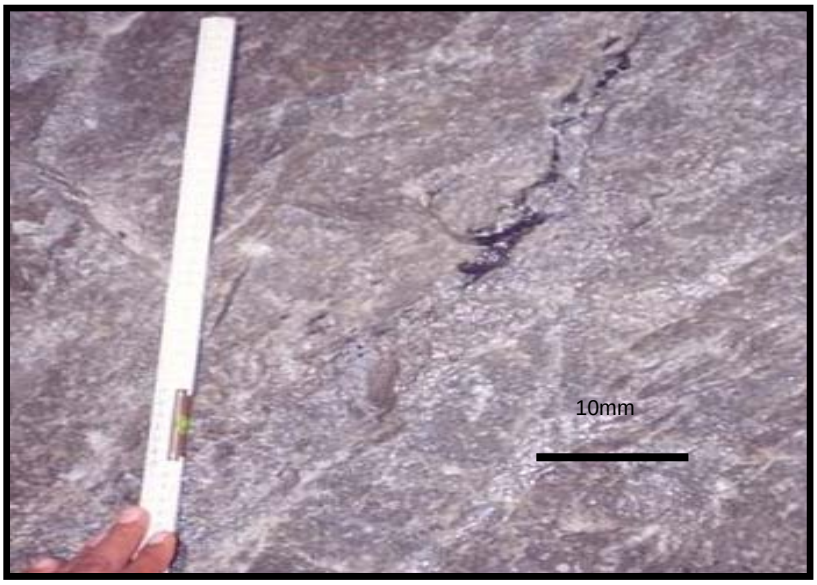

Fig. 2.23 Type B carbon in the footwall to the Vaal Reef.

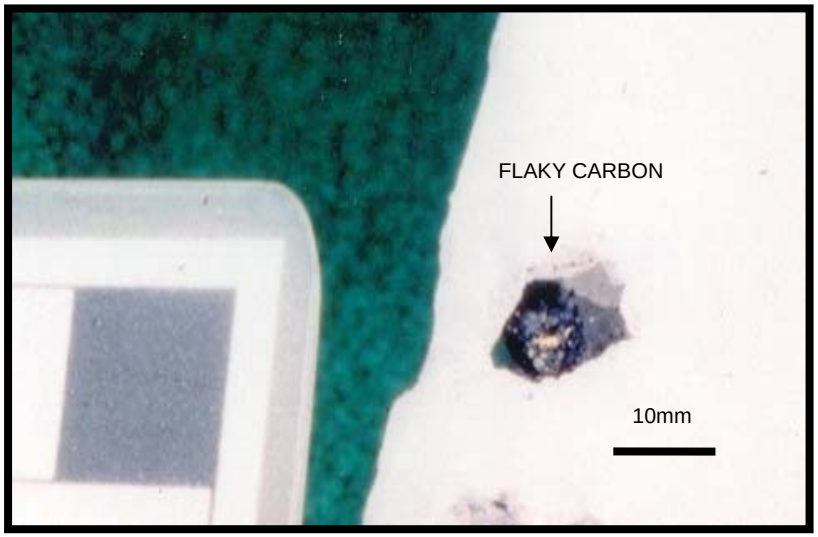

Fig. 2.24 Carbon and pyrite is present in the vug situated 1m above the Basal Reef contact Western Holdings Mine.

More detail on carbon observed is shown in Fig. 2.25. This photograph illustrates the occurrence of carbon on the VCR contact and detail along the contact.

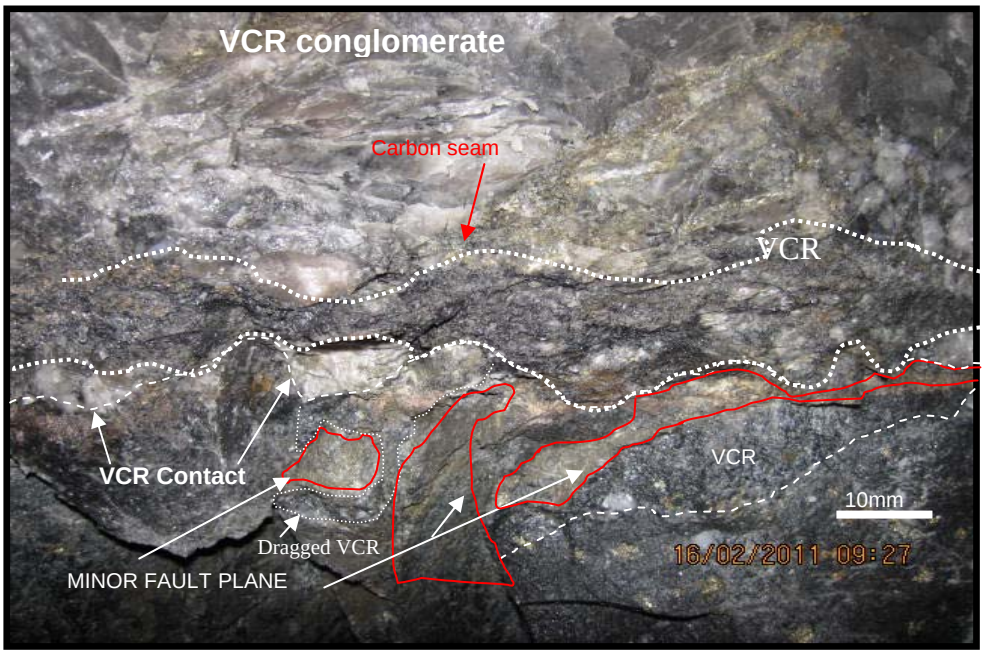

Fig.2.25 Carbon on the VCR contact 90S12A N10 panel Cooke 2#.

The carbon observed in the raise shown in Fig. 2.26 is 10mm thick. The carbon forms a solid seam all along the contact. All the fractures have been sampled in detail and these values will follow in the Chapter 6.

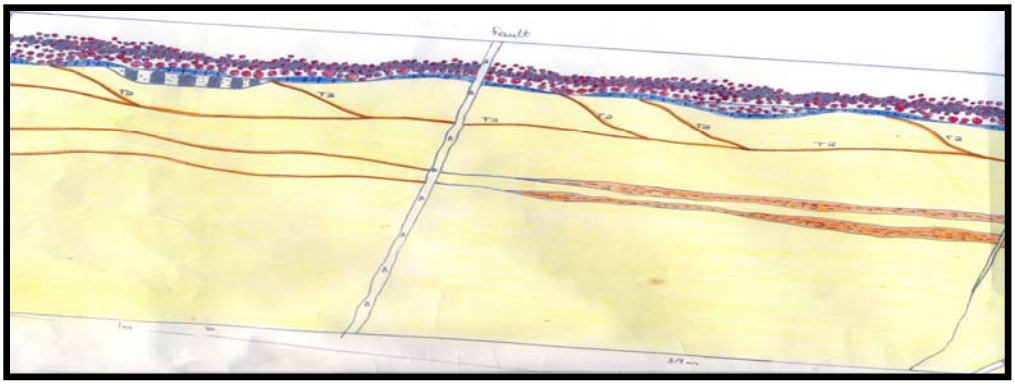

Fig. 2.26 The diagram of a raise on the Vaal Reef Mine. 70Dw 1 17 raise.

This is a diagram showing fractures (orange), carbon development in blue. Section is looking north, the dip is from the west to the east and the approximate distance from west to east is 25m.

2.5 Carbon occurrence along fault planes

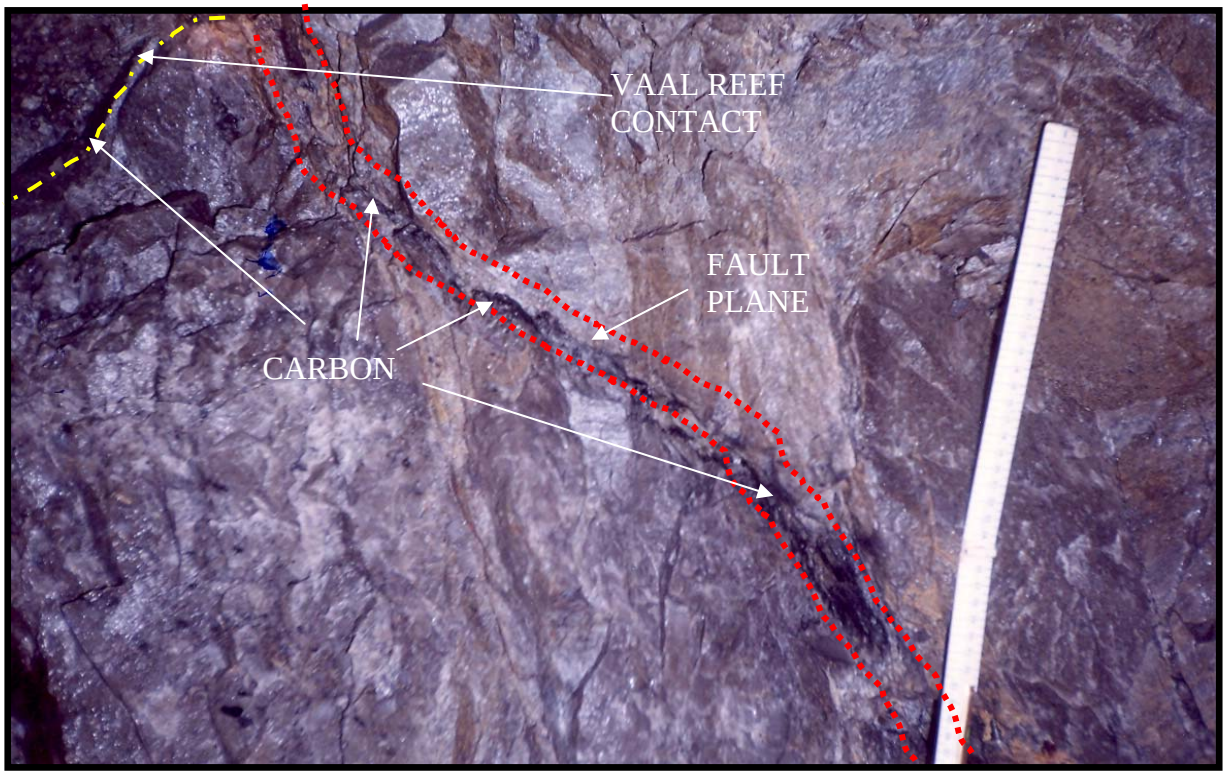

Fig. 2.27 Carbon on a fault plane at Vaal Reefs Mine. Carbon seam 1-12mm thick.

It is shown in Fig. 2.27 that the carbon is precipitated all along the fault plane and the carbon on the contact is the same as the carbon on the fault plane.

2.6 Carbon occurrences in relationship to large scale dykes

The carbon as shown in this section in Fig. 2.28 differs in thickness. The carbon on the eastern side of the dyke is thinner than the western side of the dyke. This phenomenon will be discussed in chapter 4.

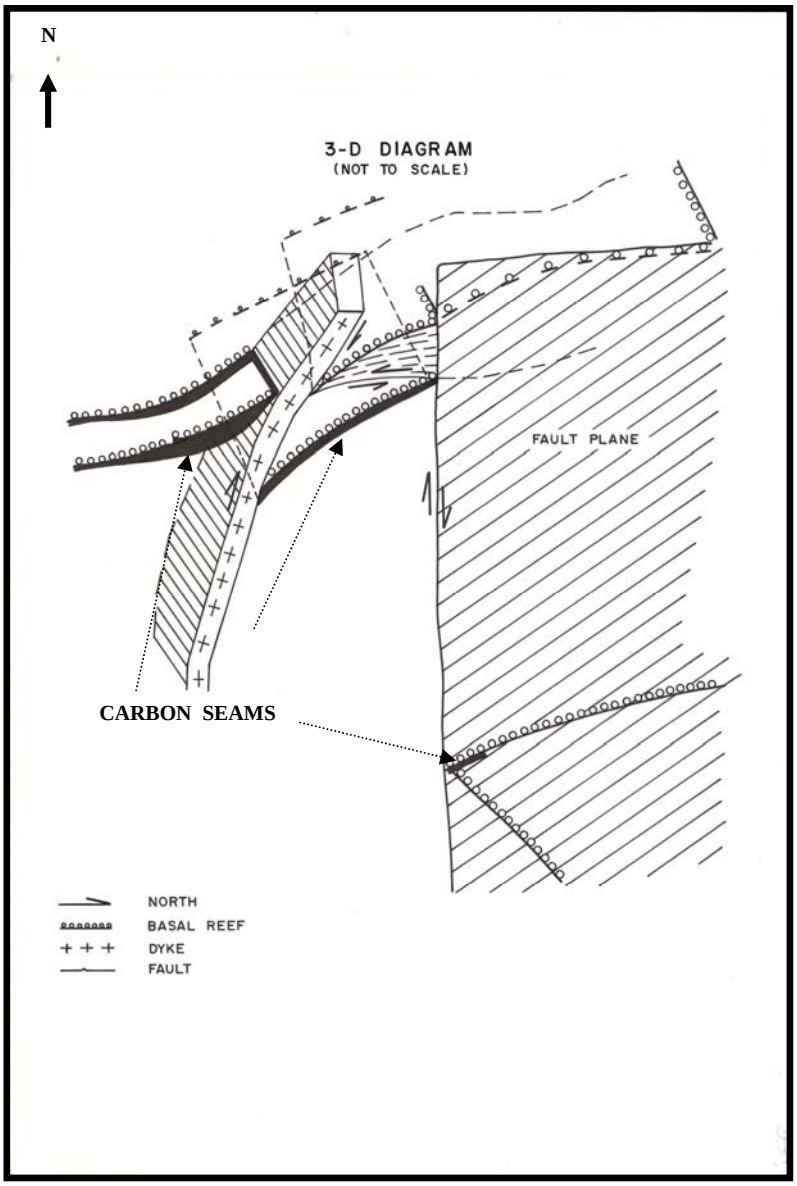

Fig. 2.28 This is a diagram from an unpublished report on the origin of carbon, showing the position of the carbon seams along a dyke with a reverse throw. Carbon is developed on both sides of the dyke but the top conglomerate band is not carbon rich.

2.6.1 Examples of Carbon and gold occurrences

Fig. 2.29 Carbon spindle plated with gold, B Reef (Tshepong Mine)

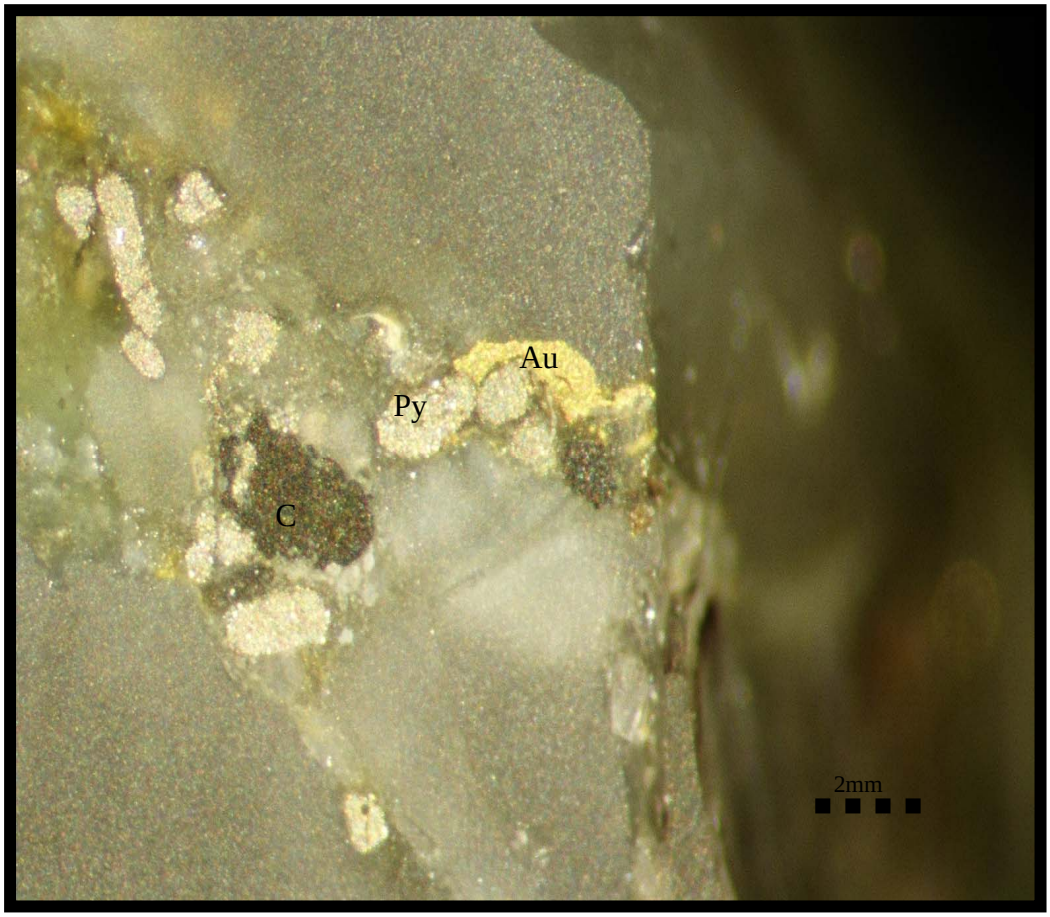

Fig. 2 .30 This is a photograph of the Basal Reef Western Holdings Mine where gold pyrite and carbon are all in close proximity within a fluid pathway around quartz pebbles.

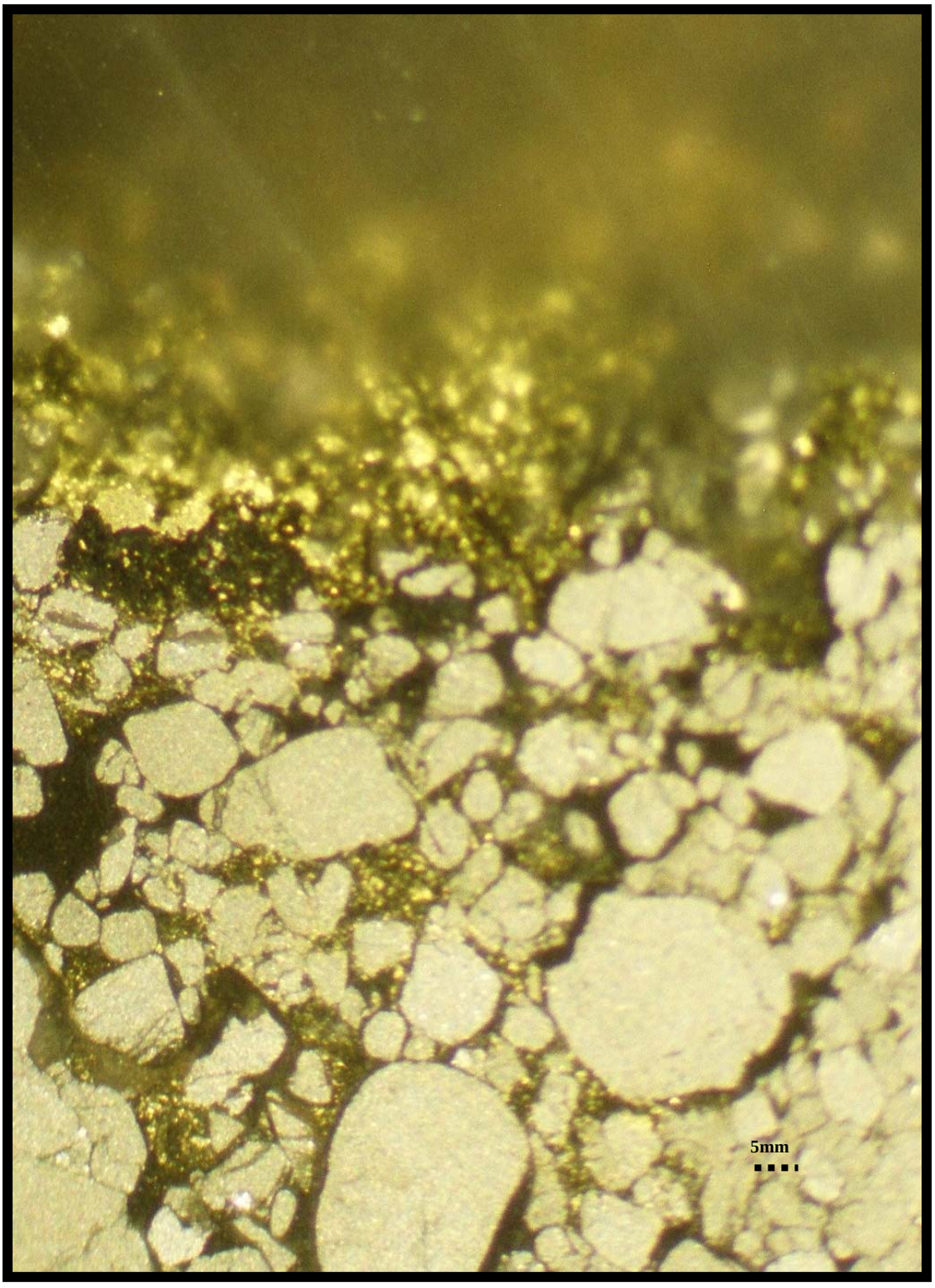

Fig. 2.31 This is a side view of gold and pyrite cut perpendicular to the contact and an inside view on the contact where the gold is plated onto the carbon, VCR at 2# (Driefontein Gold Mine)

2.7 The macroscopic description of fractures and their filling

This section describes fractures occurring in the carbon leader reef and the vein filling observed. The example to be described is a sample from Driefontein Gold Mine. The crack in this pebble is parallel to a bedding plane fracture. It is deduced that the same force that caused the bedding parallel fracturing has caused the crack in the pebble.

The event that followed filled the crack with carbon and sulphides. The carbon is coated with Bornite, and the carbon has been metamorphosed to graphite. This occurrence of carbon does explain some of the pre historic history and it reflects high energy structural deformation. There are more examples of the same intrusion but much smaller and more fascinating.

2.8 Summary

Carbon has been observed in many different localities associated with various lithologies and structures (faults,fractures and folds). Several morphological varieties were observed on the macro and meso scale namely the Type A variety (spindle, filamentous and nodular carbon). The vast subsurface development of carbon has been illustrated in Fig.2.15 and this shows the scale of carbon emplacement on the horizontal scale.

The next chapter provides more detail into the character of carbon and that data will provide more insight into the macro and meso-scale observations.

CHAPTER 3

DETAILED MICROSCOPIC STUDY OF CARBON AND RELATED MINERALS AND ELEMENTS

3.1 Introduction

The objectives of this microscopic study are to examine carbon and to investigate the spatial associations of carbon, uraninite and gold and to access the finer cracks and veins that are invisible to the eye and observe what is inside these cracks and veins.

3.2 Method

A full spectrum of 120 representative samples from core and underground hand samples were collected for this study.

Fig. 3.1 *The sample preparation lab.*

A representative population subset of 35 samples were cut for thin and polished sections and includes sections of the following: quartz veins, footwall to three different reef types, fault filling material or pseudotachylite, hanging wall quartzite to reef, shale from various sites and various fluid pathways within the footwall (Barnicoat et al.,1997). Also included are the hanging wall to various reefs and the lava above the Ventersdorp Contact Reef. All these samples were collected from underground visits as well as the studies done on the surface borehole core from AAC and Goldfields Prospecting Services.

The samples were also studied using a digital microscope in *Fig.* 3.2

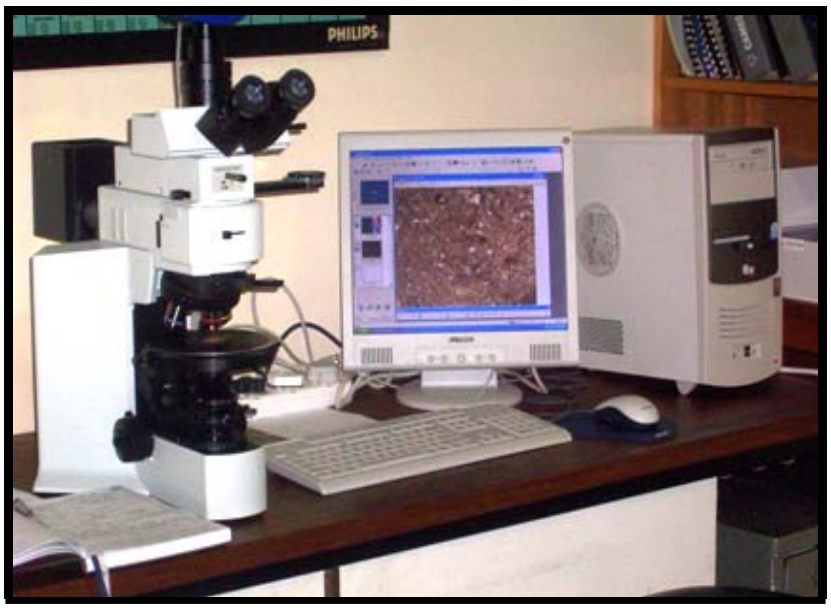

Fig. 3.2 The thin section microscope lab.

Detailed petrographic investigations were done with the Superscan Scanning electron microscope (Shimadzu SSX-550 Superscan Scanning Electron Microscope; SEM). The investigations were concentrated on the intact mineral and rock fabrics to determine the relative timing, structural control exhibited and the interrelationship between carbon, uranium and gold.

3.3 Petrographic observation on thin section scale

The observations on 60 thin and polished sections were spectacular and various metamorphic textures were observed.

The results of the electron microscope study provided evidence to the nature of the movement of fluids in the micro scale. The various minerals are deposited within the fluid pathway. See section 3.4 for definitions. From the thin section analysis of orientated core (*Fig.* 3.3), the direction of shear showed that the major direction of tectonic movement was to the north (thrust sense).

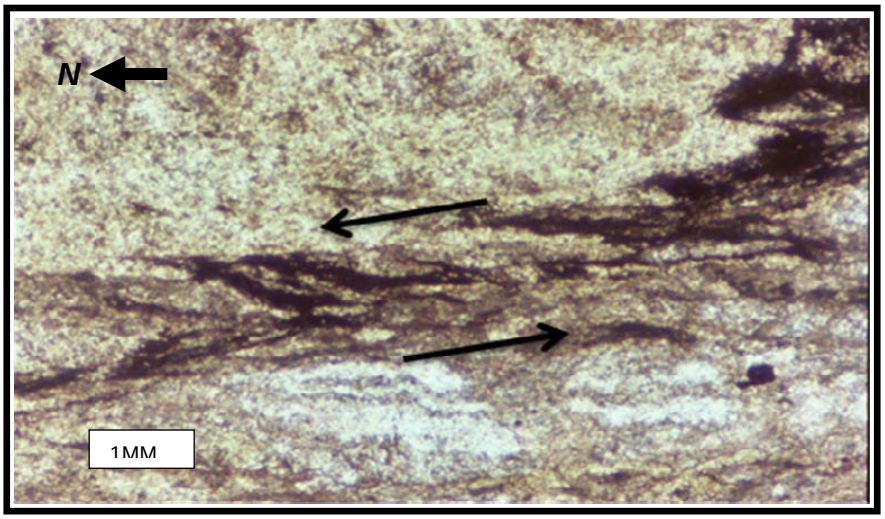

Fig. 3.3 A sigmoidal structure in a chloritic shear zone in quartzite exhibiting sinistral shear parallel to bedding in close proximity to the Master bedding plane fault at Driefontein Gold Mine. Sample no ZW741

3.4 The Fluid pathways and their carbon signature

Phylonites have been analysed by Jolley et al., (2004) and Barnicoat et al., (1997), and are defined by them as fluid pathway. The definition of a fluid pathway is a fracture or a porous rock zone or a fine grained foliated aggregate that allows fluid movement (see Fig. 3.4). Flow in these pathways is controlled by the geometry of fractures or the phylonite fabric.

Phylonite bands usually consist of quartz, chlorite/pyrophyllite and sericite. They are considered to be shear zones, associated with bedding parallel thrusting and are classified as follows:

- Type 1 exhibits a low degree of deformation and the minerals show a low degree of orientation.
- Type 2 exhibits a medium degree of deformation and the minerals show a small degree of orientation.
- Type 3 phylonite is where all the original sedimentary character of the original rock has been sheared and the deformation gives rise to a foliated rock with a distinctive foliation. Barnicoat et al., (1997) described the foliation as a schistose texture parallel to bedding.

Fig. 3.4 shows the 25cm thick phylonite band or fluid pathway. It is in these zones that different modes of cataclastic to ductile deformation took place. The orientation of minerals gives rise to a foliation (Fig.3.4b) within these zones.

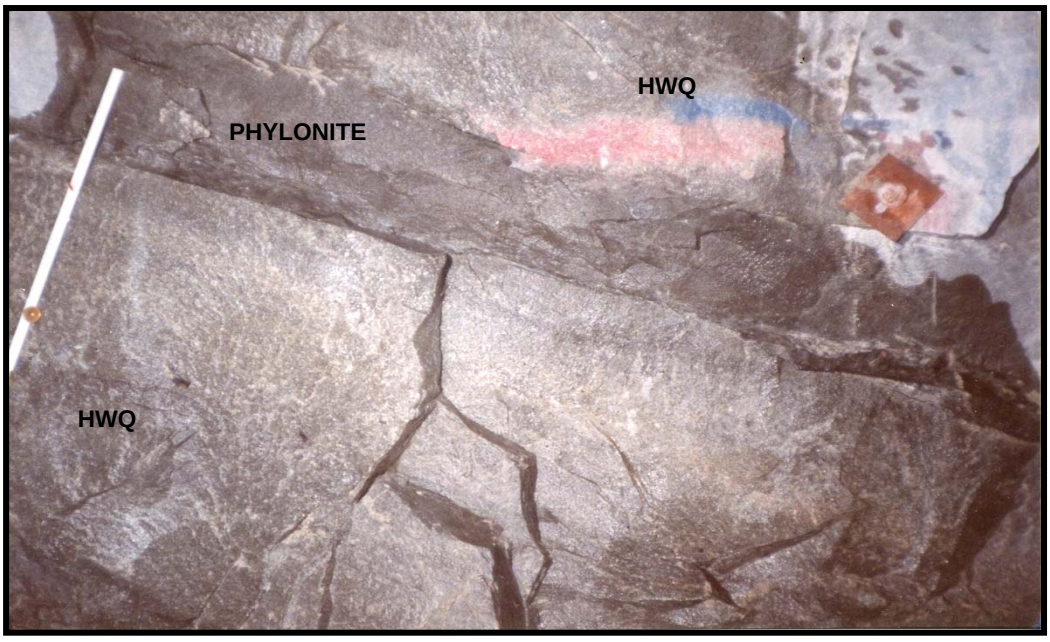

Fig. 3.4a A phylonite in the hanging wall to the carbon leader. (WHGM).

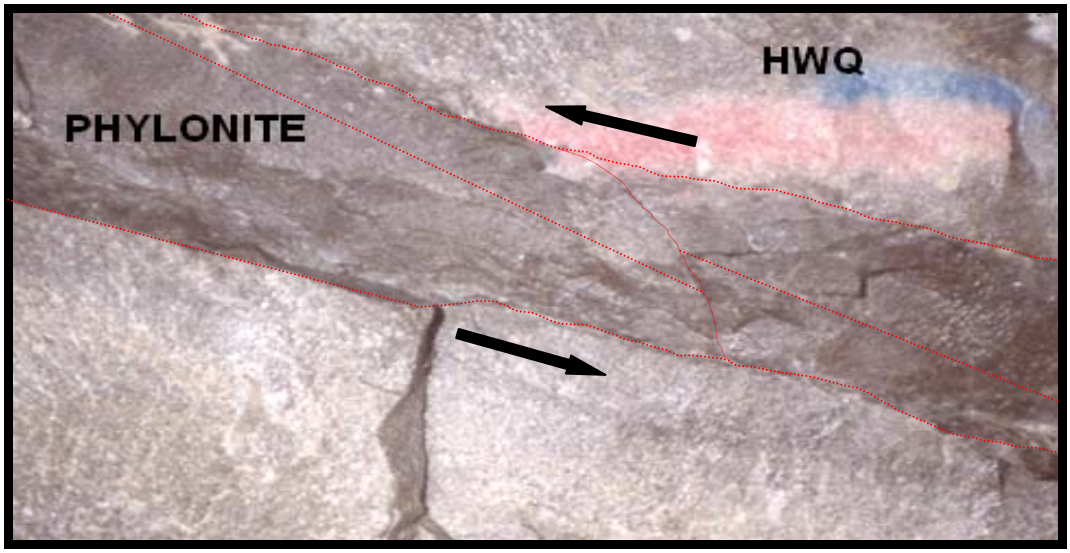

Fig. 3.4b The above phylonite band with the general foliation direction indicated by red dotted lines. The structure represents a shear zone in a bedding parallel thrust (WHGM).

Figures 3.5 to Fig. 3.10 illustrate the macroscopic and microscopic character of a phylonite. The structural age for these phylonites relate to the compressional phase at 2.8 Ga indicated by the deformation shown in the macroscopic and microscopic scale.

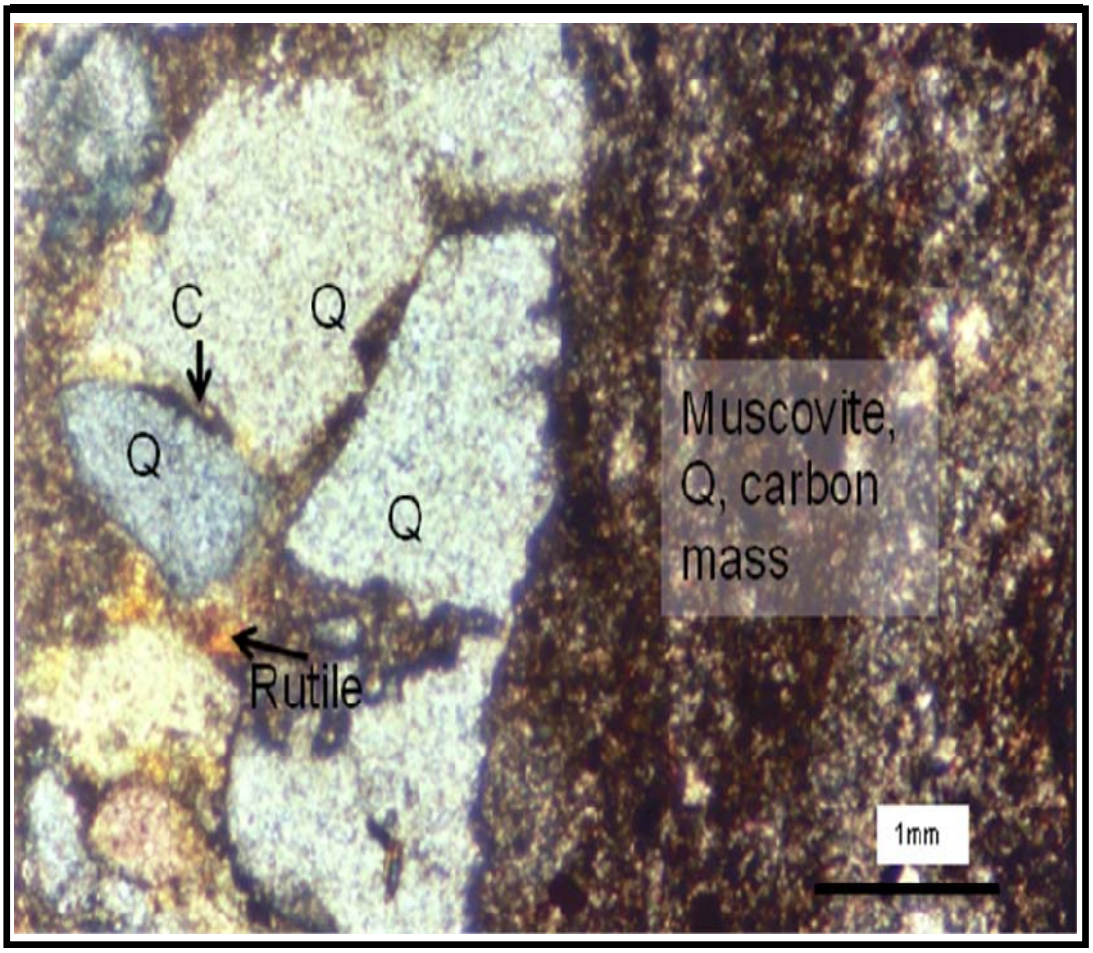

Fig. 3.5 The boundary between phylonite and quartz pebbles with rutile as a rare mineral in the fluid pathway (BH E1 T) sample no ZW 743. (DGM)

Sample ZW 743 (Fig. 3.5), is from the hanging wall quartzite to the Carbon leader reef. It is taken from a surface bore hole BH E1T. In Fig. 3.5, the brown mass is the fluid pathway, with the main minerals identified being muscovite, quartz and carbon. Carbon is disseminated throughout the fluid pathway and in between the grains.

Other fluid pathways in this study are bedding-parallel faults, thrust faults, normal faults and reverse faults. Barnicoat et al., (1997) have produced a four stage paragenetic interpretation of the complex post-depositional history of the mineralized rock or conglomerates. The author has recognised all these stages in his investigation of the minerals and rock fabrics in the thin sections studied.

The various stages of Barnicoat (op.cit.) represent the following events in the basin:

- Stage 1: Diagenesis
- Stage 2: High temperature alteration Witwatersrand Metamorfic event.
- Stage 3: Brittle fracturing
- Stage 4: Post vein fracturing

Stage 1: **Diagenesis**: Involving point contact fracturing, quartz overgrowth, illite (now muscovite) Figs. 3.7, 3.9.

Stage 2: High temperature alteration and deformation in which pyrophyllite developed after muscovite. Phyllosilicate-rich (pyrophyllite), millimetre to centimetre thick shear zones (phylonite bands) formed sub-parallel to bedding. During the formation of pyrophyllite substantial quantities of quartz has been consumed. (Fig. 3.5 and Fig. 3.6). In this study it was observed that the most intense alteration zones normally above or below conglomeratic units and contain pure pyrophyllite. In Fig. 3.6 the pyrophyllite (phylonite band) is within the K9 conglomerate but which has been sheared in this area of Cooke 2 shaft.

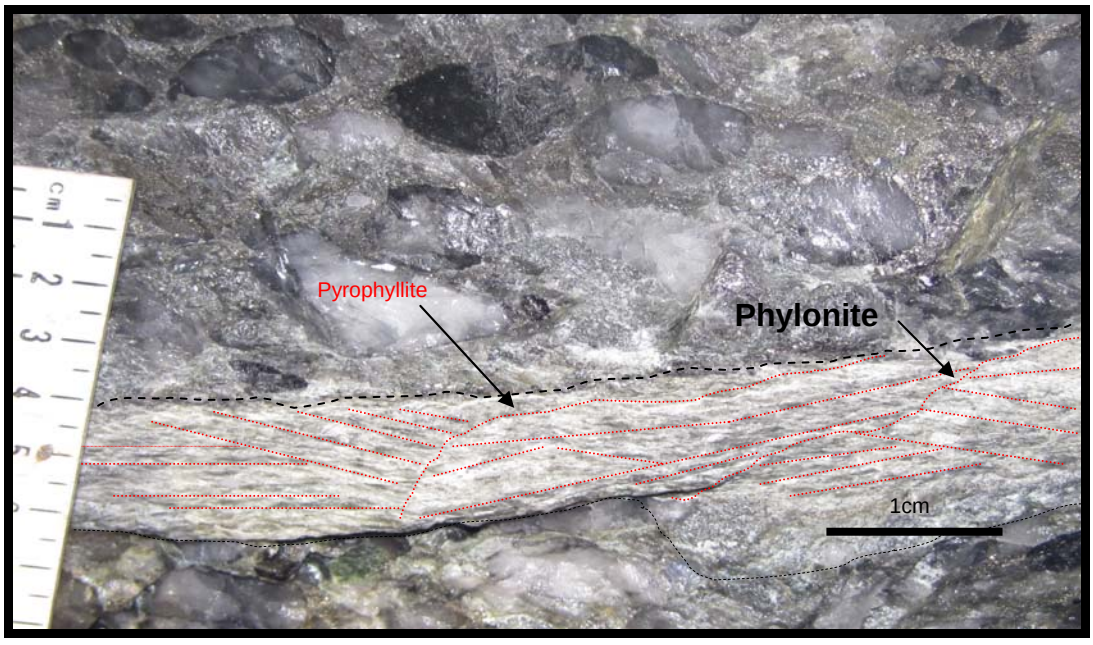

Fig. 3.6 Pyrophylite within a phylonite in the K9 conglomerate at Cooke 2 shaft exhibiting a near schistose texture. The foliation in red dotted line.

Fluid pathway is defined as a Type 3 phylonite in a K9 conglomerate. In Fig. 3.6.the fluid pathway is a Type 3- as Type 3 phylonite is a foliated rock with a distinctive foliation. The minerals are all aligned in the direction of shear. Pyrophyllite defines the fabric in the shear zone (phylonite)

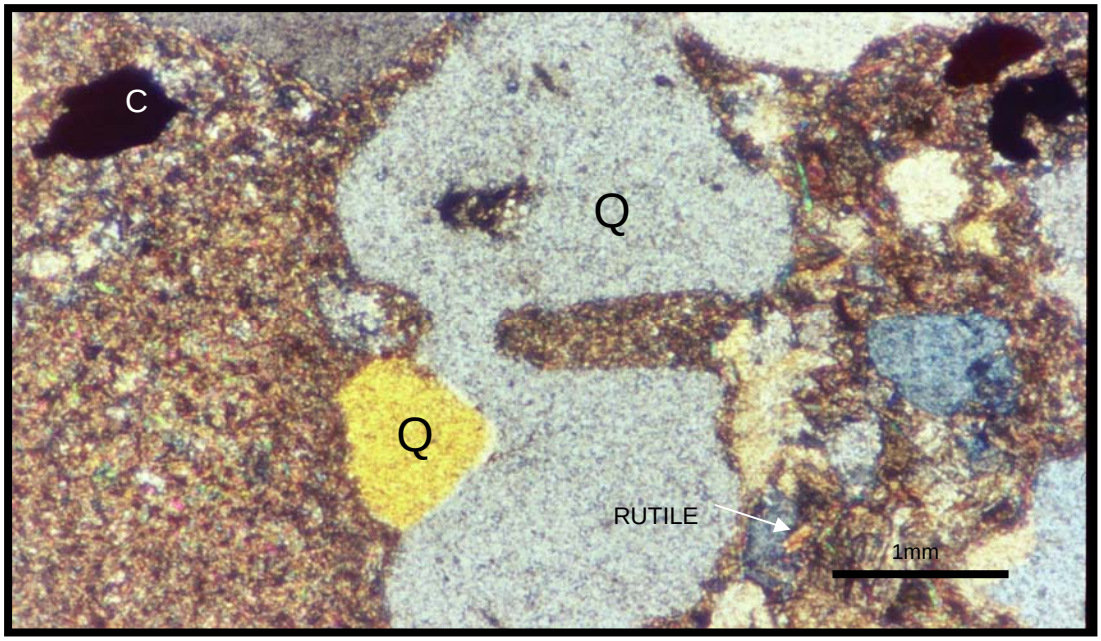

Fig. 3.7 Sample ZW 744 the quartz pebble have been dissolved by the fluid that passed through the pathway. Note the rutile, the red mineral in the second quadrant of the view and carbon within the fluid pathway (DGM).

It is observed that the quartz pebble has been dissolved by the fluid in the pathway and the volume of carbon is more than 20 percent of the brown mass of muscovite and quartz (Fig. 3.7). The red mineral in the lower right corner of Fig. 3.7 is rutile. Secondary growth of muscovite has been observed throughout the thin section. This sample is a fluid pathway from the footwall to the Middlevlei Reef. (Driefontein gold mine)

Stage 3: Brittle fracturing: This stage is characterised by sub horizontal fractures, that have been observed in Reefs the footwall below the reef in and along reef contacts, filled with uraninite, hydrocarbon, quartz, kaolinite, pyrite, pyrrhotite, gersdorffite, arsenopyrite, galena and gold in close proximity to the phylonites.

During this stage uraninite crystallization postdates phyllosilicate formation and fills fractures associated with carbon. See Fig. 3.11 to Fig. 3.17

Stage 4: Post vein fracturing: Post-mineralization events include localised fracturing, veining and shearing and pressure solution which vary in intensity across the basin. Figures 3.8-10 give some detail on the mineral character during the last stage. The minerals are all formed during the last stage and are all unaltered and not deformed.

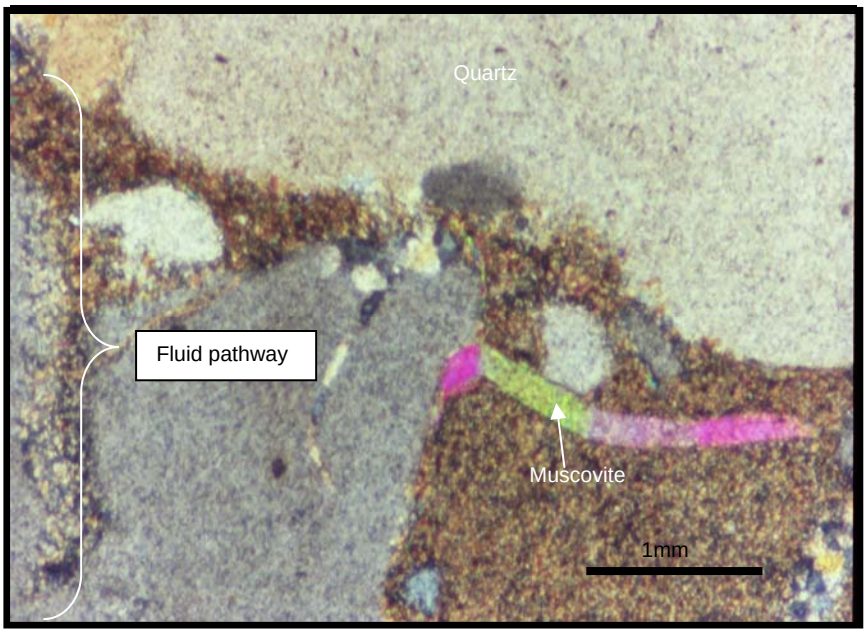

Fig. 3.8 Muscovite within a phyllonite zone indicative of secondary growth(DGM).

In Fig. 3.8 an elongated muscovite mineral is embedded in the brown mass defining the fluid pathway. The minerals are an indicator of the metamorphic changes that took place in these fluid pathways. The specific temperature and pressure can be determined from this mineral.

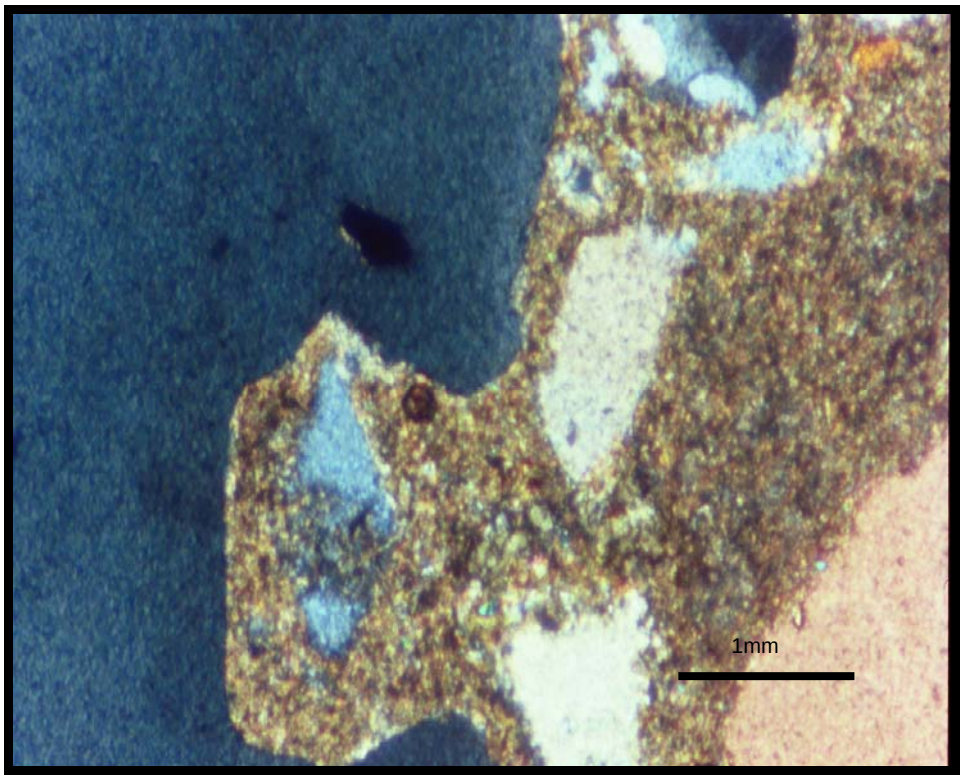

Fig. 3.9 Embayed outline of recrystallized quartz caused by dissolution by acidic fluids that moved through the phylonite zone. (Sample ZW 744) (DGM).

The acidity of fluids in the fluid pathway (Barnicoat et al., 1997) is seen in the effect it has in dissolving the edges of the quartz grain and also in forming jagged edges along the grain, in the centre and at the bottom middle of view.

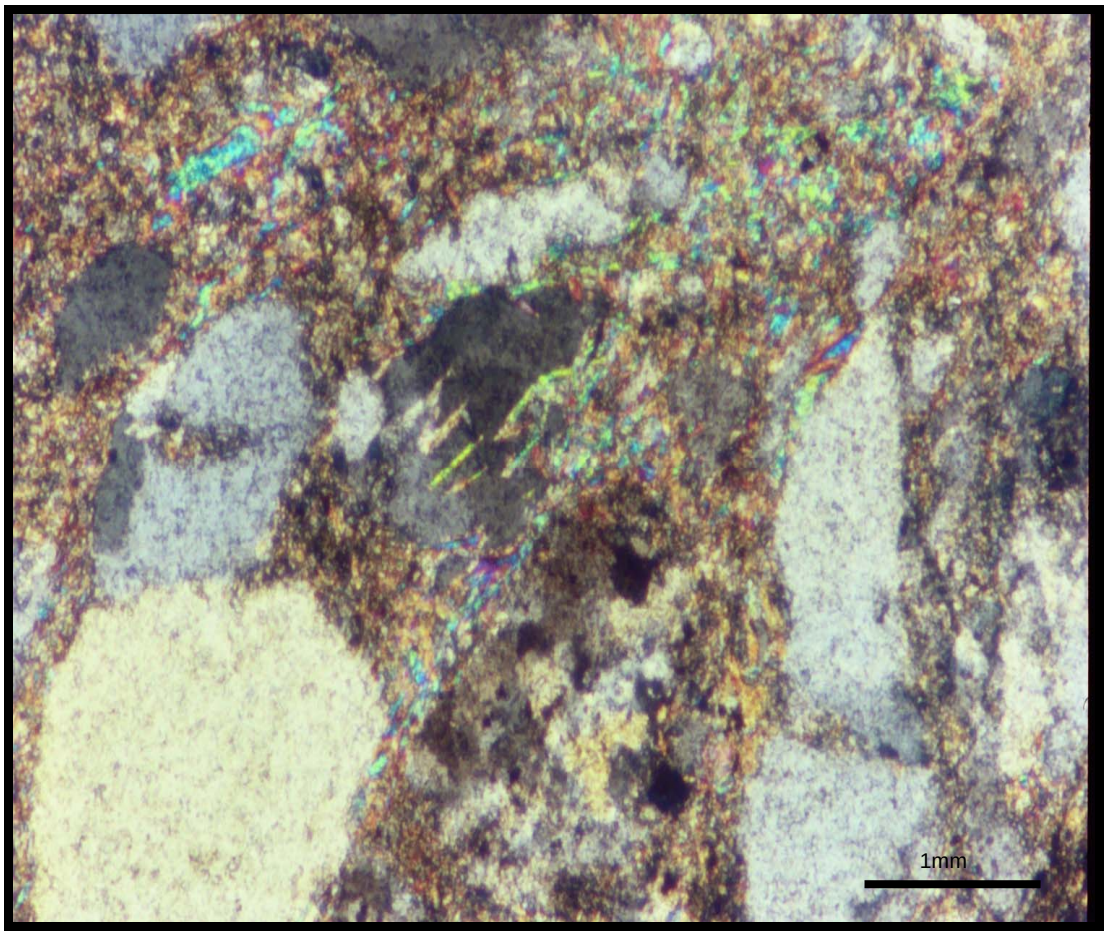

Fig. 3.10 Muscovite on the boundary of a phylonite zone indicative of secondary growth (Sample ZW745) (DGM).

3.5 The mineral associations within the fluid pathways under the SEM

The results of the SEM study on fluid pathways are extremely important as it reflects sub microscopic events, along small micrometer fluid pathways. It is analogous to what happened on the macro-scale above, below and within reef horizons.

Areas of extreme high grade to very low grade reef horizons including foot wall and hanging wall of most of the reef horizons, were chosen for study. The following figures below illustrate the sub-horizontal to horizontal fractures becoming fluid pathways within the conglomeratic reefs.

Figures 3.10 to 17 (Sample number RBB112228) illustrate the mineral signature of the fluid pathways under the electron microscope. This scale

opens the way to interpretation on the mineral faces within the fluid pathways; and many of these pathways reveal the paragenetic sequence of events.

A summary of the mineral associations in the fluid pathways is illustrated in Table 3.1

Table 3.1 Mineral associations and relevant figure number.

MINERAL ASSOCIATIONS	FIGURE
U- CARBON	3.11,3.22
U-PYROPHYLLITE	3.11
U-PYRITE	3.14,3.15,3.17
Au-PYRITE	3.20,3.21
Au-CARBON	3.18,3.19,3.21
Au-C-U-PbS	3.23
C-Au-Ta	3.25,3.26
Ca –CARBON	3.12B
Ta- CARBON	3.24

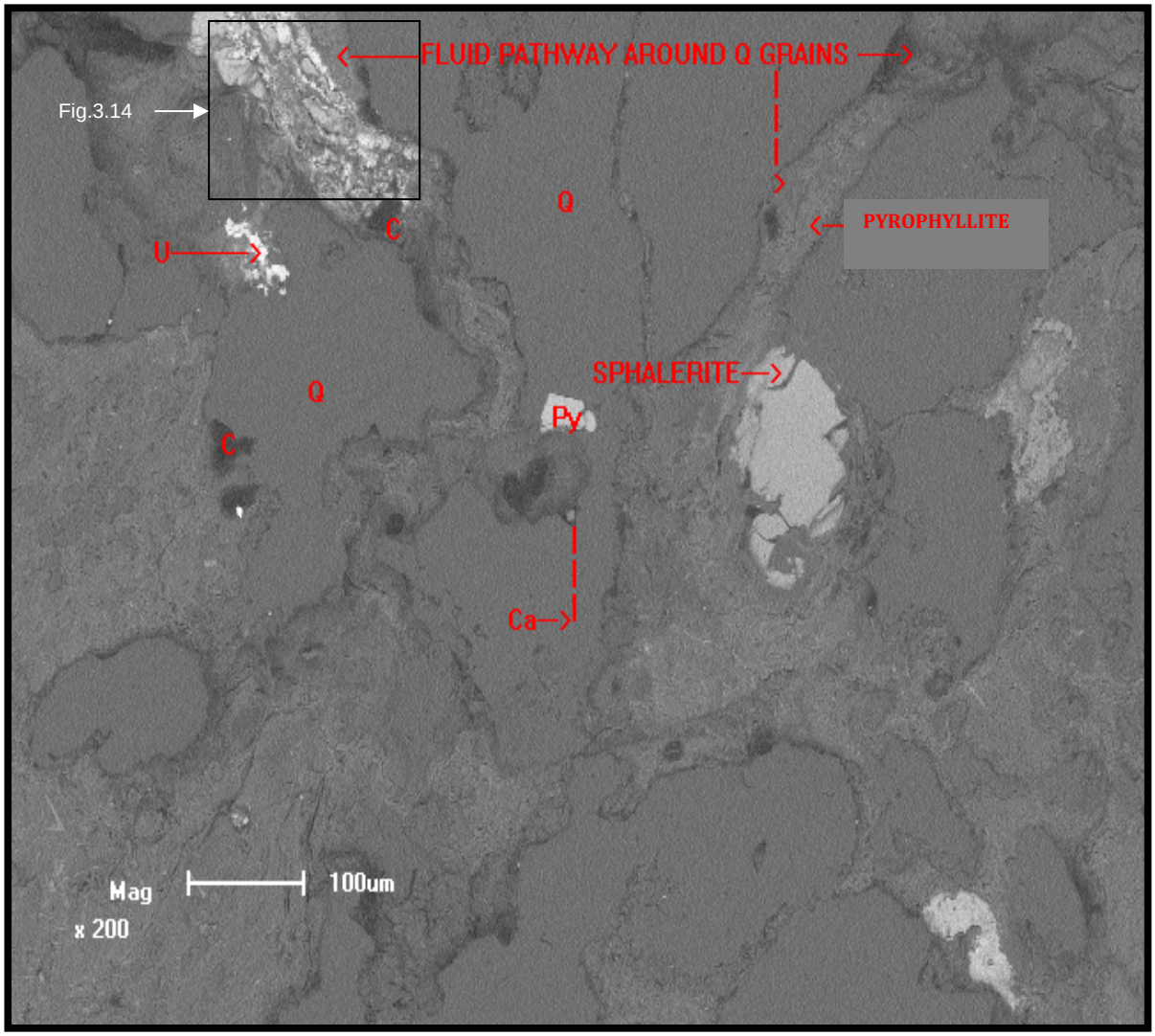

Fig. 3.11 This is a sample of the Basal Reef Western Holdings Mine (RBB 112228) note the fluid pathway around the Q grains .

Abbreviations : Py =Pyrite, Ca =Calcite ,C=carbon,U=Uraninite

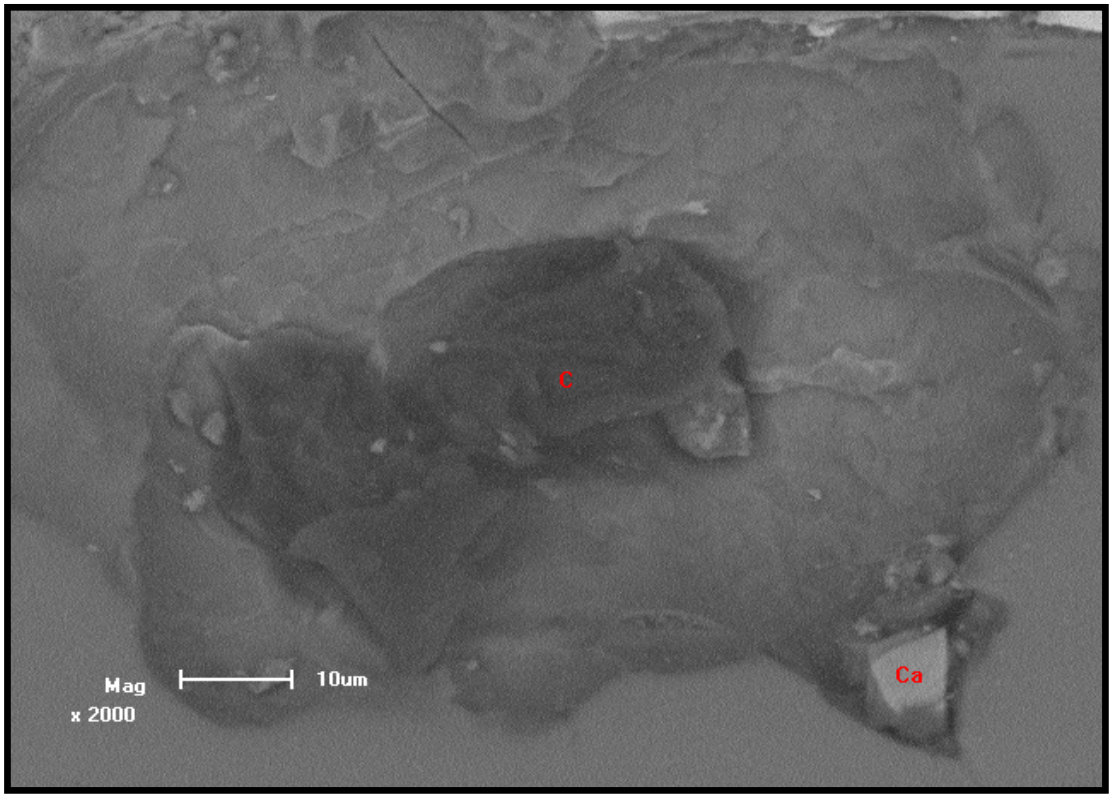

Fig. 3.12a This is a sample of the Basal Reef Western Holdings Mine (RBB 112228) Note the calcite and carbon in contact with each other.

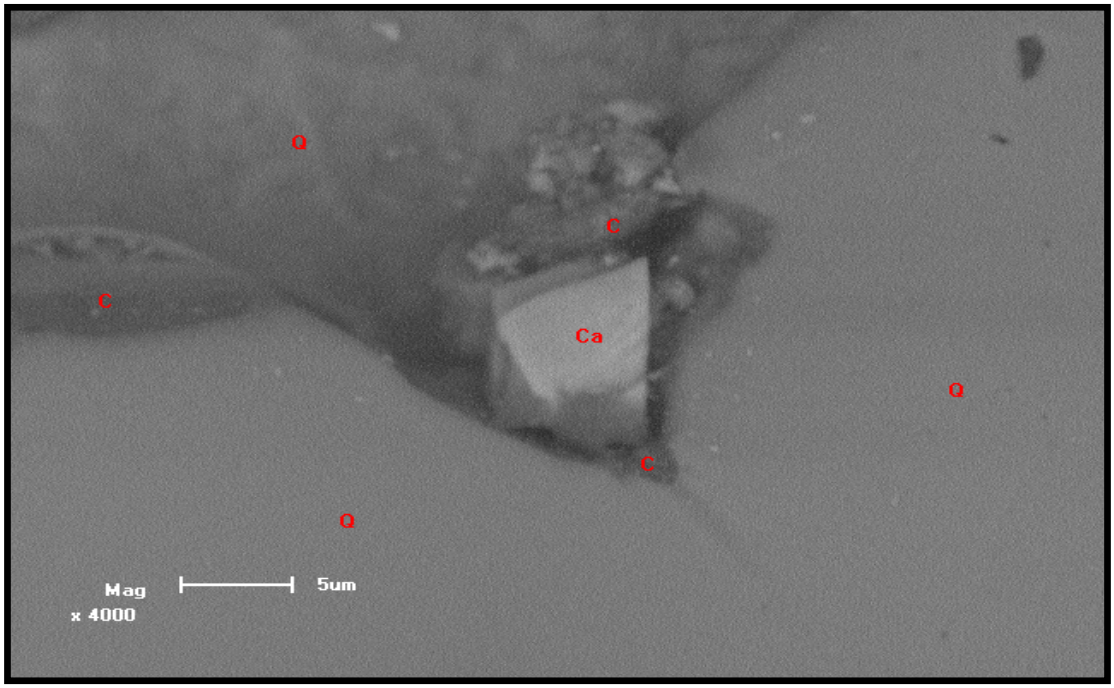

Fig. 4.12b This is a sample of the Basal Reef Western Holdings Mine (RBB 112228) Note the calcite (Ca) crystal in an open space between carbon (C) and quartz (Q).

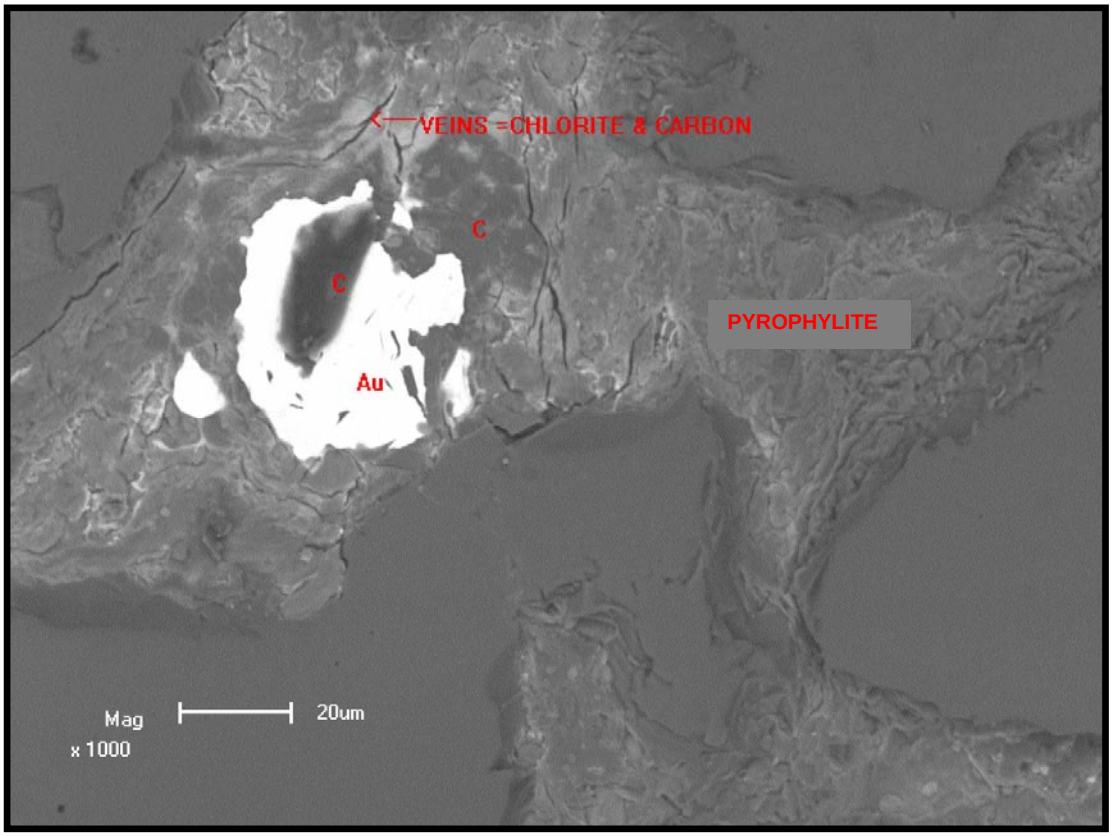

Fig. 3.13 This is a sample of the Basal Reef Western Holdings Mine (RBB 112228). Note the gold nugget within the pyrophyllite rich fluid pathway. The Au-C's are inclusions in the fluid pathway. The Au and C came into the basin at the same time.

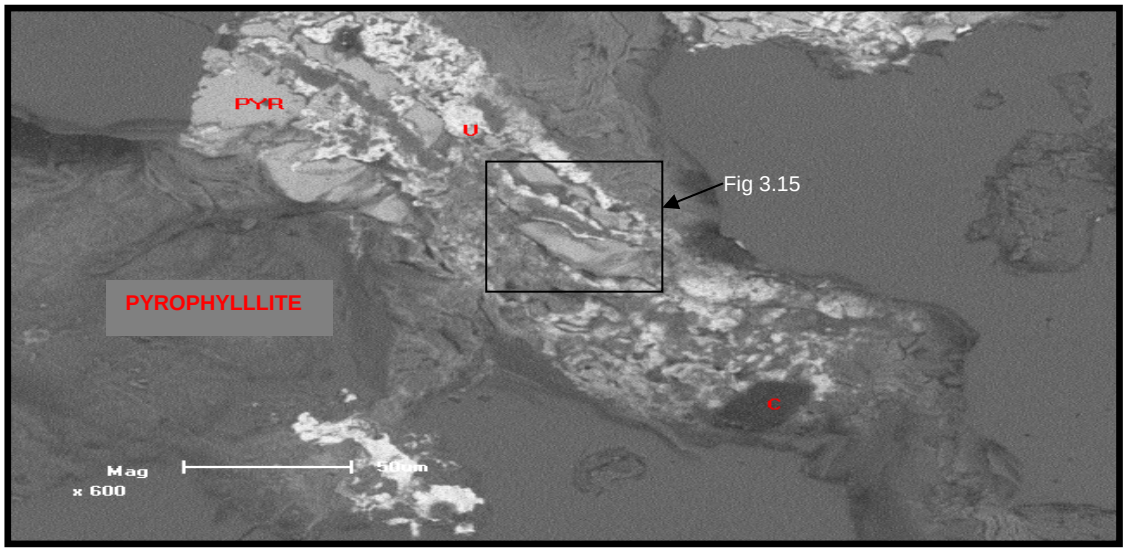

Fig. 3.14 This is a sample of the Basal Reef Western Holdings Mine (RBB 112228). Note the white reflectance inside the fluid pathway is uraninite.

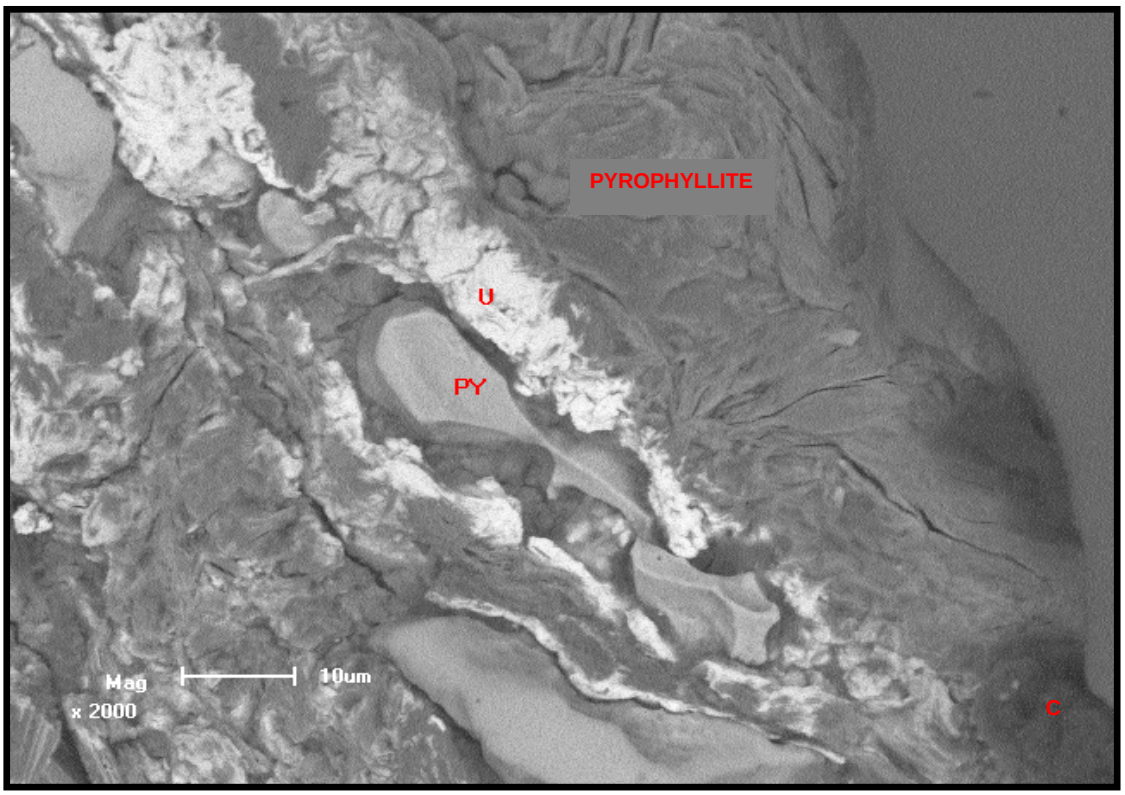

Fig. 3.15 This is a sample of the Basal Reef Western Holdings Mine (RBB 112228). Note the occurrence uraninite and pyrite within the Type 3 fluid pathway define by pyrophyllite.

The two minerals (U,Py) in Fig. 3.15 are in the same fluid pathway and close to it is gold .(See Fig. 3.11) The pyrophyllite is replaced by uraninite and pyrite is precipitated in the fluid pathway. This is not a polished sample but a fresh surface therefore giving the 3-D effect. The detail nature of the shape of pyrite and contact relationships with pyrophyllite is hown in Fig.3.16.

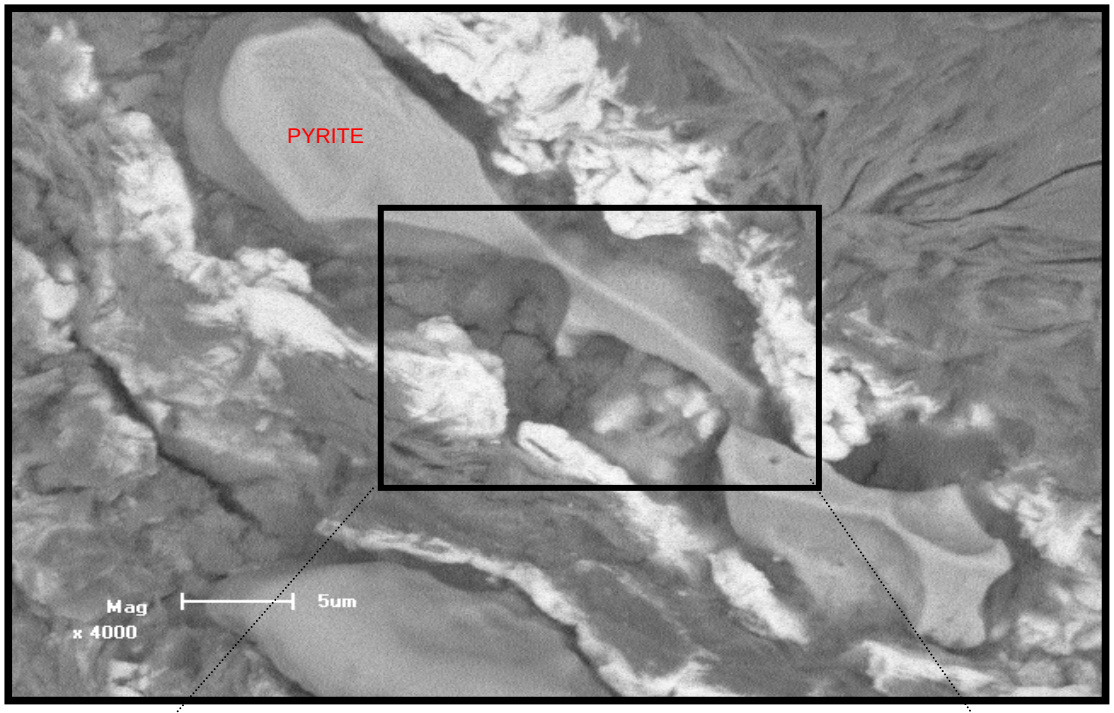

Fig. 3.16 This is a sample of the Basal Reef Western Holdings Mine (RBB 112228).Note the pyrite is embedded in carbon and quartz. The pyrite is a vein filling and no typical cubic crystals present in this view.

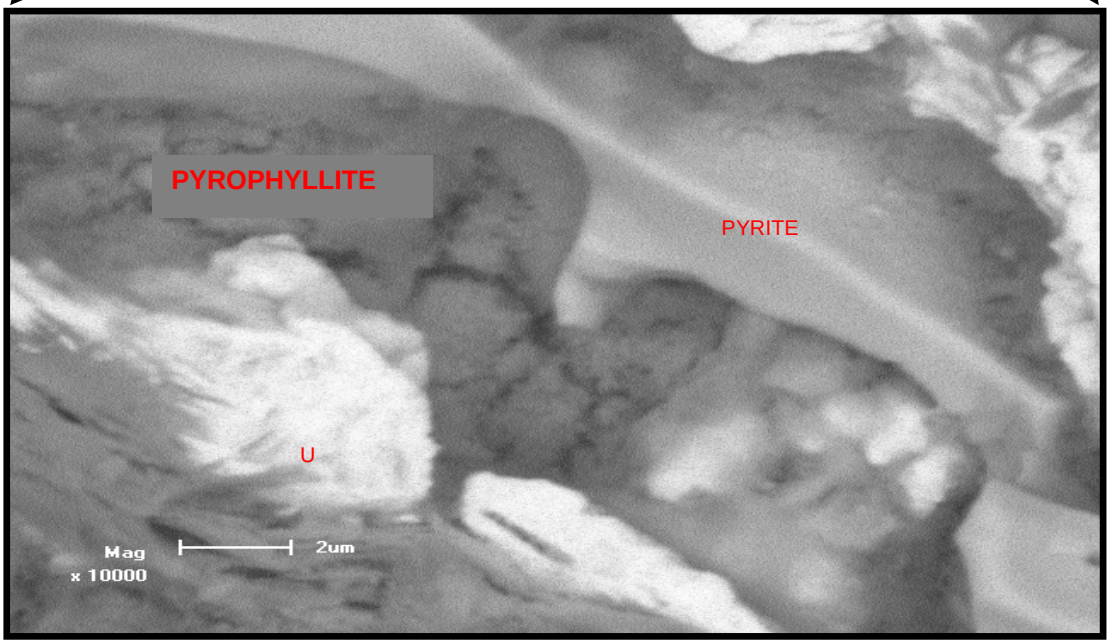

Fig. 3.17 This is a sample of the Basal Reef Western Holdings Mine (RBB 112228).This indicates the sequence of crystallization of different minerals within the fluid path way.

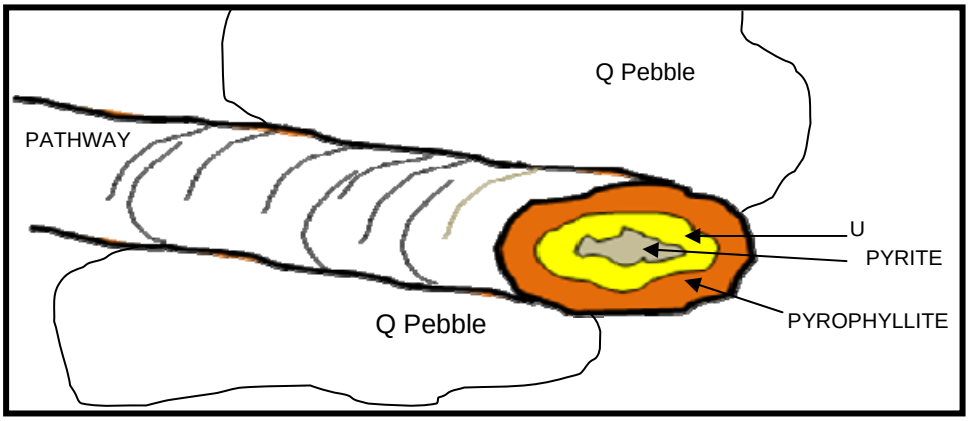

Fig. 3.17a Three dimensional view of a fluid pathway ref. Fig. 3.15&3.17.

The SEM analysis showed new mineral associations which have not been documented in the literature nor been photographed before. The mineral phases are shown in three dimensions. The pyrite in the centre fills the space in the vein. The shape of the pyrite in Fig.3.16 resembles the space it filled. The uraninite replaces the pyrophyllite from the inside of the vein. The uranite came in with the pyrite into the vein at the same time.

3.6 Detailed observations of carbon and gold under the microscope and SEM

The association of carbon and gold in the fluid pathways suggests that there is a strong relationship with each other and the mineralised fluid. Carbon and gold occur in close proximity to each other.Gold also occurs as inclusions in carbon. Gold has been observed as a vein in quartzite (Fig. 3.18,19).

The next example is where the gold has precipitated in the quartz matrix between quartz pebbles (Fig. 3.20).

The VCR sample (Fig. 3.21) shows gold imbedded in chlorite and quartz, with minor carbon nodules present in close proximity to the gold nuggets. The carbon from this sample has been scanned under the SEM and shows the carbon nodule contains at least 5% of uraninite (Fig. 3.22).

The mineral association in Fig. 3.23 are gold, uranium, carbon and lead sulphide (Au-U-C and PbS).

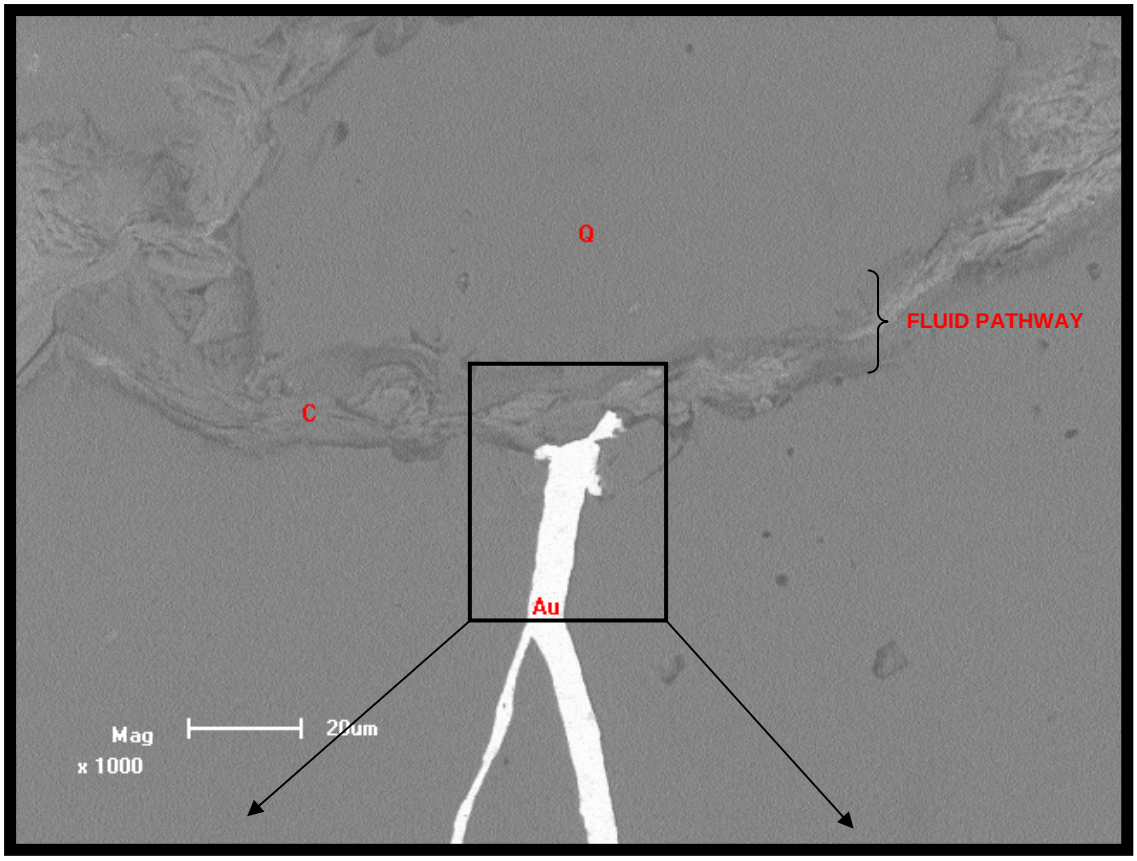

Fig. 3.18 This is a sample of the Basal Reef Western Holdings Mine (RBB 112228). Note the fluid pathway is filled with carbon and the gold in fracture originating from the fluid pathway.

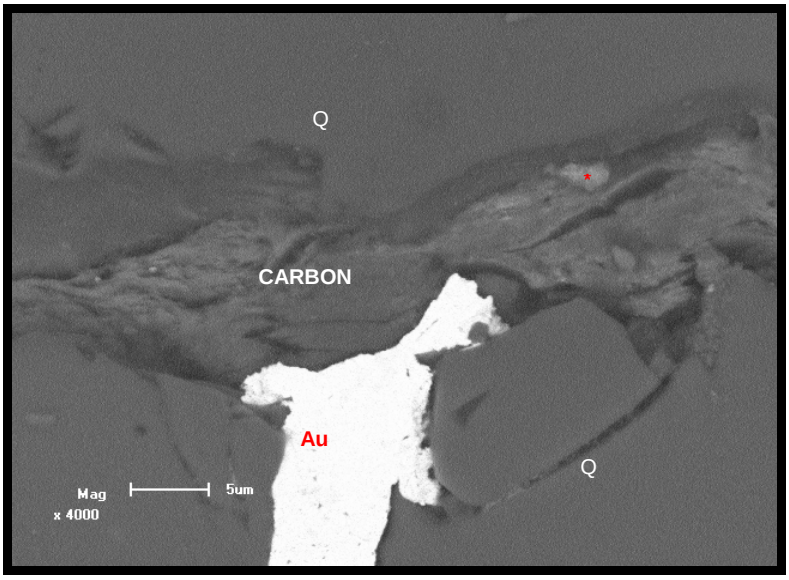

Fig. 3.19 This is a sample of the Basal Reef Western Holdings Mine (RBB 112228. Note the fluid pathway is filled with carbon and the gold in fracture originating from the fluid pathway.

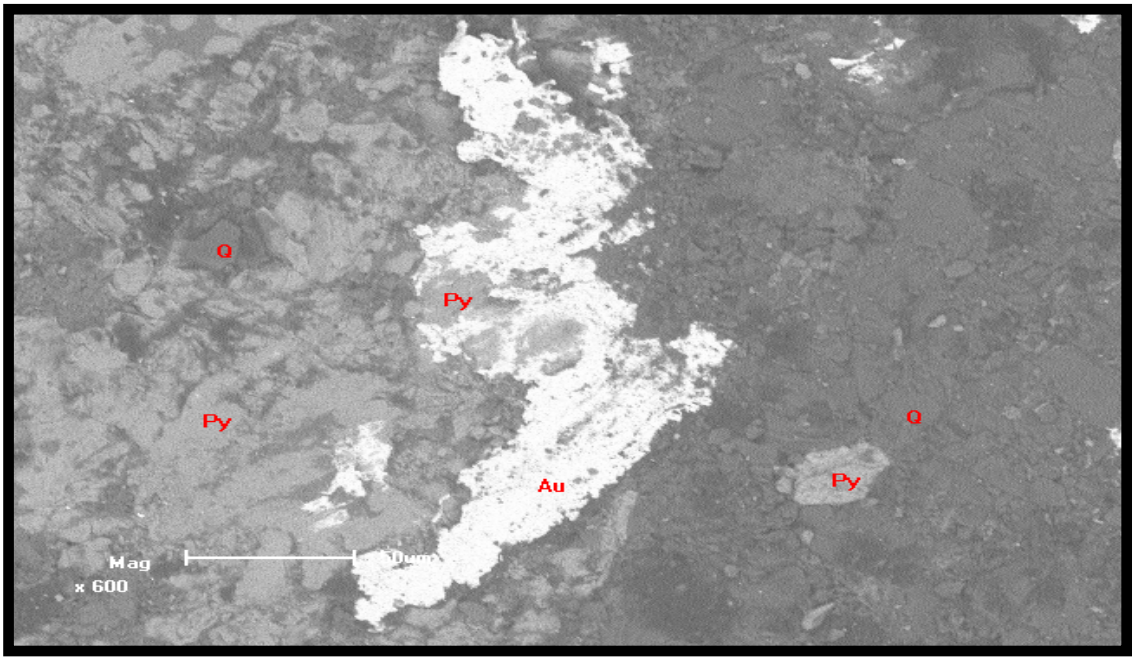

Fig. 3.20 This is a sample of the VCR DGM mine gold in the matrix between quartz and pyrite in the conglomerate. (Sample 2036).

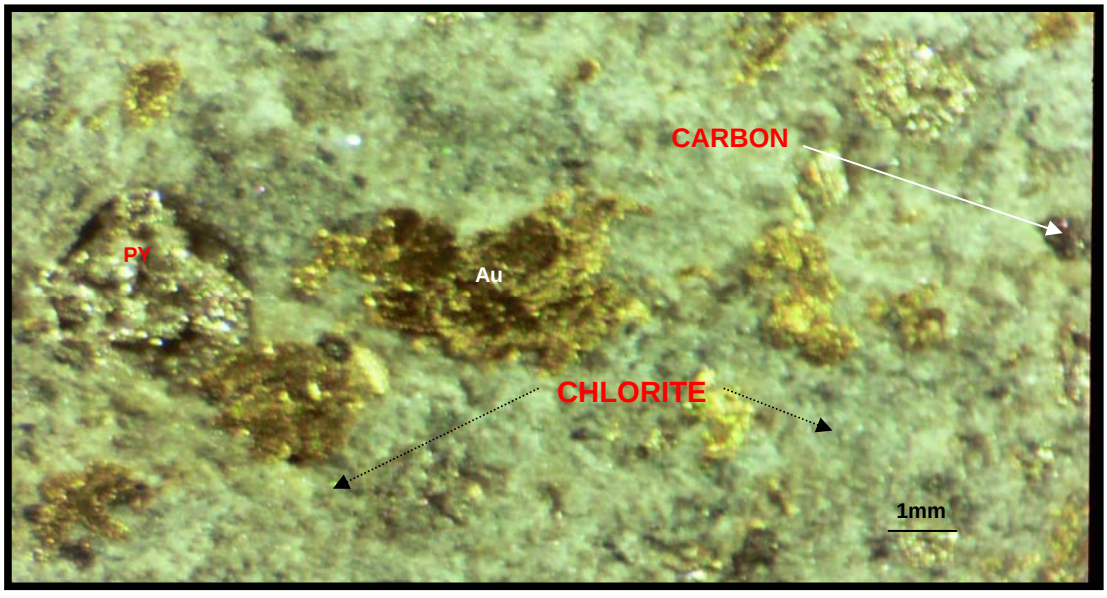

Fig. 3.21 This is a sample of the VCR DGM Mine (sample 2036). The gold and carbon occurs in foliated matrix of quartz and chlorite.

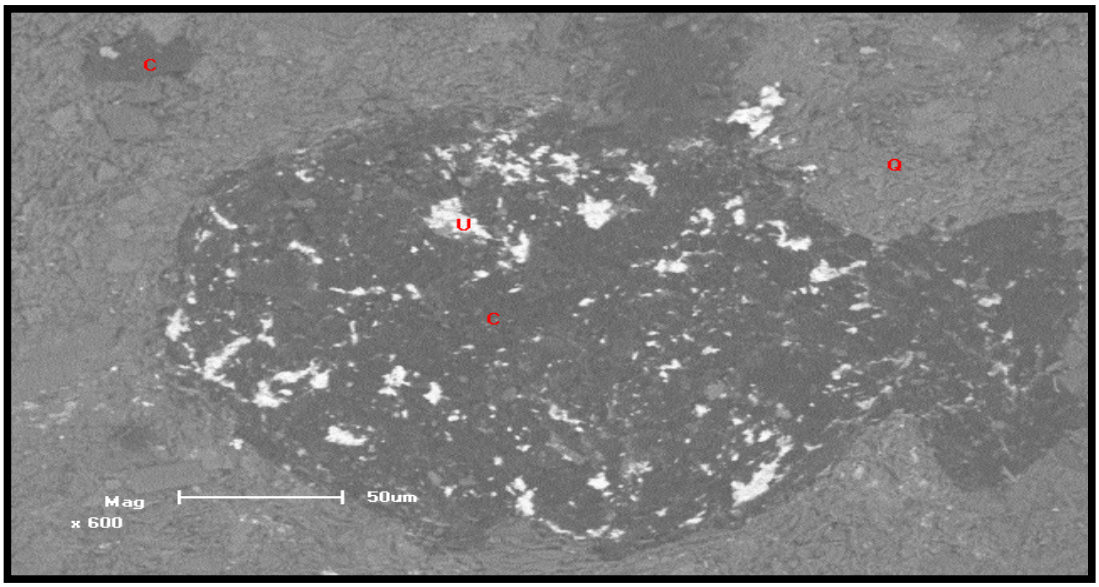

Fig. 3.22 Close view of the carbon in Fig. 3.21(VCR DGM Mine (sample 2036). Uraninite intergrown with carbon.

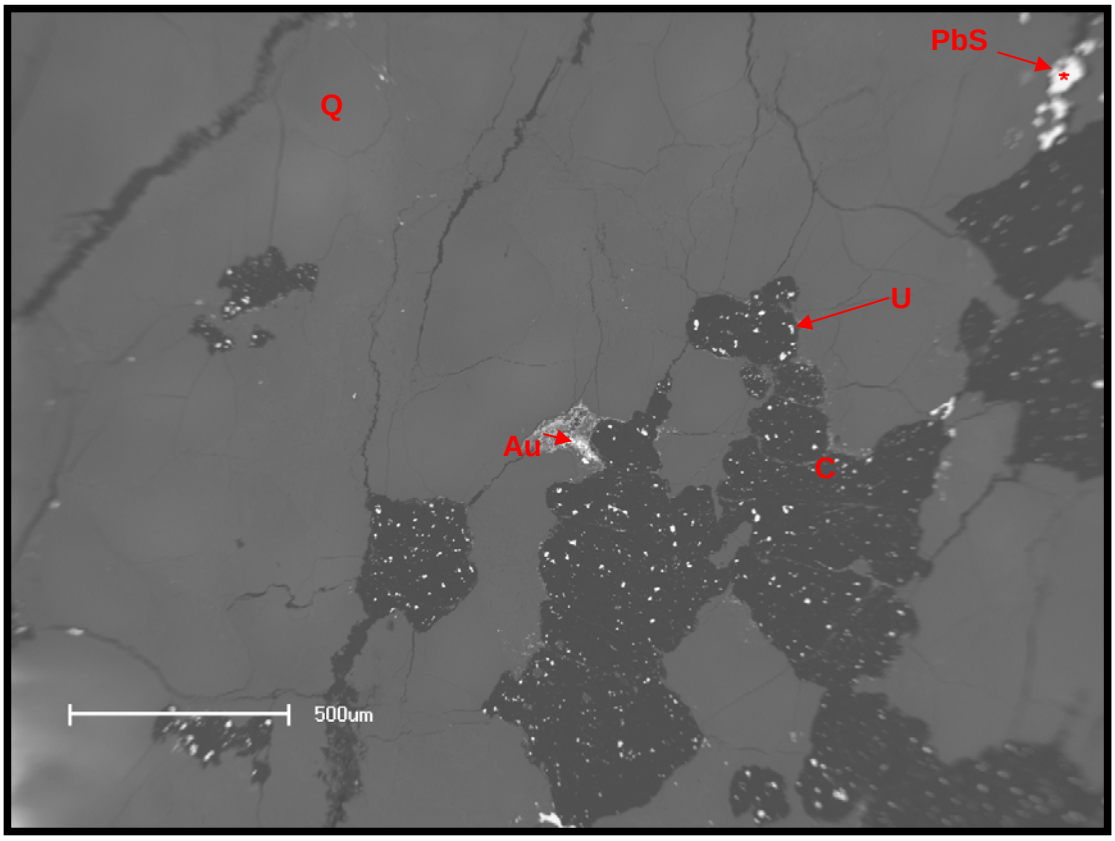

Fig. 3.23 This is a sample of the Basal reef WGM 3741 raise line. Note the gold, carbon, uraninite and galena (PbS) association.

3.7 The electron images of TaSiO2

Tantalum has been detected in the carbon seams collected from Western holdings Gold Mine (WHGM) from the Free State. The emissions recorded by the SEM are listed in the table in the appendices.

The location of the tantalum is from the cracks within the carbon seam. The visual image of tantalum silicate is from the same carbon seams as what were used for the research done at the university of Johannesburg in 1998.The emissions of Ta was extremely high and this came from three different samples.

Tantalum silicate is the catalyst to dehydrate the carbonaceous gas. The reaction leads to the precipitation of carbon as drops of carbon fluid. The drops on top of one another forms the carbon spindles on the contact and within faults and within the conglomerates.

In Fig.3.24 one can see the TaSiO2 associated with the carbon. Fig.3.25 is the backscatter image of Ta. The graph in Fig. 3.26 proves the existence of Ta.

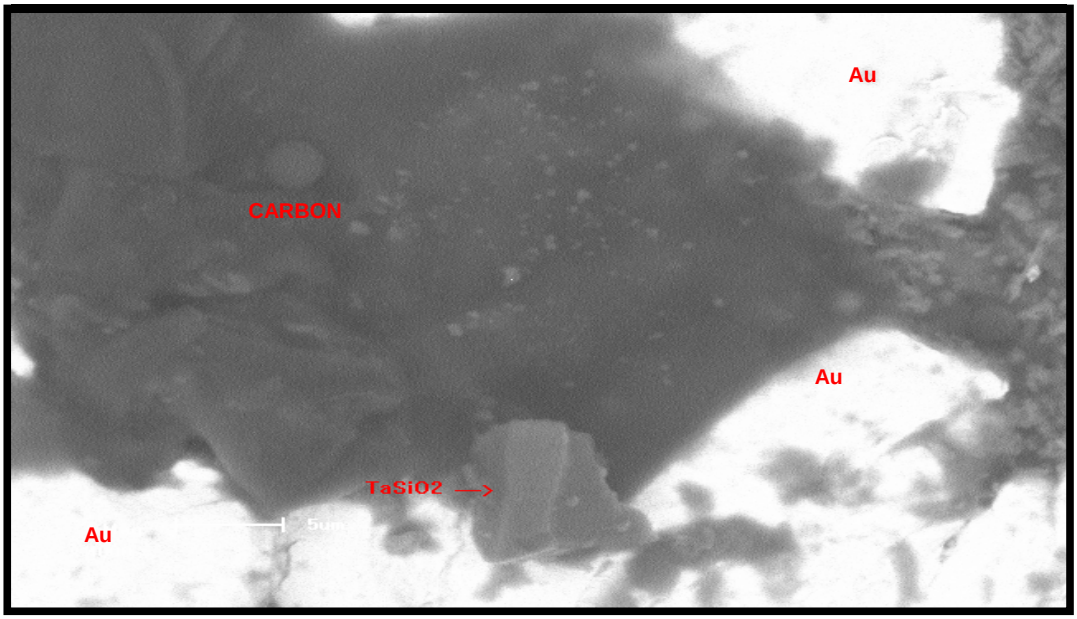

Fig. 3.24 This sample is from the Western Holdings 2# pillar note the Ta in the centre of the photo.

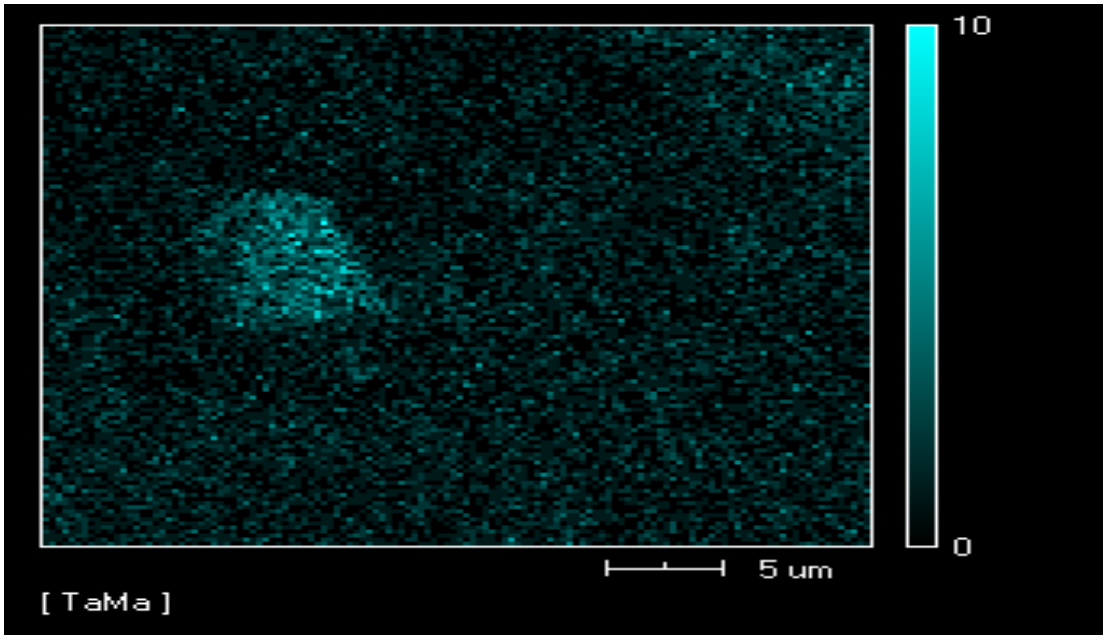

Fig. 3.25 This is a backscatter image of the sample above indicating the Tantalum content in the view.

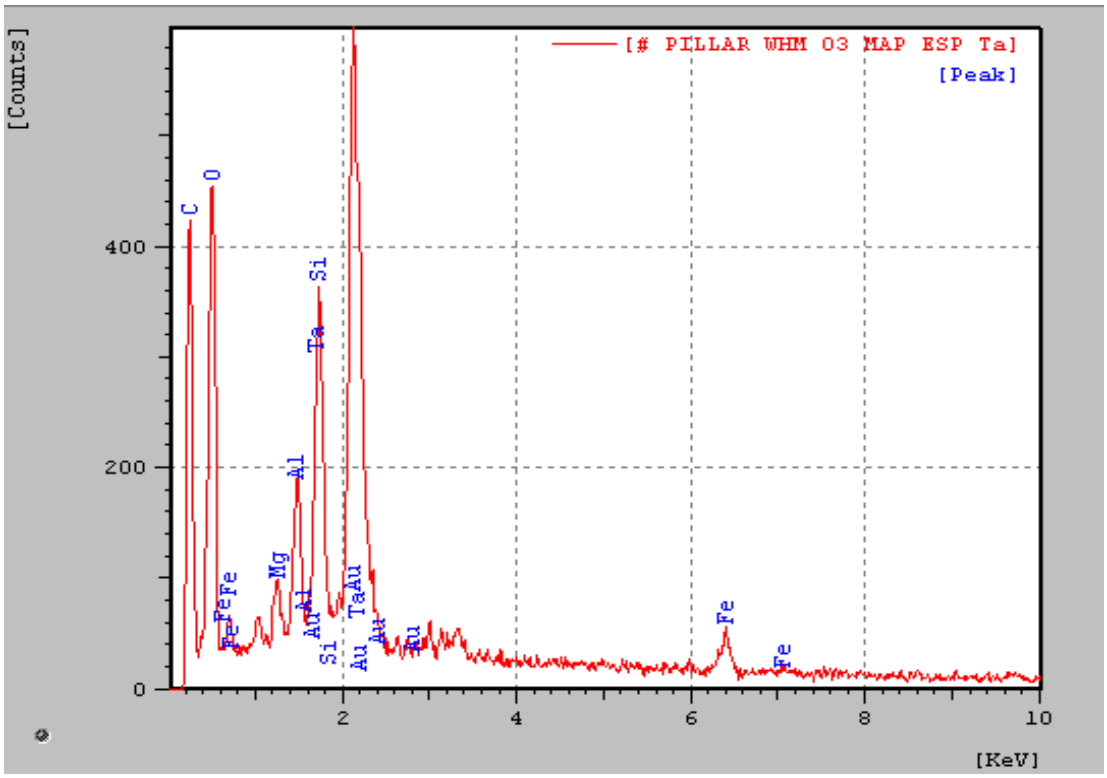

Fig. 3.26 This is a graph of the sample above indicating the Tantalum content in the view.

3.8 Carbon spindles and the close relationship of carbon gold and uranium

The carbon nodule in Fig. 3.27 is situated in a Type 3 Fluid pathway in pyrophyllite and is rimmed with gold. Uraninite is enclosed in the carbon matrix of this nodule.

This occurrence of carbon, gold and uranium is very unique in that the carbon and the other two elements are genetically closely associated with each other.

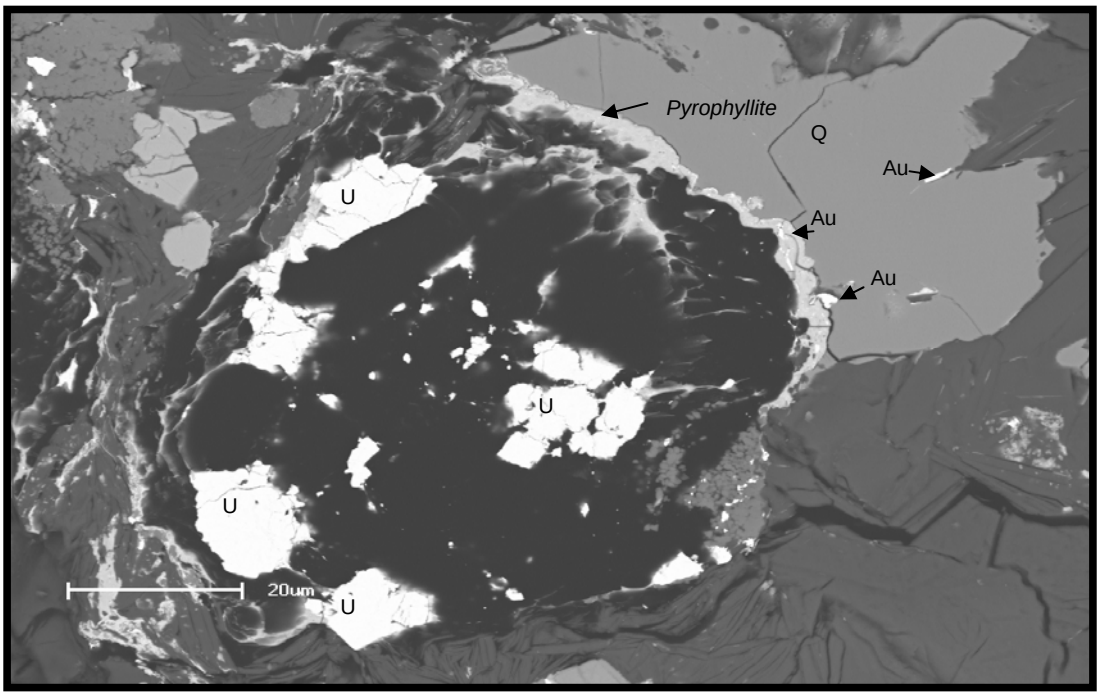

Fig. 3.27 This sample of the basal reef from the Western Holdings 2# pillar grade 13kg/t. Carbon nodule with inclusions of U_3O_8

3.9 Summary

Petrographic observations showed that minerals were precipitated in fluid pathways. The fluid pathways are interali a shear fabrics formed during bedding-parallel thrusting, of which these types were recognised - based upon the degree of strain, bedding parallel fractures in various lithologies, thrust and extensional faults, and sedimentological structures.

The SEM analysis showed new mineral associations which have not been documented in the literature before nor been photographed. The mineral phases are shown in three dimensions and the order of precipitation can be deduced within the pyrophyllite filled pathway which is the older metamorphic mineral, the precipitation of uraninite is taken place simultaneous with the precipitation of pyrite and gold and carbon are precipitated together in the same sample but in different fluid pathway.

The high grade gold samples and low grade sample differ in uraninite and tantalum content, but it is noted the uraninite content is the highest in the high grade gold samples. The element tantalum is also prominent in one of the high grade samples. The most prominent metamorphic mineral in the fluid pathways within the matrix of the various reefs is pyrophyllite.

A three dimensional diagram depicts the order of precipitation in the fluid pathways. The carbon is emplaced within the pyrophyllite defining the fluid pathway. The uraninite replaced the pyrophyllite and the pyrite has been crystallized in the fracture within the pyrophyllite and exhibits the shape of the area in which it has been crystallized.Uraninite also occurs as inclusions within carbon.

It is concluded that the three main minerals carbon, uranium and gold were all contained in the same gas/fluid that entered the basin. The microstructure indicates the sequence of events and the timing of the different events as discussed above.

From the literature it is suggested that the date for uraninite and pyrite is 3.5Ga - 2.9Ga. Pyrite from the Vaal Reef dated at 2.99Ga and gold dated at 3.5Ga-2.9Ga. Carbon is dated at 2.3Ga.

CHAPTER 4

STRUCTURAL-STRATIGRAPHIC CONTROLS ON CARBON IN THE WITWATERSRAND BASIN

4.1 Introduction

In this chapter the aim is to present observations on the controls of the deposition of carbon and to integrate the microscopic observations made previously (Chapter 3). The origin of carbon is not explained by the theories nor the models in the literature. To a certain degree all the research work done to date by scientists are indicative of fluids and fluid migration as to the origin of carbon.

4.2 Sedimentological control on the distribution of carbon

4.2.1 Case study Vaal Reefs Mine (Kopanang shaft) Fig. 1.2

The control on carbon emplacement by the physical character of the different stratigraphic units has been observed underground and the lithostratigraphic features of the Vaal Reef and the Kalkoenkrans Reef have been highlighted by a compilation of the footwall topography of both reef horizons. The footwall topography of the Vaal Reef is shown in Fig. 4.1a. This model was created from drilling data points. The topography resembles the floor of an ancient sea bed with channels and dunes (fine grained siliceous quartzite- wind blown remnant) that had a big influence on the depositional character of the Vaal Reef (Bailey et al., 1990). The heavier sediments were deposited into the channels in the low lying areas in between the dunes. This physical

characteristic of the Vaal Reef was the key to the control on the carbon emplacement. The physical attributes of the host rock, in this case the footwall quartzite below the conglomerate, controlled the emplacement depositional pattern of carbon seams Fig.4.1b. It was observed that the quartzite type, an argillaceous quartzite, had more permeability and exhibited more fracturing than the siliceous quartzite. The siliceous quartzite formed the cap of the dunes and the argillaceous quartzite was observed in the low lying areas. The carbon was observed in the low lying areas where the larger pebble conglomerates were deposited. Thus it can be deduced that the permeability potential of the conglomerates in the low lying areas was the highest and the conglomerates on high lying areas had the lowest permeability potential.

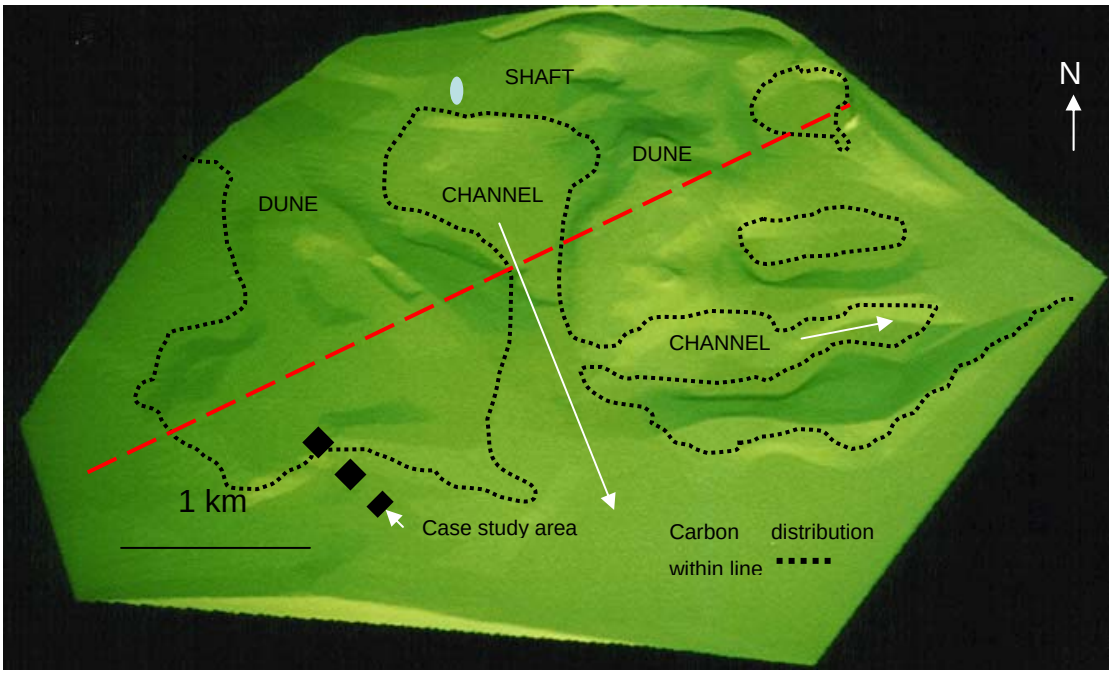

Fig.4.1a The depositional model using drilling data at Vaal Reefs Mine. It represents a shallow marine environment for the Vaal Reef at Vaal Reef Mine. The channels of argillaceous quartzite are filled with conglomerate. Carbon is deposited along the argillaceous quartzite and the conglomerate below. Section line in red (Fig.4.14b).

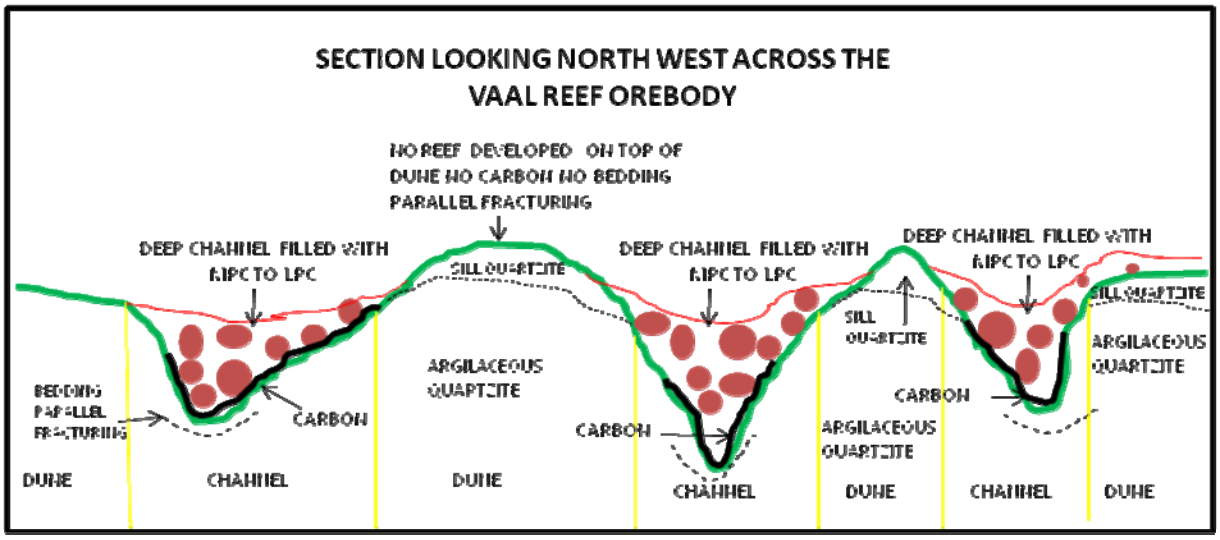

Fig.4.1b The section across the depositional model of the Vaal Reef (Kopanang Shaft)

One specific area was selected (see Fig.2.26) to show the sedimentological observations mentioned above. (Author's own underground observations). The carbon was in most cases deposited at the intersection of fluid pathways and the reef. The carbon is the thickest where the pebbles are the largest.

The mapping of the carbon emplacement for this particular area was done in detail at 70 sw1 17 raise and 59 dw2 10 x/c (Fig.2.26). The columnar carbon varied in thickness from 1mm to 10mm and contained visible gold along the filaments. The controls on the carbon emplacement were the physical properties of stratigraphic sequences and the structural permeability potential of the Vaal Reef conglomerate.

The carbon distribution corresponds well with the type of footwall and the amount of fluid pathways within the footwall type. The low lying areas are characterized by the argillaceous footwall quartzite with abundant phylonites and fluid pathways. The high lying areas are areas, which could not be eroded and formed the crest of the dunes. These zones are characterized by a siliceous quartzite with no fluid pathways present in the zone. The conglomerate on top of this zone is thin bedded to a single pebble lag. This indicates that the carbonaceous fluids were precipitated along the most permeable layers, within multiple bedding parallel fractures in thy footwall Mb5

q and the more fractured conglomerate. Several thrust faults are interlinked by fluid pathways as seen in Fig. 2.26. The observations include the following. The ramps or fractures are called fluid pathways and they are labeled according to the degree in which the minerals are orientated along the bedding planes.

4.2.2 The Free State gold fields Beatrix 4# Case study

The case study on Beatrix 4# involves the Kalkoenkrans Reef (Fig. 4.2)

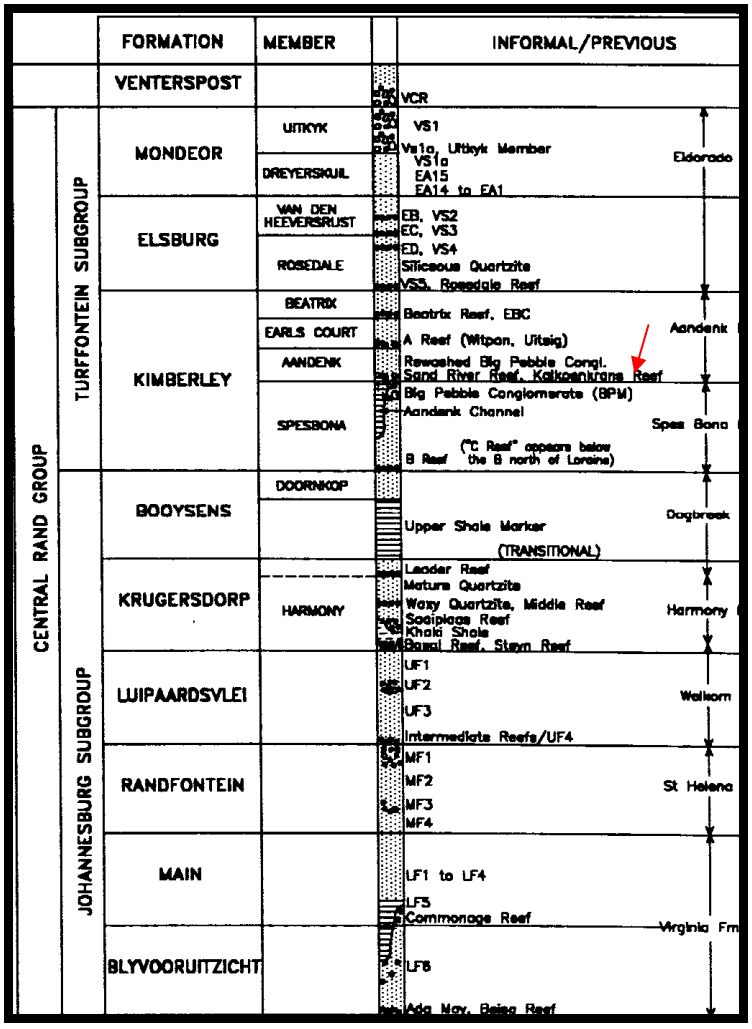

Fig.4.2 The stratigraphic column of the of the Free State goldfield with the Kalkoenkrans reef indicated with red arrow.

The model in Fig. 4.15 indicates the same pothole system as observed on the Vaal Reef. The potholes are smaller but much deeper in the vertical dimension. The potholes are filled with cobbles and pebbles of various sizes. Secondary permeability of the reef and the footwall controlled the emplacement of carbon. The type of footwall determines the % bedding parallel fracturing that is characteristic of the argillaceous quartzite.

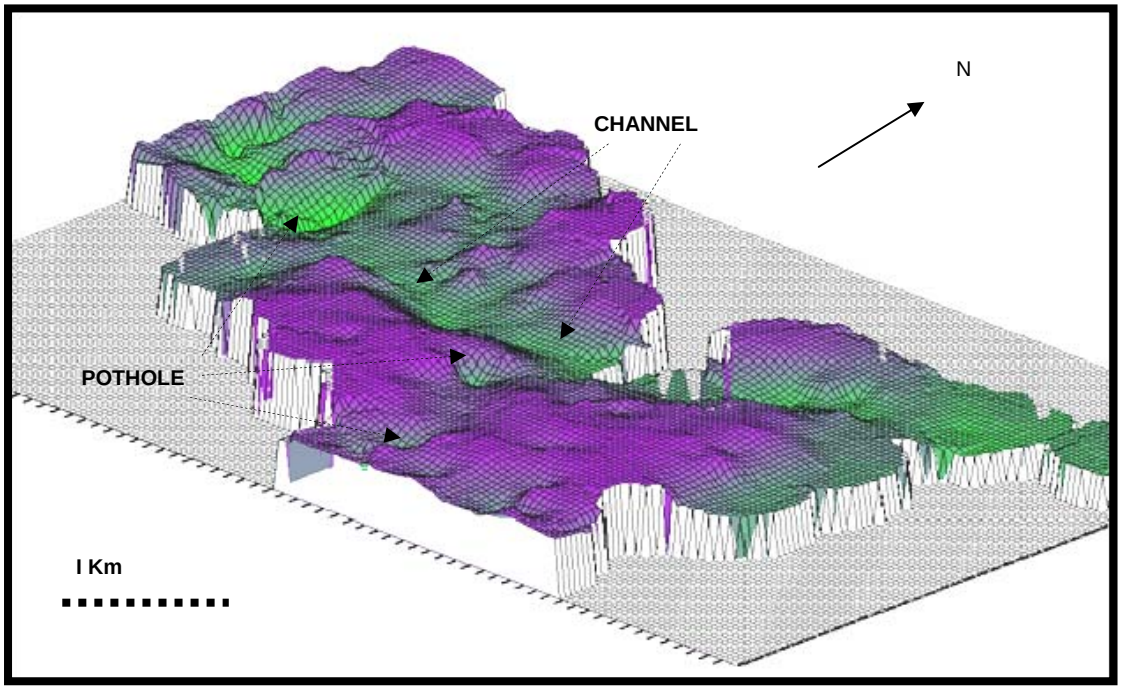

Fig. 4.3 The three dimensional footwall model for Beatrix 4 shaft. Carbon observed in the areas indicated by dark green colour. Note the potholes in channels.

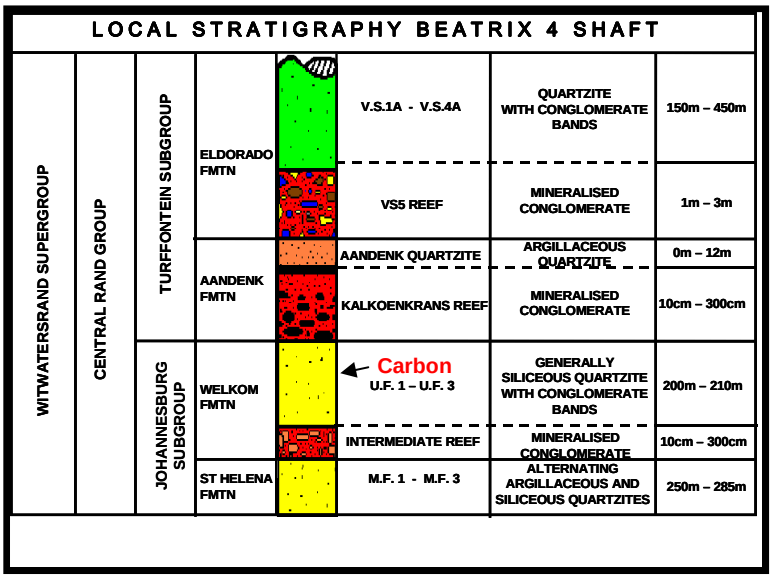

Fig. 4.4 The stratigraphic column for the southwestern gold field.

Various channels have been mapped and photos of the best exposed channels were chosen. The first Fig. 3.18 and 3.19 show the dimension of the reef package and show the carbon emplacement morphology.

The complete package is shown in Fig. 4.5 and the carbon seams are situated on the bottom contact of the Kalkoenkrans Reef and on the channel edge to the right of the photo.

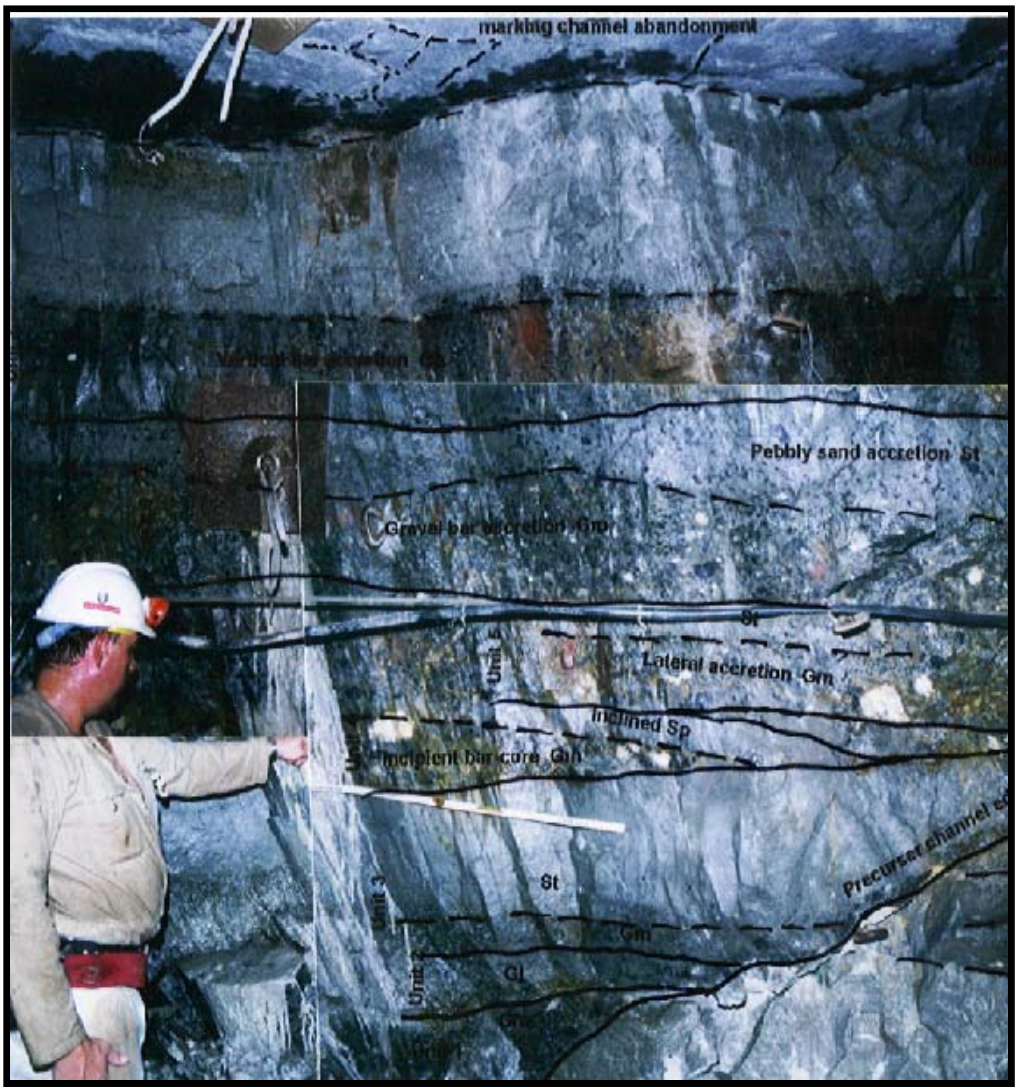

Fig. 4.5 The channel fill consists of various conglomerates of the Kalkoenkrans Reef with the channel edge to the right of the photo.

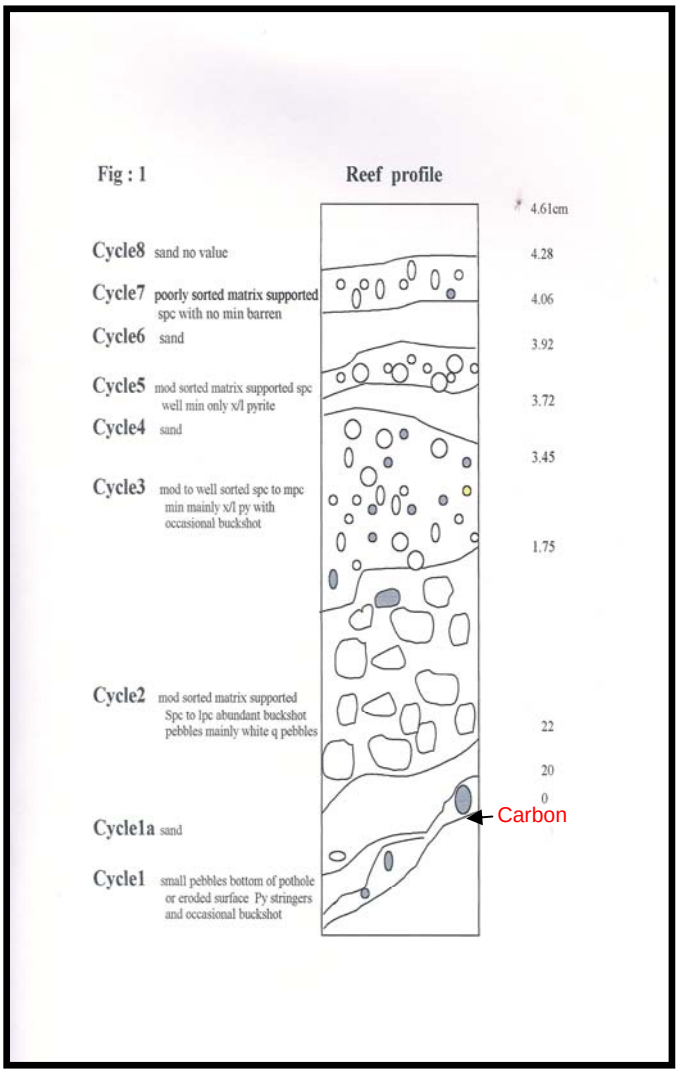

Fig. 4.6 The eight cycles that could be identified underground, see Fig.4.5 above.

The carbon observed underground is mainly localized within the thick conglomerate packages within the channels as depicted by the green colour in the model.

The carbon is situated at the bottom contact of the Kalkoenkrans reef conglomerate. The spatial distribution within this zone is not more than 5 meters on strike and dip and is concentrated along the contact.

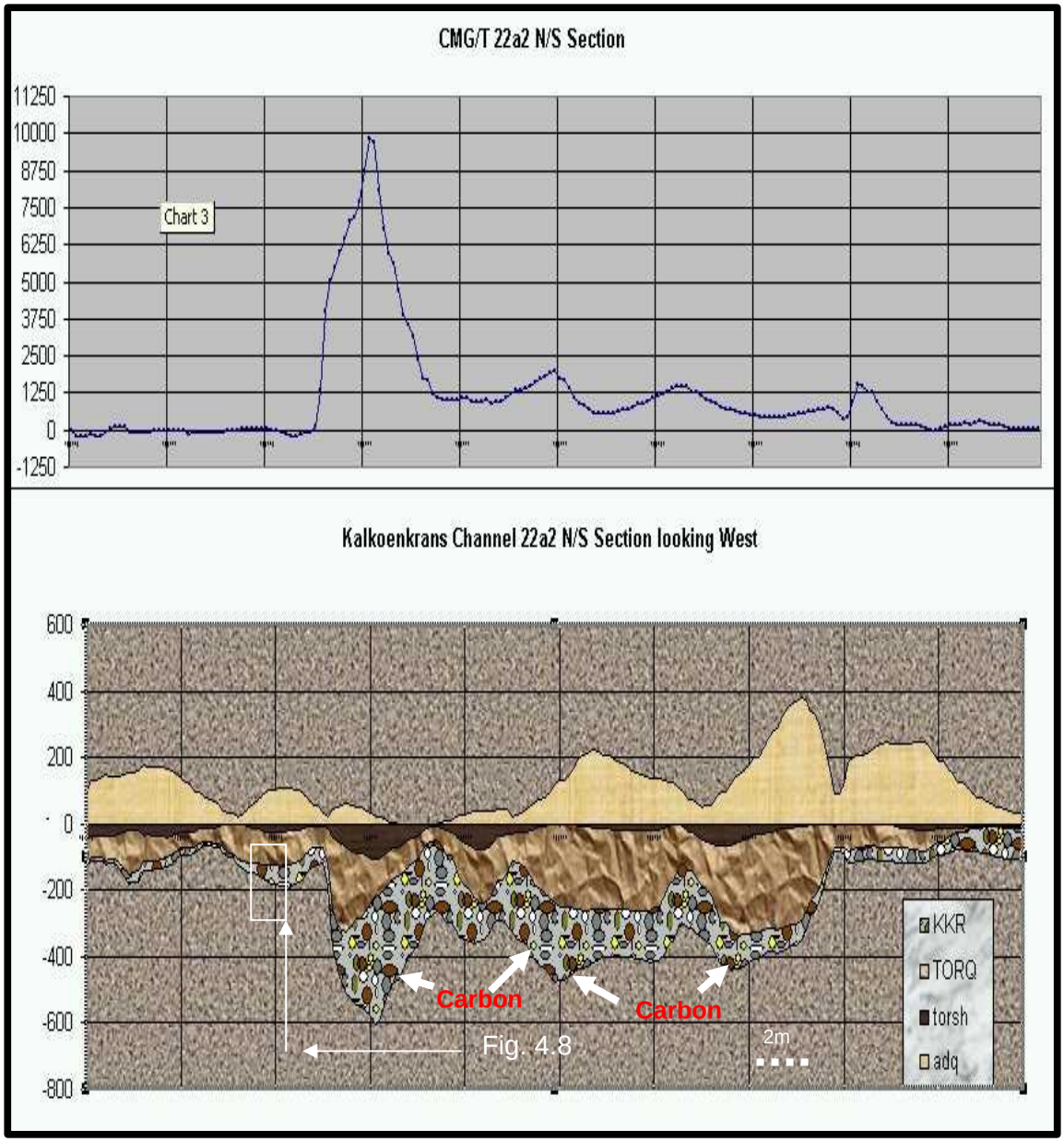

Fig. 4.7 The eight cycles that could be identified underground see photo above. See Fig.4.8 and Fig.4.20.

The carbon is concentrated at the bottom of the deep channel and the channel value reflects the close association of carbon and gold (Fig. 4.7). The edge is shown in Fig. 4.8. Microscopic scale will highlight the detail relationships within the reef package. Free gold is also abundant along the bottom edge of the conglomerate band.

Fig. 4.8 The pothole edge within one of these channels of the Kalkoenkrans Reef (see Fig. 4.3 and Fig 4.7).

The most westerly edge of this ore body together with the Beisa Reef has been overturned and is curved over the ore body edge. The carbon distribution along this edge is not high. The percentage carbon deeper down the slope towards the syncline increases substantially.

4.3 The structural control on Carbon distribution

The general characteristics of the regional structural controls on carbon in the Witwatersrand Basin are summarized as follows.

4.3.1 Bedding plane structures

Carbon seams are commonly associated with bedding parallel thrusts. These structures occur throughout the Central Rand Group and are shown in Fig. 4.21.

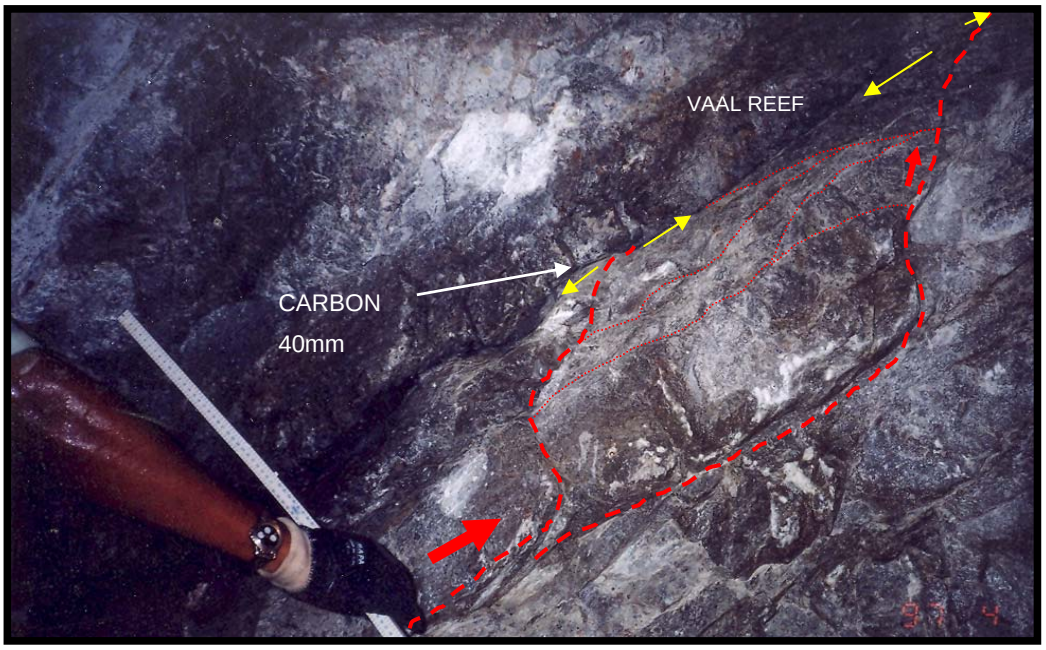

Fig. 4.9 Carbon development on the contact of the Vaal Reef on both sides of the 50 cm mark on the ruler carbon 40mm thick, the fluid pathway at the index finger of my assistant to the second ramp is 1m up dip. The flow of fluids indicated with yellow arrows. Main ramps and bedding parallel thrusts in dotted red line. Minor bedding parallel thrusts in thin red line.

The structural controls on carbon emplacement have the effect that the sedimentological features are cut by faults and carbon is emplaced around pebbles and through the pebbles as carbon filled fractures. The emplacement followed a sequence and the injector paths have been seen within the conglomerates.

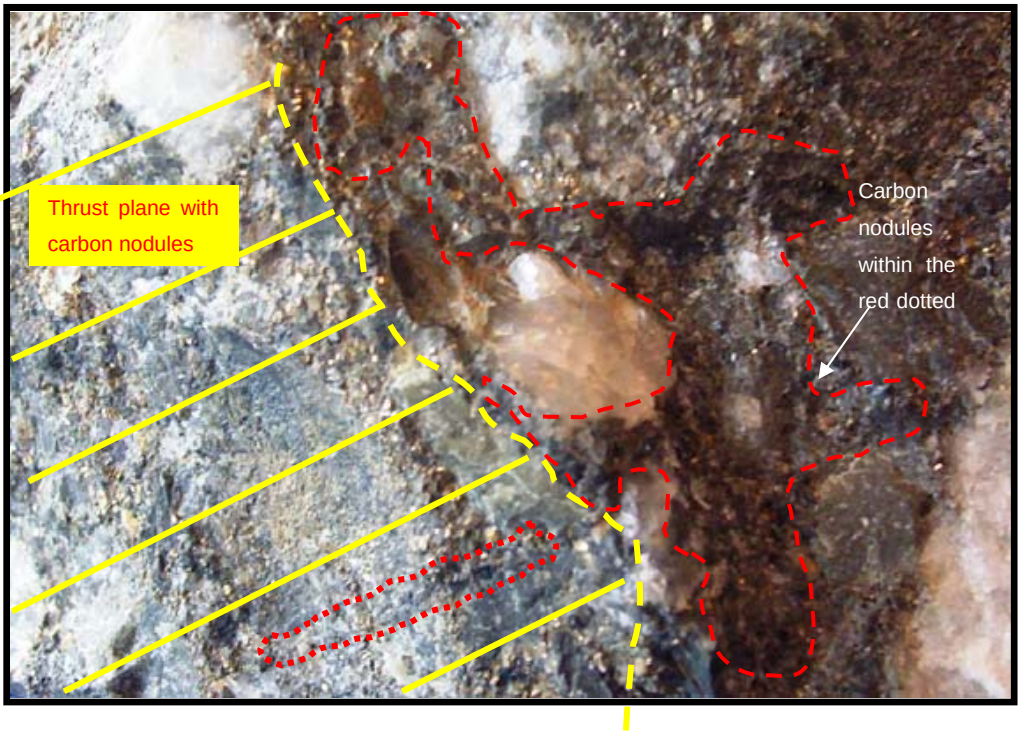

Fig. 4.10 The sediment (conglomerate) has been intersected by a thrust plane and the carbonaceous gas ingressed along this plane.

A fracture in Fig. 4.23 that is filled with carbon is indicative of the time and the events that lead to the fracturing of the pebbles. The observations are unique to this study and will be discussed in Chapter 5.

The figure below is a fracture in quartzite filled with a combination of pyrite and carbon.

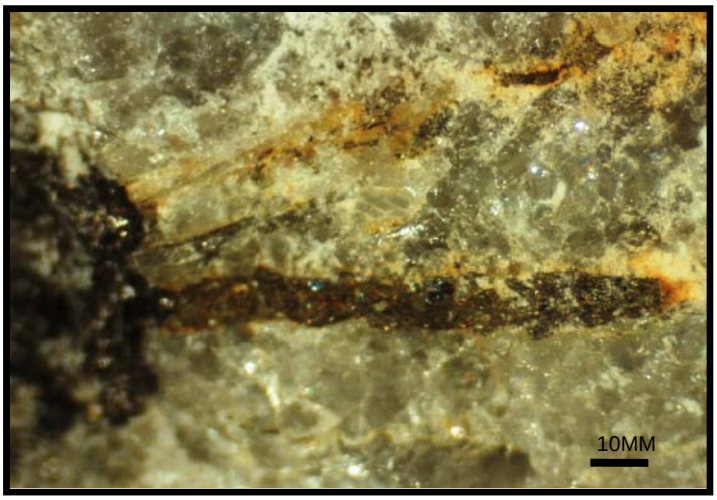

Fig. 4.11 Fracture filled with pyrite and carbon.

4.3.2 Brittle deformation control on carbon deposition

Hayward et al., (2005) described their observations on the brittle fracturing on the contact of reefs as follows. “The consistent location within the paragenetic sequence, the wide regional and stratigraphic extent of the brittle deformation, together with mineral chemical and petrological data suggest that the Vredefort Impact Event (2.02 Ga) was the cause of this late deformation, and that post-impact fluid-poor metamorphism resulted in crystallization of a significant proportion of the gold on and within mineral grains that were deformed during this event.” The brittle deformation that has been observed by the author is shown in Figs. 4.12 and 4.13.

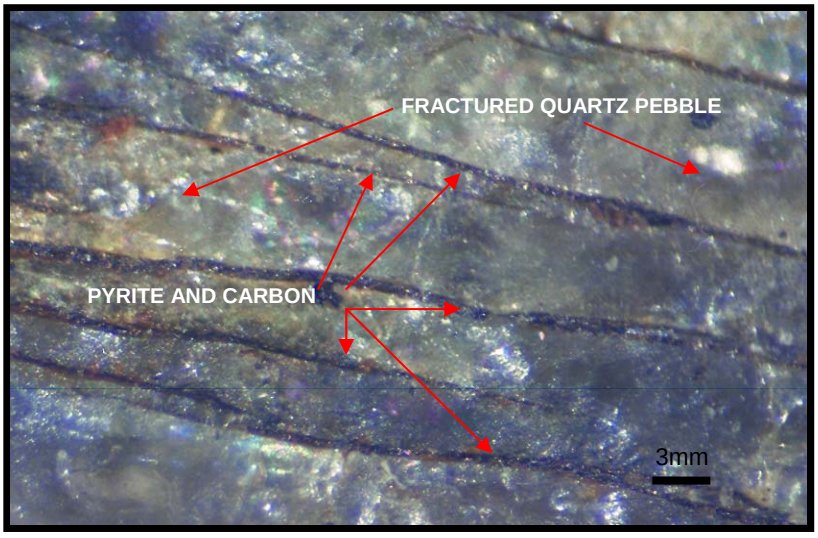

Fig. 4.12 Carbon filled fractures within a quartz pebble.

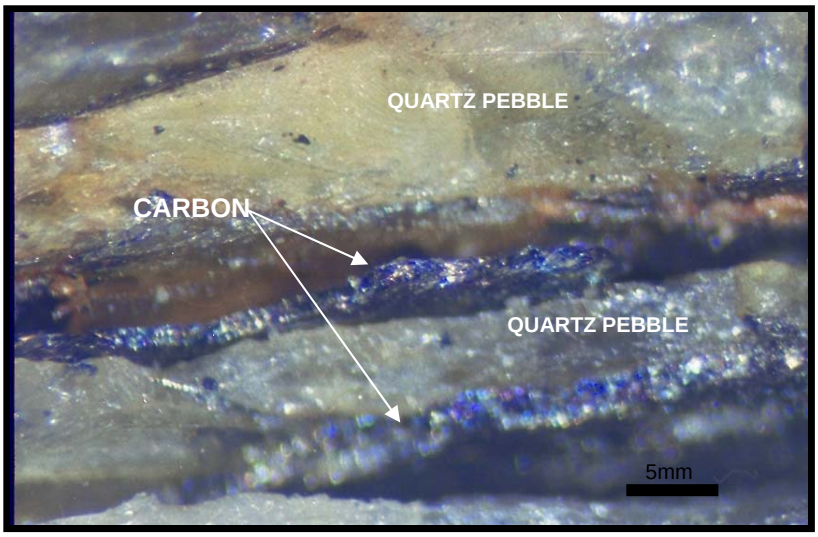

Fig. 4.13 Carbon fills the brittle fractures within a quartz pebble.

4.3.3 Large extensional faults

The large extensional faults are definitely controlling the flow of carbon rich fluids into the basin Jolley et al., (2004), examined the progressive evolution of fault architectures through late orogenic compression- to post-orogenic extensional deformation in the Witwatersrand Basin. The results indicate that rapid extrusion of mafic lavas of the lower Klipriviersberg Group formed a rigid 'lid' over the thrust front, changing its mechanical character and thereby driving a change of structural style from fold growth to passive roof duplex. Flexural tightening of folds in the core of the triangle zones at this time may have helped provide the dynamic secondary permeability for distributed ingress of hydrothermal fluids and consequent gold mineralization. This is a basin wide phenomena (Fig. 4.14).

An example of the structure that controls carbon emplacement is from the Vaal Reef in the Klerksdorp goldfield. In this Fig. 4.14 it is clear that the structural character of the ore body controls the emplacement of carbon. This is a normal fault of probable Platberg age.

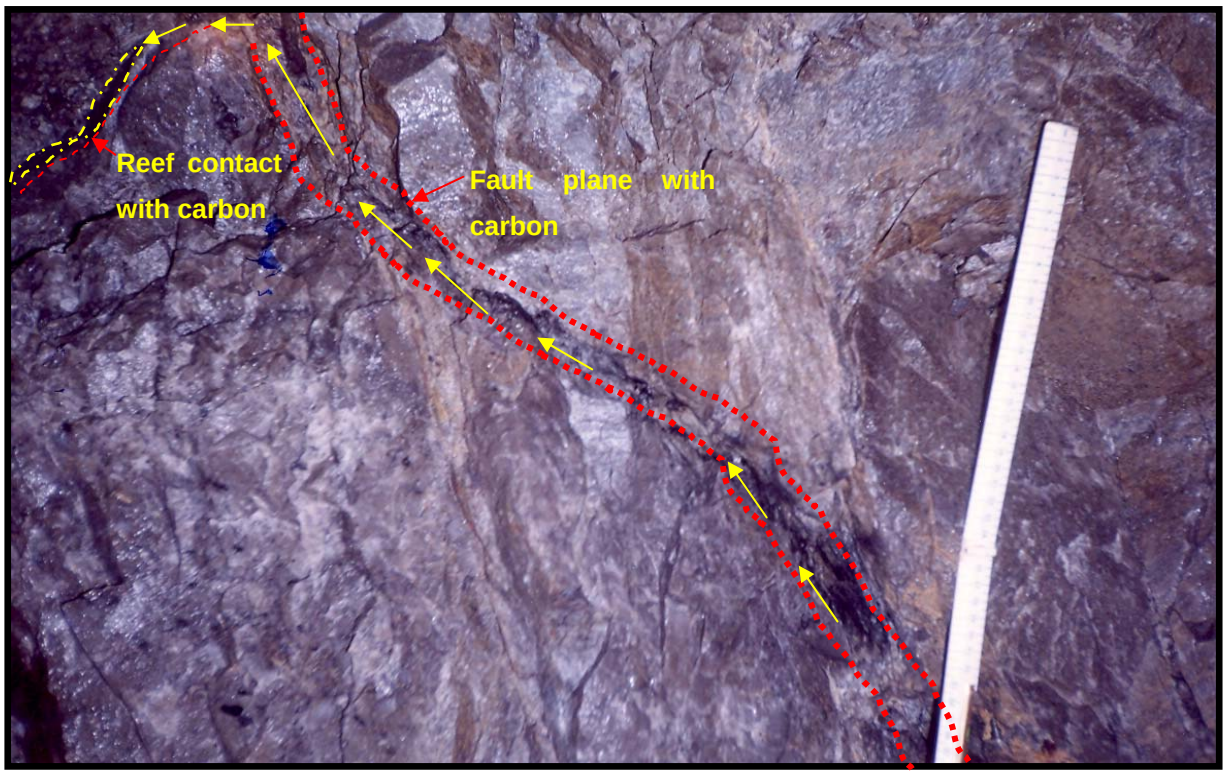

Fig. 4.14 Carbon on a normal fault at Vaal Reefs Mine.Carbon seam 1-12mm thick.The possible flow direction of fluids is indicated by yellow arrows. The fault plane acts as the conduit for the fluids.

4.3.4 Large scale to small scale dykes

Large scale to small scale dykes serve as feeders of fluid basin wide and many mineralized zones have been exposed underground near these structures.

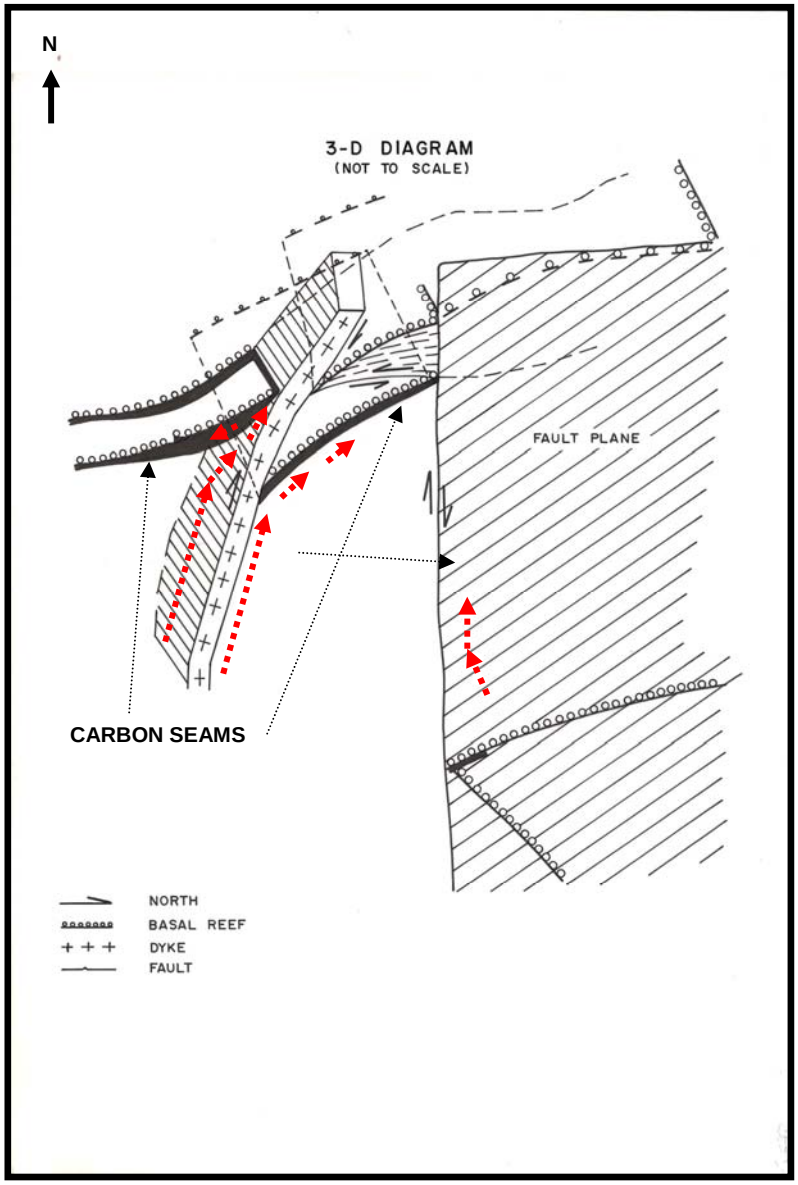

Fig. 4.15 This is a diagram from an unpublished report on the origin of carbon, showing the position of the carbon seams along a dyke and opposite sides of reverse fault. Carbon is developed on both sides of the dyke but the top conglomerate band is not carbon rich. See red arrows indicating the fluid flow. The highest concentration of carbonaceous fluids is on the eastern side of the dyke.

4.4 Specific structural controls observed at various mines in the Witwatersrand basin are: See Fig.2.15

1. **Western margin:** Welkom gold field: thrust faulting, extensional faults, brittle deformation.

2. **Central margin:** Kloof / Carletonville gold field: thrust faulting, extensional faults, brittle deformation.

3. **Eastern margin:** Evander, and **Central margin**: Western area gold fields: thrust faulting, lystric faulting Extensional faults. Brittle deformation, folding (anticline structures at Cooke mine).

Figs. 4.16 and 4.17 show structural controls on the distribution of carbon in the Witwatersrand Basin on the macroscopic scale which range from small scale thrust faults and thrust related fracture to major thrust fault systems. Fig. 4.16 show a major thrust fault. From the thrust fault small scale ramps or thrust fractures were observed intersecting the Carbon Leader Reef.

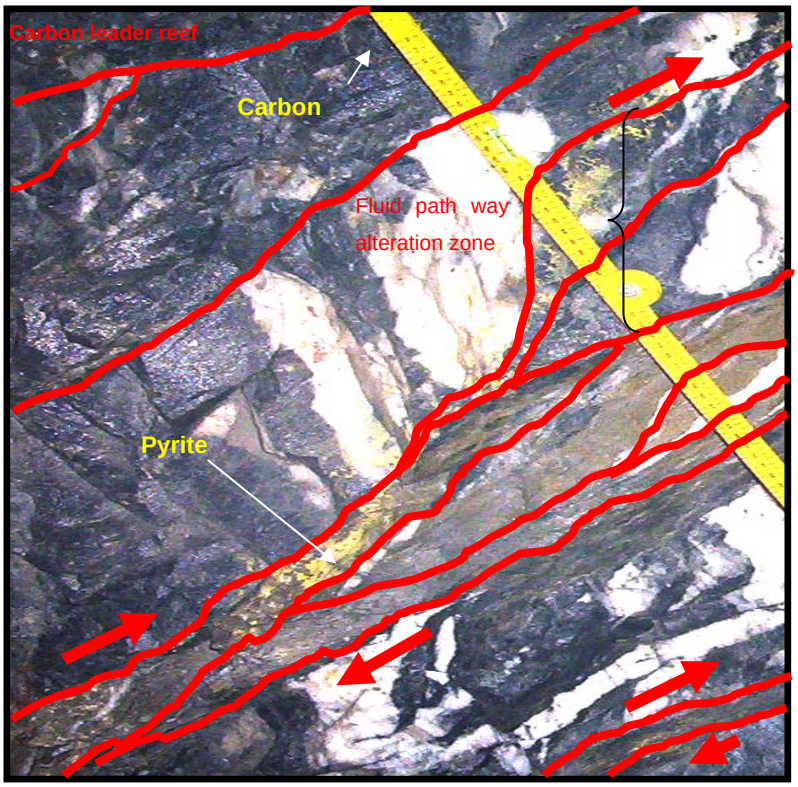

Fig. 4.16 A complex thrust fault system below the Carbon Leader reef DGM.

From the above Fig. 4.16 one can see that carbon is developed where the ramps intersect the reef horizon.

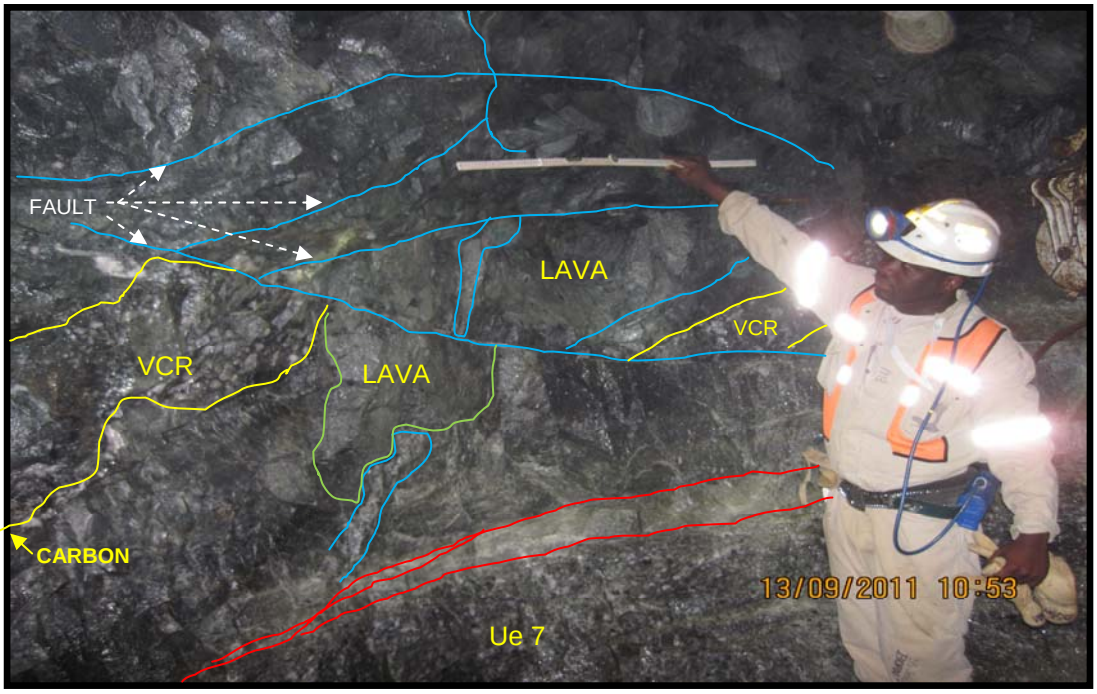

Fig. 4.17 Fluid pathways below the VCR Cooke 2#, 1mm carbon developed on VCR contact.

The examples of carbon seams in Figs. 4.18 and 4.19 from the Welkom goldfield are from the Western Holdings goldmine. In these figures the thickness of the carbon is well over 10mm and these particular samples rendered a glimpse into the pressure regime that existed during deposition of carbon. The conglomerate has secondary permeability (fractured) and the penetration of the gas pushed the two contacts, top of footwall contact and bottom of conglomerate contact apart and followed the contact - probably on an existing bedding parallel fracture under high pressure. This process allows for the deposition of 10mm of carbon in between the footwall and conglomerate in Fig. 4.18. Carbon can now be seen as a vein on the contact of the Basal Reef.

Fig. 4.18 Carbon seam Type A from Basal Reef from 2# WHGM.

This sample below is from Western Holdings Mine and is nearly 40mm thick

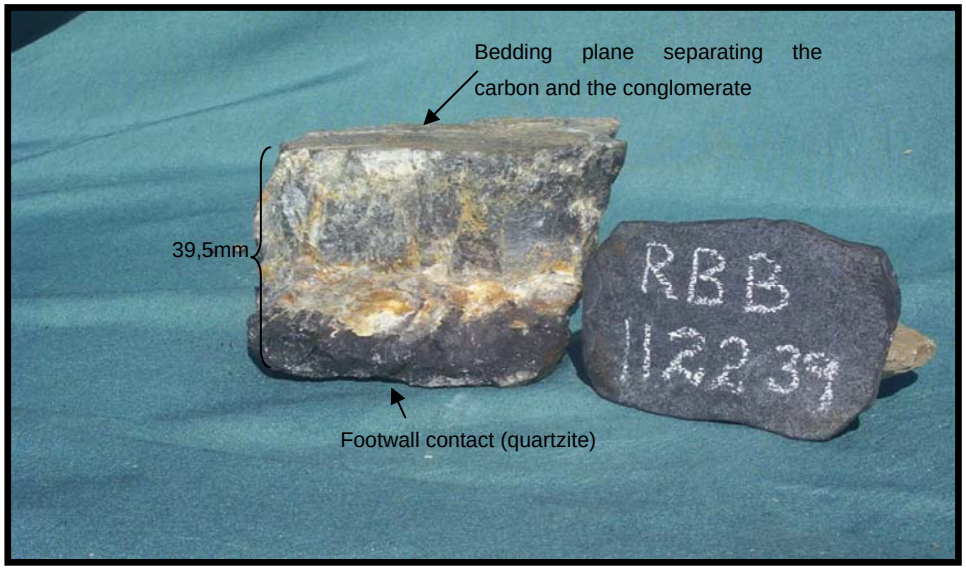

Fig. 4.19 Carbon, 40mm thick, locality 30/41 rse, 2# WHGM.

An example of the structural control on carbon in the Welkom goldfield is illustrated in Fig.4.20 from the Beatrix mine in the southern Welkom goldfields.

In this figure it can be seen that the carbon is emplaced in between the edge of a channel and the Kalkoenkrans conglomerate.

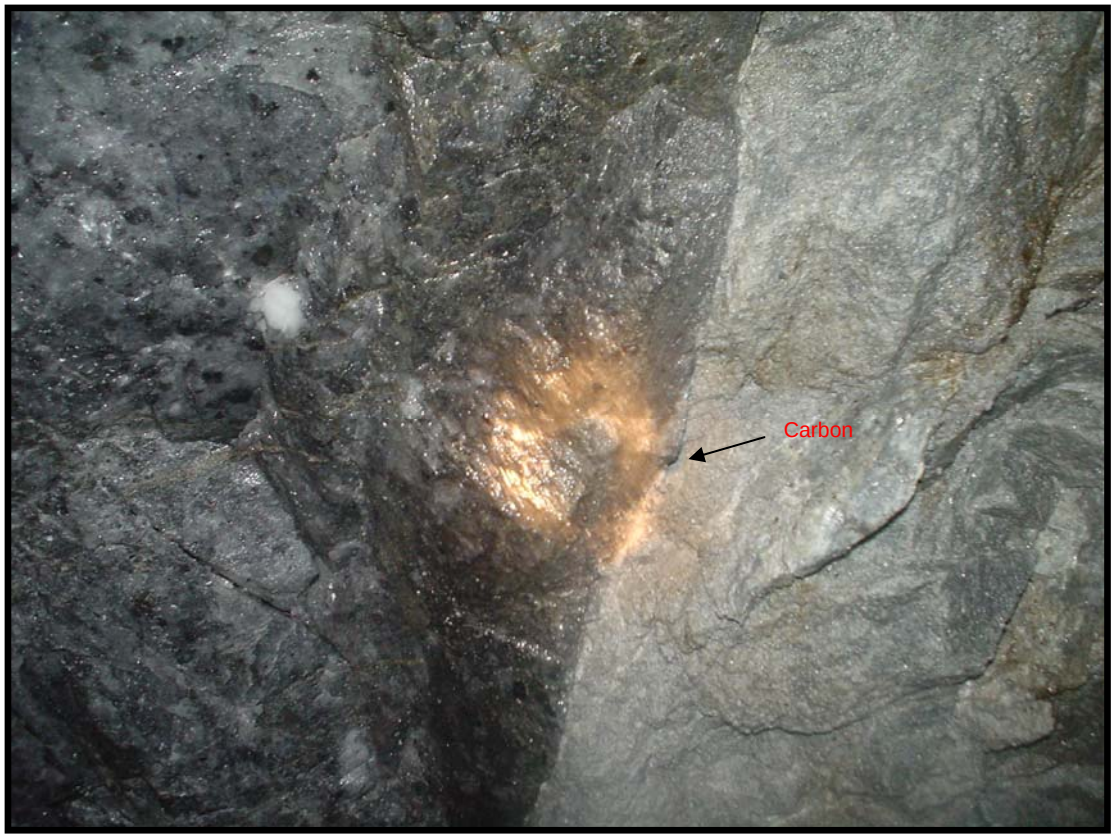

Fig.4.20 Carbon on a channel edge, Kalkoenkrans Reef, 4# Beatrix Mine.

4.5 The structural relationship between carbon emplacement and the related structures

In Figs. 4.21 and 4.22 samples are shown which contain carbon veins with wall rock inclusions. The carbon is classified as Type A carbon (spindles). Fig. 4.21 exhibits a fracture along the reef contact plane and one can clearly see that the spindles are perpendicular to the fracture and that the growth of carbon was along the vertical axis of the fractural space. The space in between the carbon seam fractures is wall rock. (Conglomerate and quartzite).

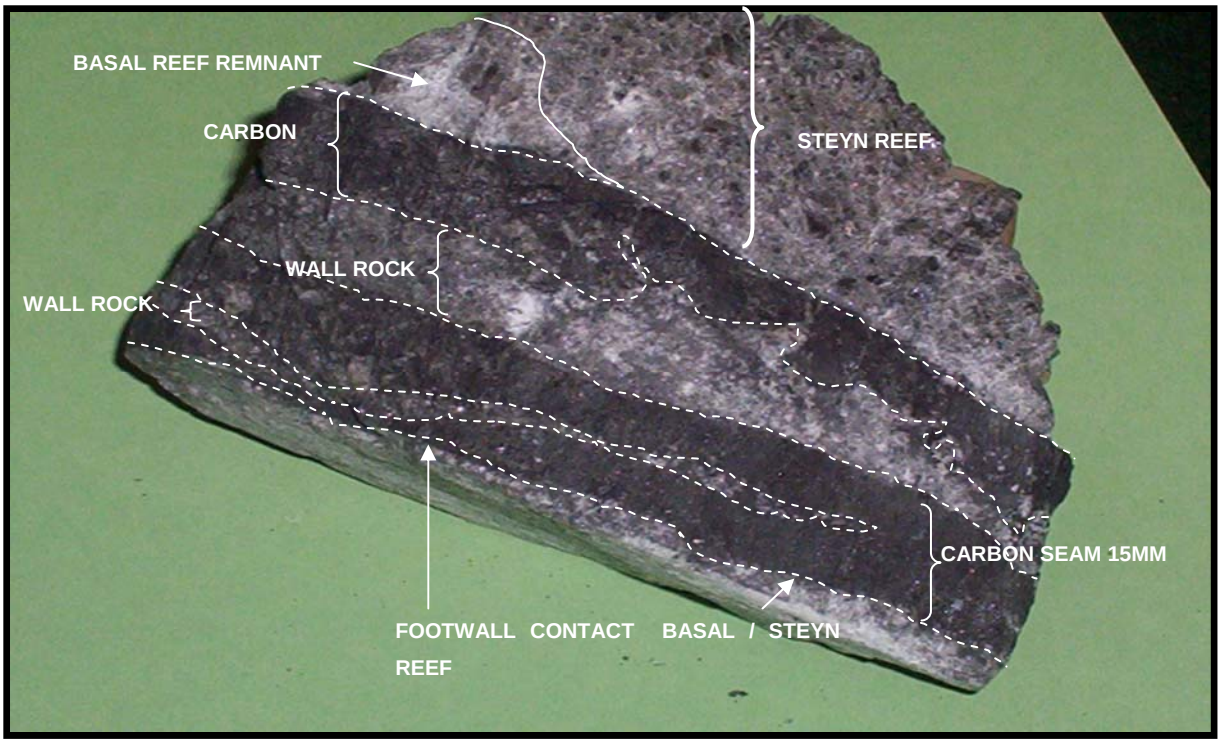

Fig. 4.21 The carbon seam Type A in the reef sample, has been injected into the three fractures as a gas/ fluid as seen in the photo.(WHGM).

Fig. 4.22 This photo shows the foliated bottom contact of the reef contact with the carbon seam(Type A).

The carbon spindles (Figs.4.21 and 4.22)have been described by England et al. (2001) as nodules that have been stretched perpendicular to bedding to form the spindle structure. The structure type will be discussed in more detail in Chapter five.

The location of the samples in Figs. 4.21 and 4.22 are shown in Fig.4.3. One can see the position of the samples as indicated, but the sample (Fig.4.22) must be turned by 180^0 as it is the mirror image of the face sketch.

The structural relationship between carbon and the related structure is shown in Fig. 4.23 illustrating a thrust fault duplicating the reef horizon (Steyn Reef). The bottom contact of the reef package forms the plane that the reverse thrust, the footwall to the thrust contains the complete reef package (Basal Steyn Reef). Carbon has been emplaced within the fractures along the reef contact with footwall quartzite. The details of the relationships of this relationship are shown in Figs. 4.21 and 4.22.

The reverse thrust plane is the main fluid pathway and in this case the secondary permeability potential of the wall rock on both sides of the fault determined the fluid flow direction. In this case it preferred the bedding parallel fracturing on the bottom contact. The timing of carbon precipitation is post the compressional deformation phase. These facts refute the sedimentary origin of the carbon on the Steyn Reef package. The footwall reef sequence formed a buffer and did not allow flow of fluids through to the hanging wall reef sequence.

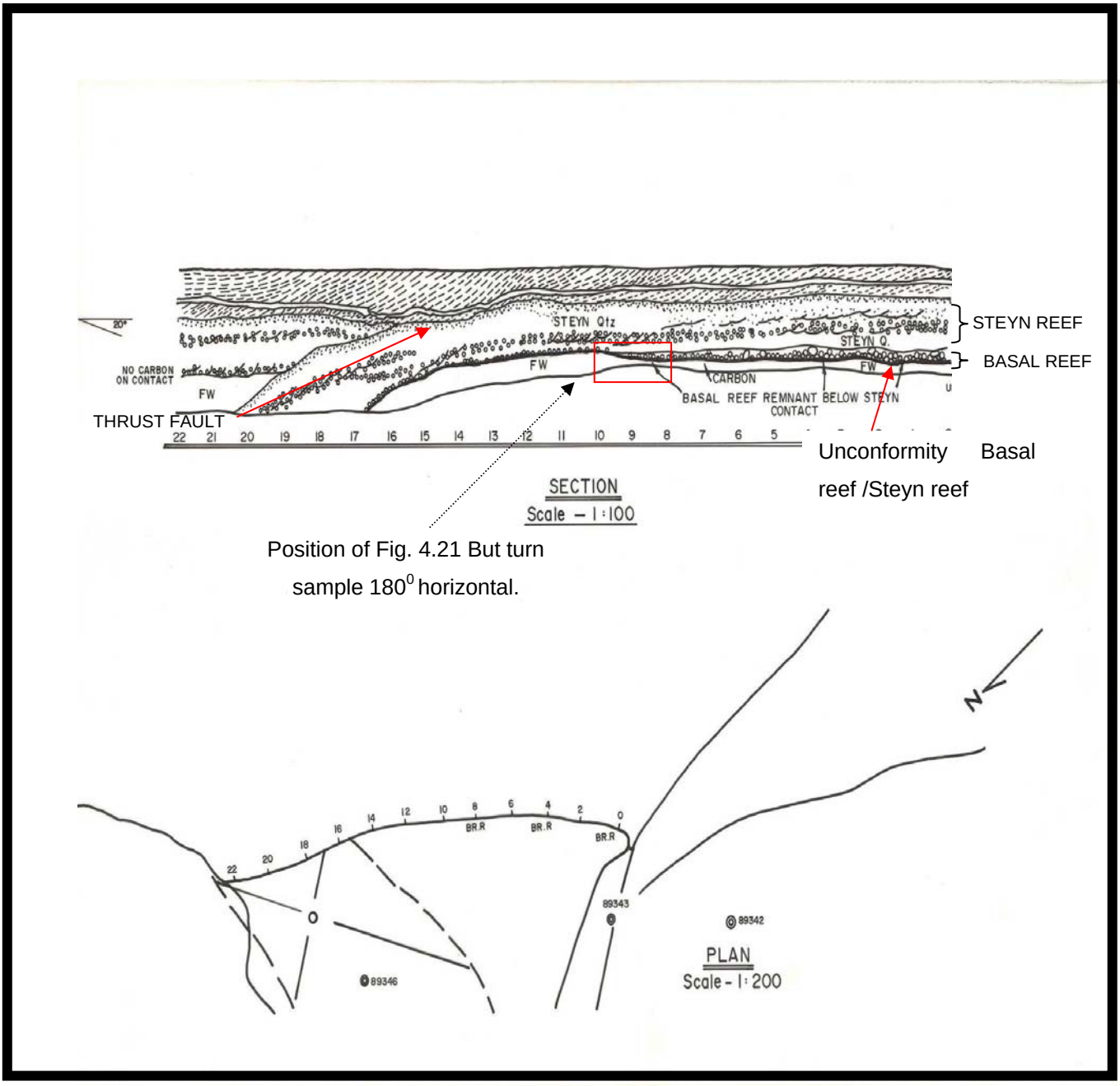

Fig. 4.23 Section of stope face at 2# Western Holdings Mine on 37/41 lineBasal / Steyn Reef stope. A thrust fault duplicates the reef sequence, with carbon seams being emplaced on the footwall to the thrust.

The Fig. 4.24 below depicts the spindle carbon with gold plated along the carbon spindles. The structural deformation of the carbon and the gold plating on the carbon are post precipitation and it can be deduced that both,carbon

and gold, precipitated out of solution at the same time and were deformed at the same time.

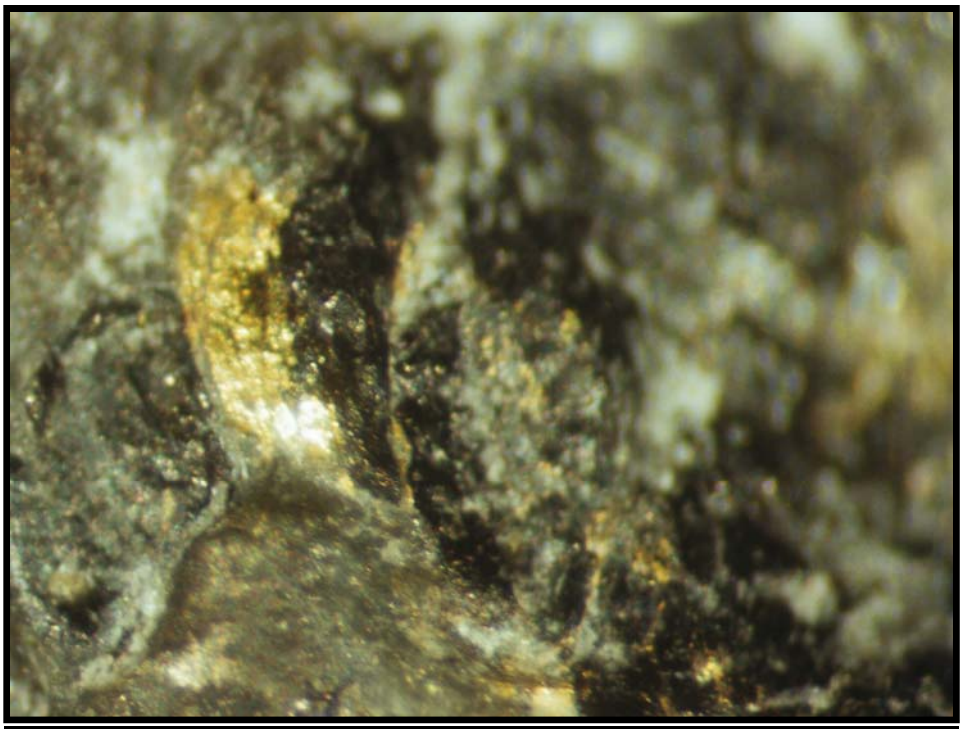

Fig. 4.24 Gold on carbon spindles.

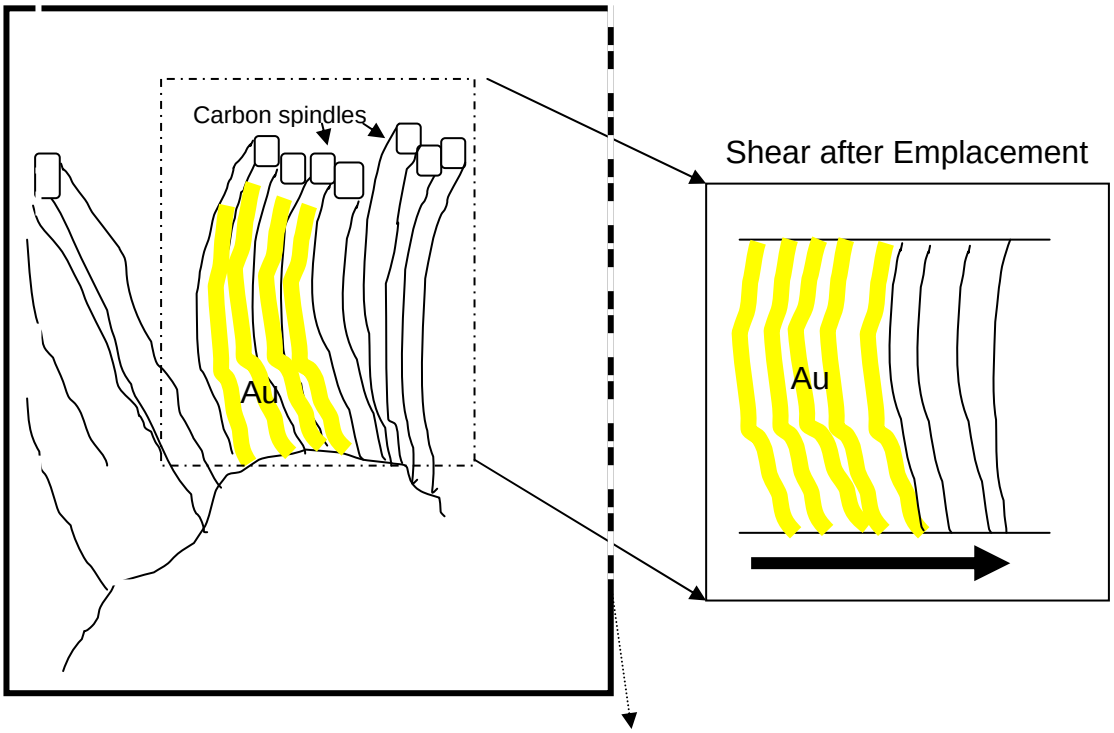

Fig. 4.25 Diagram of gold on carbon spindles.

The deformation of both C and Au shows that the structural relationship between carbon emplacement and the related structures are post precipitation, and could form part of the relaxation phase syn Vredefort Impact event.

The next diagram (Fig. 4.26) shows the emplacement of carbon along a major fault with different percentages of carbon on either side of the fault. The percentage carbon increase closer to the faults on all the mines.

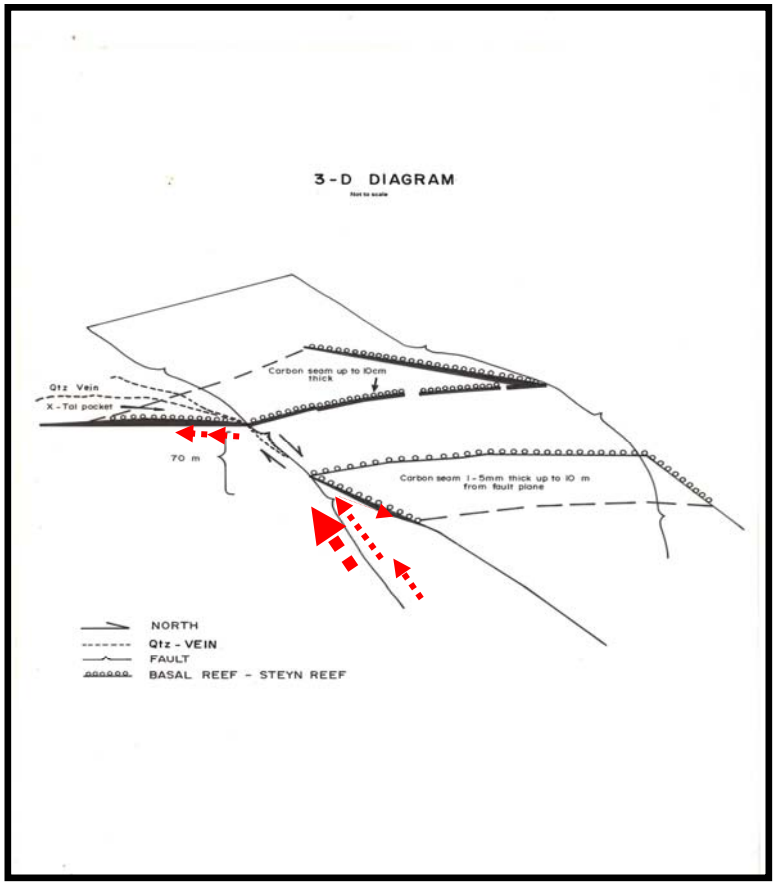

Fig. 4.26 Type A carbon seams are not the same thickness on both sides of the normal fault. The thickness on the up-throw side of the fault is 10 cm and on the down throw side is only 1-5mm. Fluid flow direction indicated with red arrow. The highest volume of inflow indicated with large red arrow.

4.6 The interpretation of the specific carbon observations from underground to SEM

Carbon is observed within and on the contact between the quartzites and the phylonite defines the fluid pathway, suggesting that the age of carbon postdates the formation of the phylonites. The SEM images confirm the mesoscopic observations.

In Fig. 3.16 and 17, it appears that the pathway at high magnification is hollow and that pyrite is precipitated from a fluid into the voids. This indicates the mode of deposition of the mineral phases. The mode of deposition of the mineral phase is suggested then as being from fluid to solid (precipitation of minerals out of fluids) associated with the process of fracturing and fluid injection.

All this suggests that these minerals and metals crystallized more or less at the same time. The occurrence of these mineral phases in fractures suggests that a high fluid pressure must have been present at the time. Parnell, (1996) suggested a high hydrocarbon pressure needs an abundant source of carbon. It is this injection of carbon into the fractures that suggests a high pressure injection of hydrocarbon fluids into the Witwatersrand Basin. These views of carbon and uraninite and pyrite, mitigate against a sedimentary process for all these minerals. The uraninite and pyrite in this view is post metamorphism and are embedded in the metamorphic mineral, pyrophyllite. The physical appearance of uranium replacing pyrophyllite is indicative of the sequence of precipitation and the timing. The suggested timing for carbon emplacement is 2300 Ma (Rob et al., 1989) and is based upon an isotopic study of uraninite imbedded in carbon. Fig. 3.17 shows that the uraninite mimics the shape of the pyrophyllite grains and suggests that the timing of the uraninite emplacement post-dates peak metamorphism. It is suggested that the three main minerals carbon, uranium and gold all came in at the same time into the basin.

4.7 Discussion on new model for the origin of carbon

An attempt to find the origin of the carbon on the contact of the reef horizons has been done using the SEM to determine the element that could be associated with a chemical reaction to bring about the precipitation of carbon. The clearest evidence for the time aspect within the Wits Basin is the presence of carbon within the VCR.

If the carbon pre-dated the Klipriviersberg lava, then the carbon would be altered on contact with the hot lava (as in Fig.2.25). This however is not the case and it is therefore deduced that the carbon post-dates the Ventersdorp lava event at 2.7Ga.

In Fig. 2.26 the mapping indicates how the fractures and the ramps dominate as locations for the carbon distribution (in blue) on the reef horizon. These small scale thrusts are the result of a thrust fault below the raise, deep into the footwall. The thrust movement is normally very small. These ramps are consistent with the front end, low displacement part of the bigger thrust system (Jolley et al., 2004).

The above examples are not the only structural controls on carbon. The influence of intrusive and major fault systems on the distribution pattern of the carbon emplacement has been mapped basin wide. The studies of (Jolley et al, 2004) have a major impact on the prospectivity of the Ventersdorp Contact Reef.

More detail on carbon observed on fault planes is shown in Fig. 4.27. Fig. 4.27 shows carbon on the VCR contact and details of shape change along the contact.

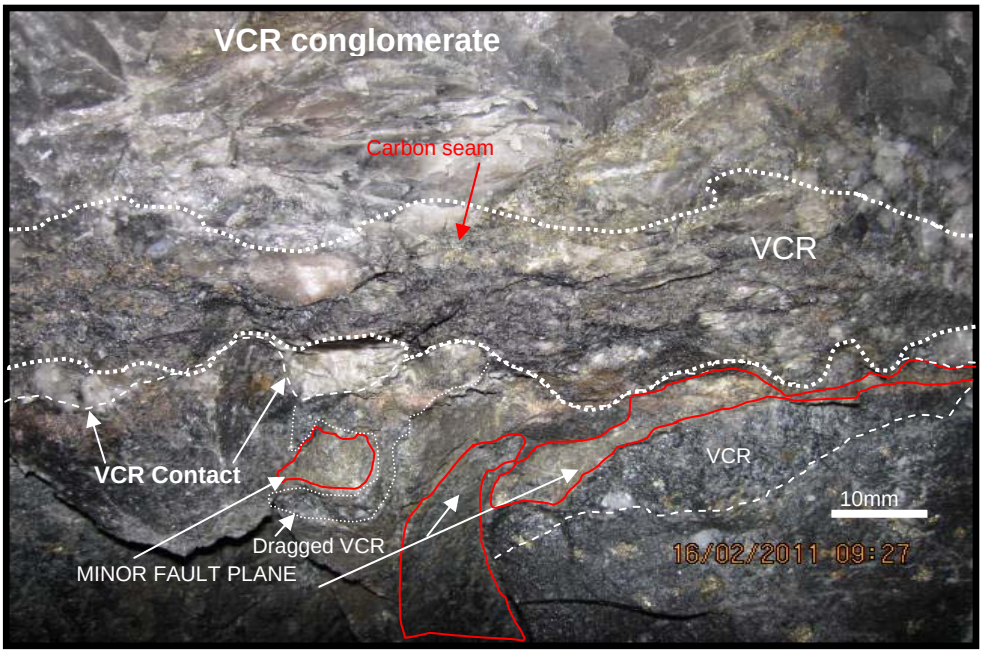

Fig. 4.27 Carbon on the VCR contact 90S12A N10 panel Cooke 2#.

The carbon observed in the raise shown in Fig. 4.28 is 10mm thick. The carbon (Type A) forms a solid seam all along the contact. All the fractures have been sampled in detail and these values will follow in Chapter 5.

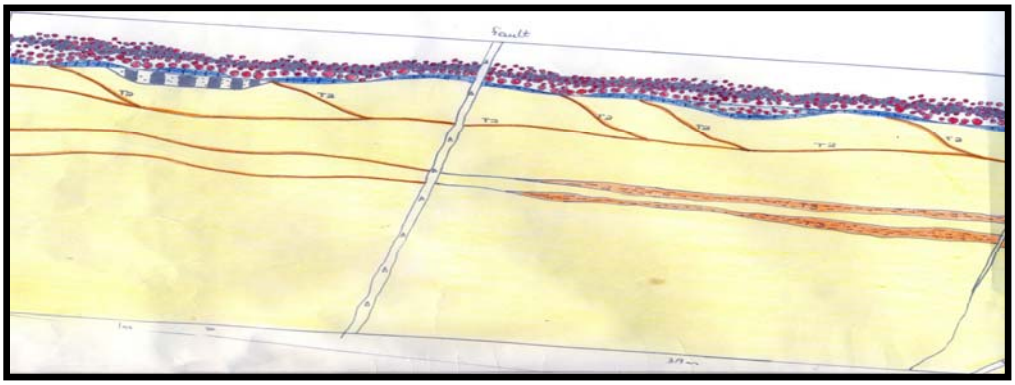

Fig. 4.28 The diagram of a raise on the Vaal Reef Mine. 70Dw 1 17 raise. This is a diagram showing fractures (orange), carbon development in blue. Section is looking north, the dip is from the west to the east and the approximate distance from west to east is 25m.

4.8 Carbon occurrence along fault planes

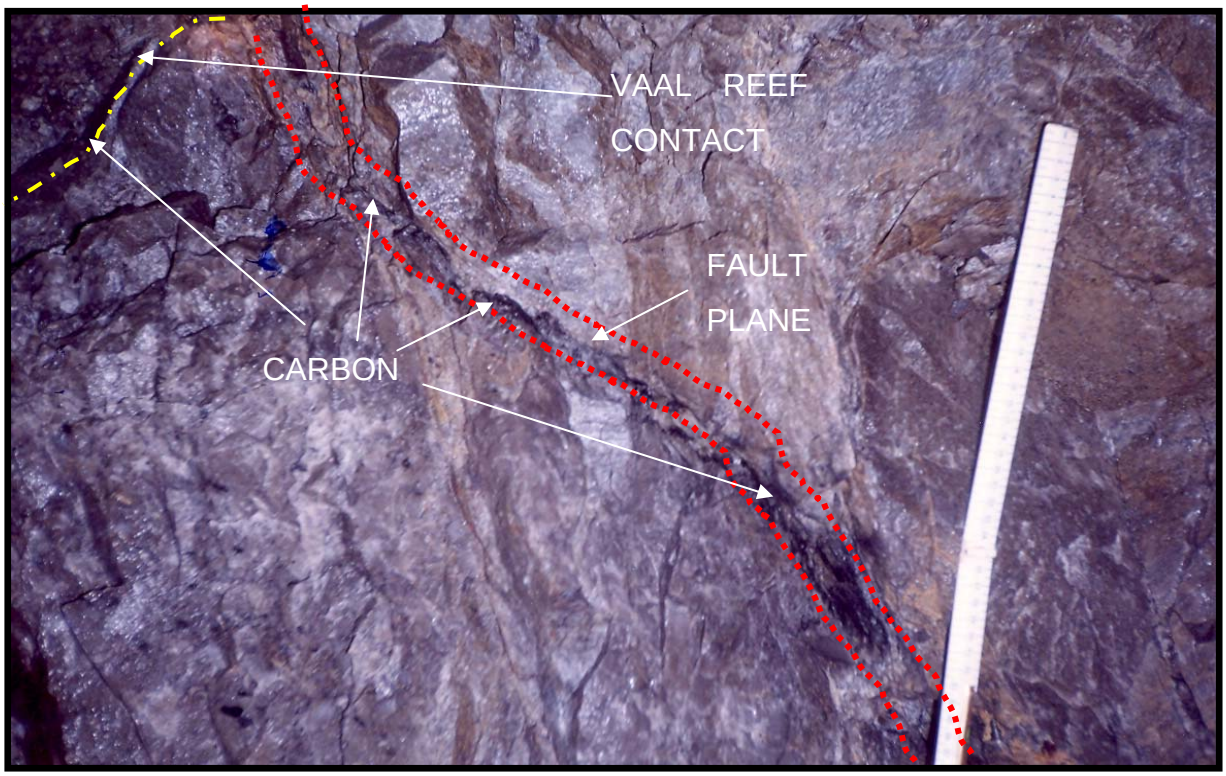

Fig. 4.29 Carbon on a normal fault plane of Platberg age at Vaal reefs mine. Carbon seam 1-12mm thick.

It is shown in Fig. 4.29 that the carbon is precipitated all along the normal fault plane and the carbon on the contact is the same as the carbon on the fault plane.

4.9 Carbon occurrences in relationship to large scale dykes

The carbon as shown in this section in Fig. 4.30 differs in thickness. The carbon on the eastern side of the dyke is thinner than the western side of the dyke. This suggests that the volume of gas is unequal on both sides of the dyke and that there is a difference in permeability potential of the conglomerate bands.

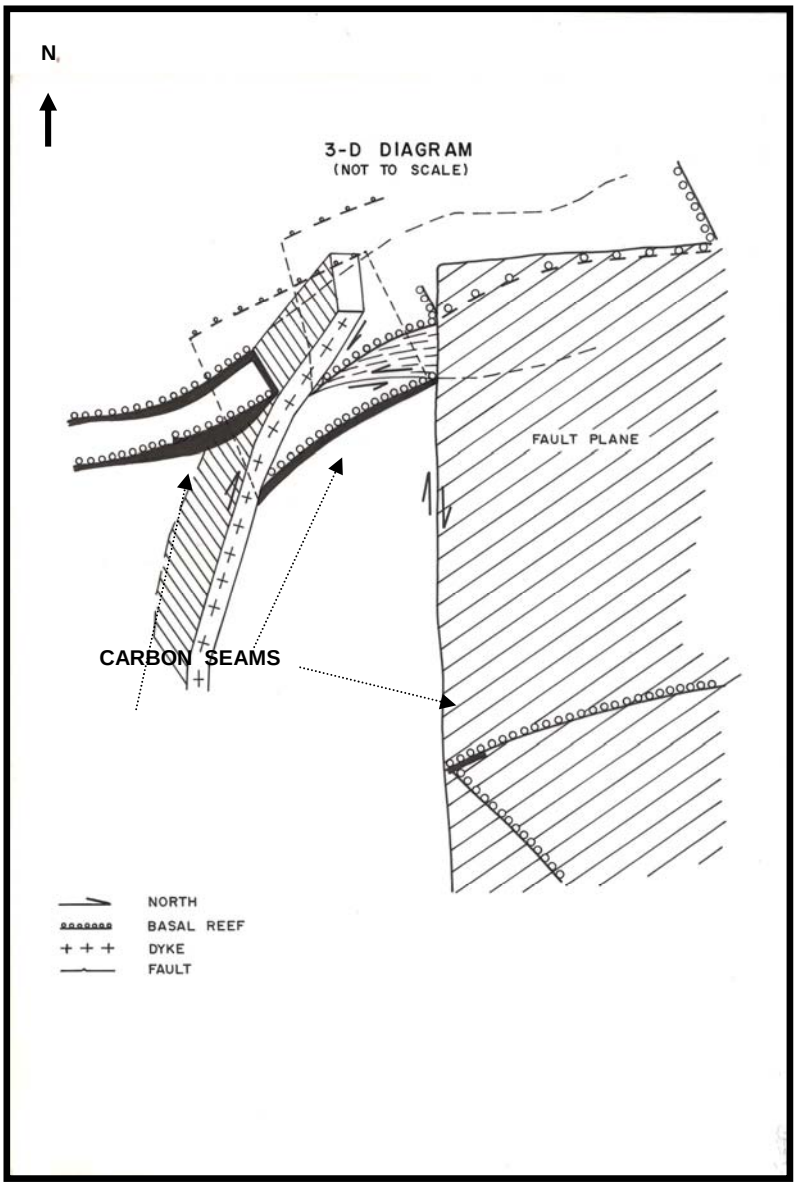

Fig. 4.30 This is a diagram from an unpublished report on the origin of carbon, showing the position of the carbon seams along a dyke with a reverse throw. Carbon is developed on both sides of the dyke but the top conglomerate band is not carbon rich.

4.10 Examples of Carbon and gold on the contact

Fig 4.31 shows the nodular carbon with its strong relationship with Au.

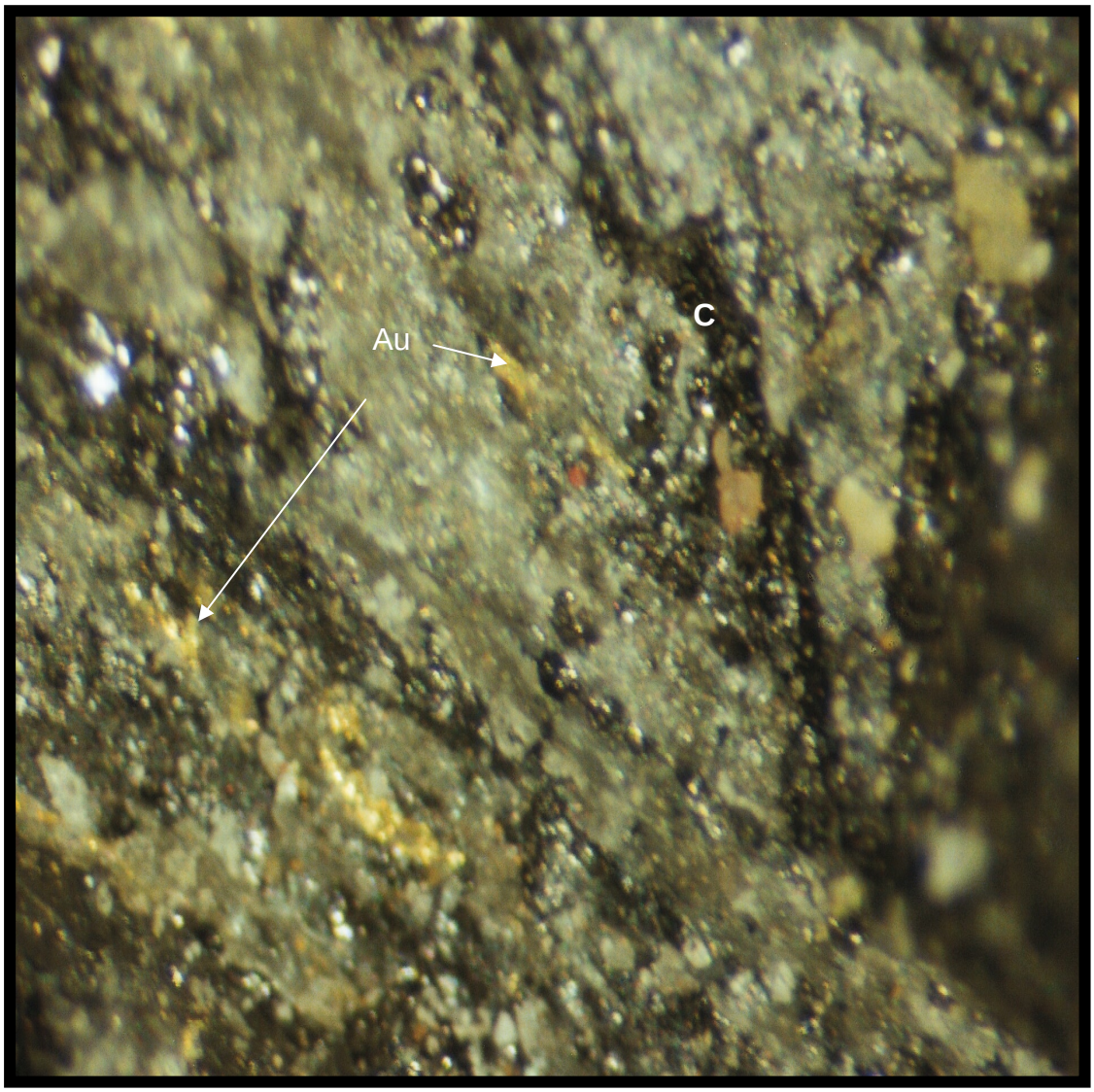

Fig. 4.31 Carbon and gold, B Reef (Tshepong Gold Mine)

Fig.4.32 shows the strong relationship of carbon and pyrite within Type A carbon.

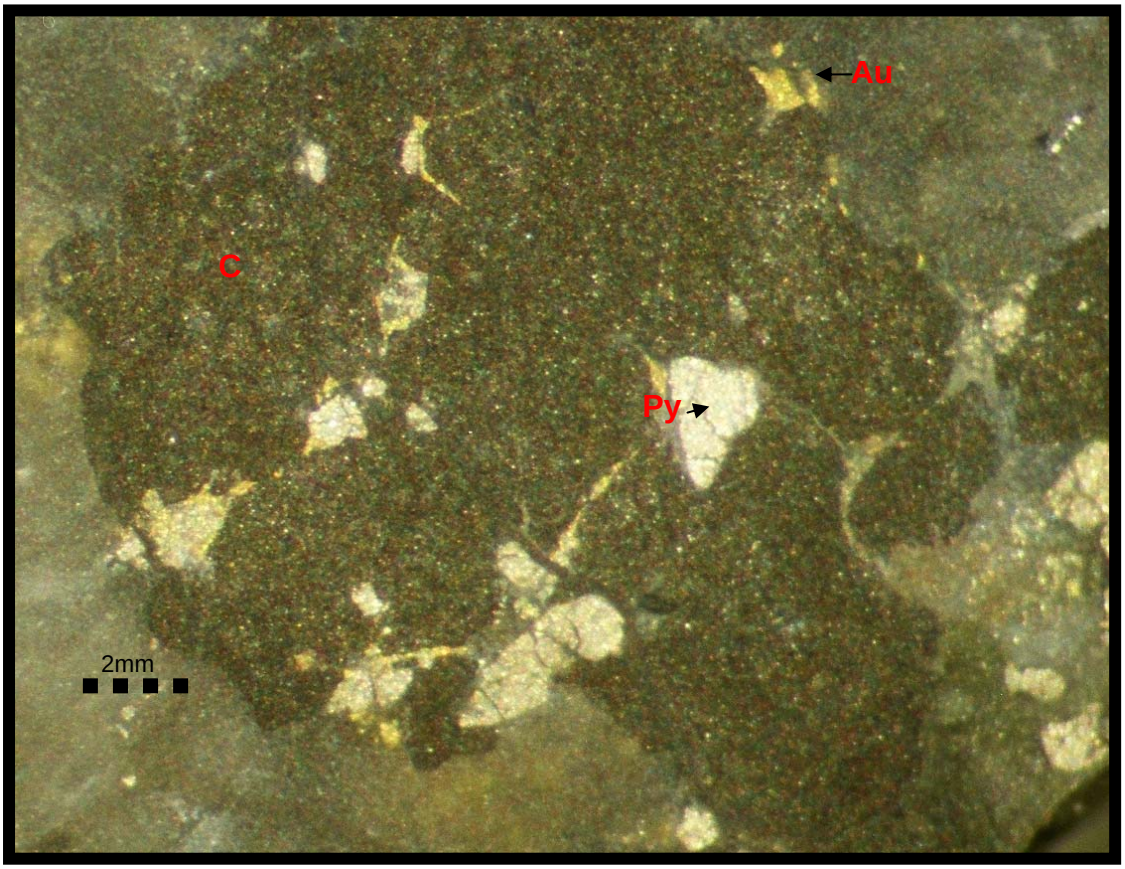

Fig. 4.32 This is a photograph of the Basal Reef Western Holdings Mine where gold and pyrite are in between carbon nodules.

Fig.4.33 is a carbon seam from the B Reef at Tsepong mine and the gold is situated in between and on the carbon filaments and nodular carbon.

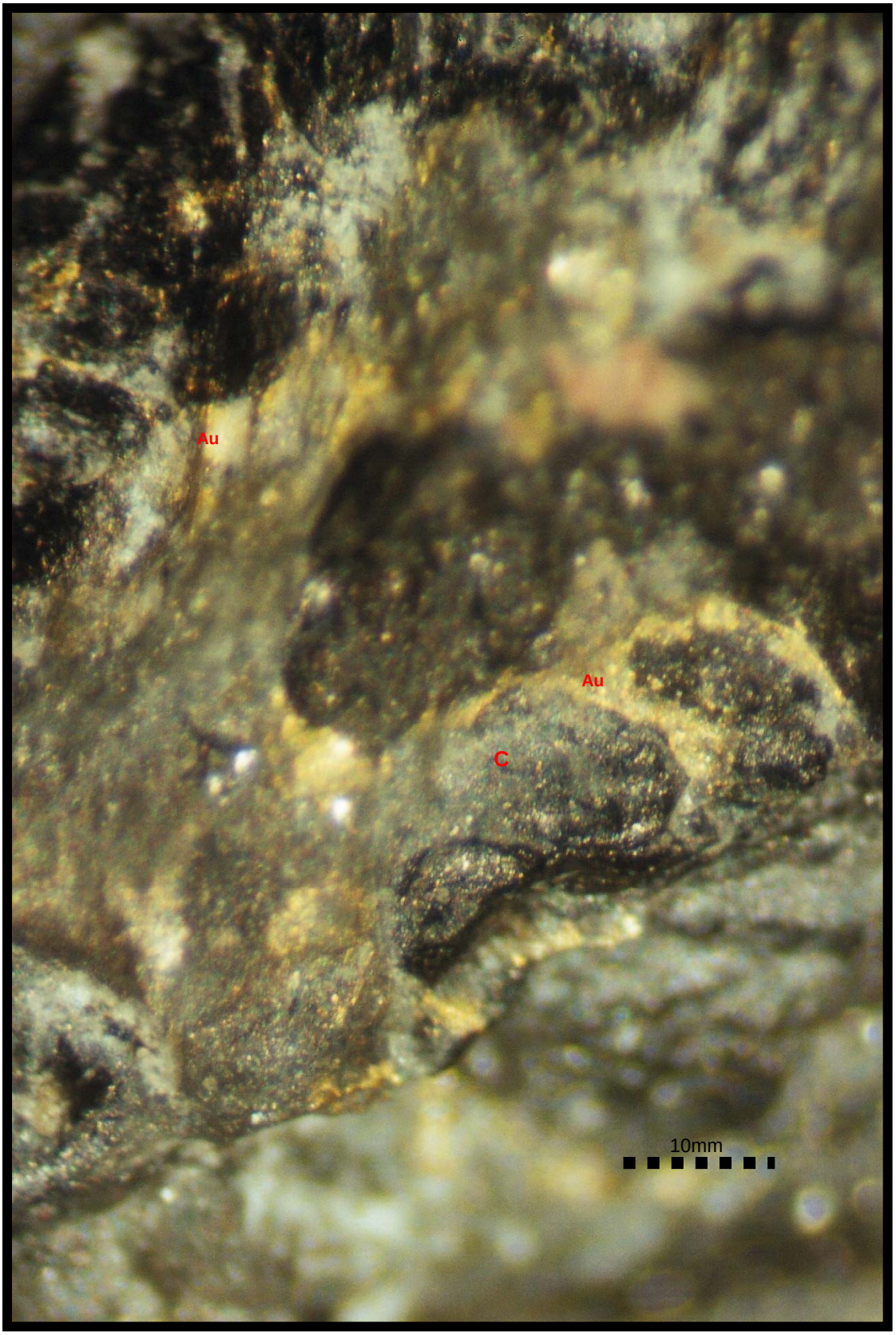

Fig. 4.33 This is a view of gold and carbon where the gold is plated onto the carbon filament, B Reef (Tshepong Gold Mine)

4.11 The macroscopic description of fractures and their filling

This section describes fractures occurring in the carbon leader reef and the vein filling observed. The example to be described is a sample from Driefontein Gold Mine. The crack in this pebble is parallel to a bedding plane fracture. It is deduced that the same force that caused the bedding parallel fracturing has caused the crack in the pebble.

The event that followed filled the crack with carbon and sulphides. The carbon is coated with bornite, and the carbon has been metamorphosed to graphite. This structural occurrence of carbon does explain some of the pre-historic history and it mitigates against the hypothesis of carbon being an algal mat.

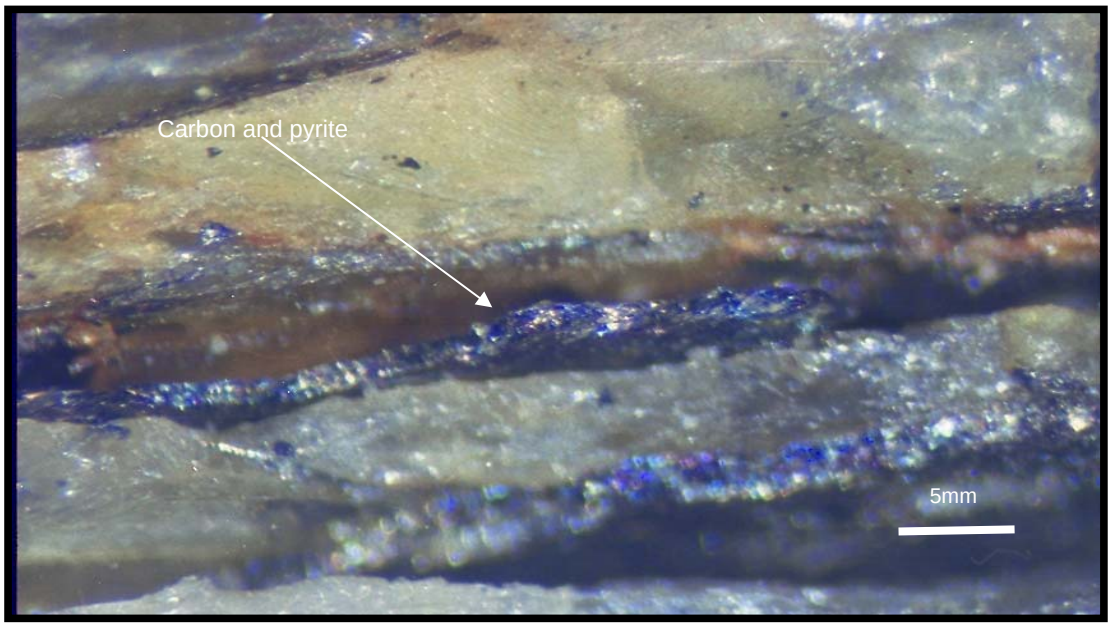

Fig. 4.34 A bedding parallel fracture filled with carbon.

4.12 Summary and interpretation

- Stope mapping on 22 different shafts all indicate carbon and related minerals (pyrite, gold, uraninite) are associated with sedimentological structures(crossbeding,unconformities,channelsurfaces).Paleo-depressions, bedding planes, conglomerate bands (below, within and above) all these sedimentological structures are all fluid pathways.

- The occurrence of C, U, Py and Au in conglomerates is not a function of its sedimentary processes; it is rather a function of induced secondary permeability due to deformation.

- Carbon is also emplaced near dykes.

- A major control on the deposition of carbon is tectonic structures. Bedding parallel fractures in reefs and within pebbles containing carbon are indicative of the influence of large scale deviatoric stresses in the ore body.

- Tantalum silicate ($TaSiO_2$) occurs within fluid pathways and in C.

- Timing of C and Au is post Platberg.

It can be concluded that:

- Carbon emplacement is controlled by structure and stratigraphy.
- Carbon is emplaced as a late fluid post Platberg faults.
- Carbon itself controls gold and uranium deposition.

Carbon, gold and uranium are all associated with fluid pathways.

CHAPTER 5

SUMMARY AND DISCUSSION

5.1 Summary on carbon deposition

5.1.1 The structural control on carbon deposition

The map in Fig. 2.15 illustrates the distribution of carbon in association with faults and Central Rand Stratigraphy. Observations made on these associations suggest that faults (extensional and contraction/compressional) may be regarded as fluid pathways. Some of the thickest carbon (up to 10cm thick, Fig. 4.26) occurs within the fault zones. Bedding parallel thrusts (Fig. 2.14) and massive thrust faults are very prominent fluid pathways throughout the basin and form part of the contraction faulting which pre-dates the Klipriviersberg extension at 2.7 Ga. The carbon is deposited on or close to the faults. The detail on the carbon distribution on faults is described in Chapter 2 & 4 and illustrated in Fig. 2.27 and Fig.4.29.

It is observed that the more structurally deformed the area is, the higher the gold content. It is thus deduced that the structure determined the inflow of mineralized gas/fluids to the area. Figure 5.1 shows the anastomising fluid pathways and ramps that stem from a 20m down throw fault to the left of the section. The gold value on the ramps and fluid pathways confirms the presence of gold and also confirms the presence of hydrothermal fluids which deposited the gold. The sampled value of the Vaal Reef contact at the fluid

pathway intersection is 445g/t. Note that the carbon seam starts where the pathway or ramp intersects the contact.

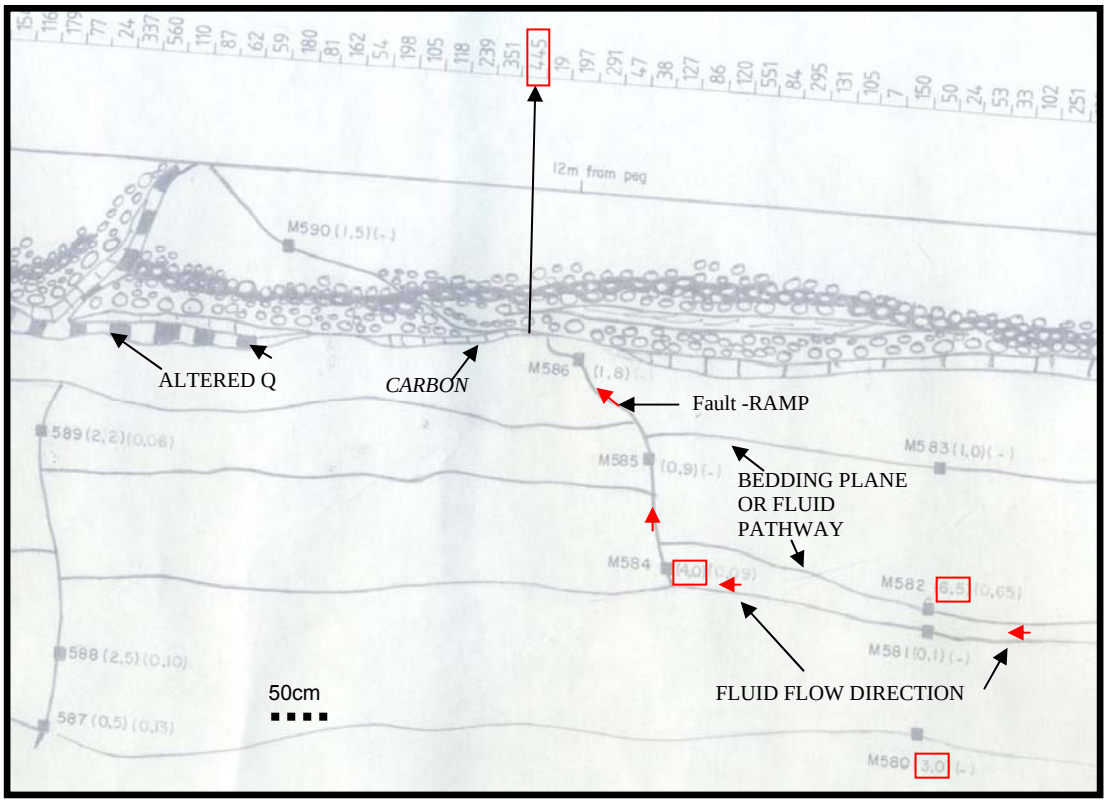

Fig. 5.1 Detailed raise mapping on the Vaal Reef (MB5's) and sampling; note Au value in g/t. Carbon is deposited along the bedding plane contact between quartzite and conglomerate. Fault presumed to be of Platberg age. Gold occurs along faults.

The value on the contact increases close to where the ramp intersects the contact with the conglomerate/quartzite. The footwall ramps have values between 1- 6g/t.

If the rock is fractured, the hydraulic properties of rock masses are likely to be highly heterogeneous, even within a single lithological unit (Fig. 5.1). The main difficulty in modelling fluid flow in fractured rock is to describe this heterogeneity. Flow paths are controlled by the geometry of fractures and their open voids. Fluid flow in fractures is dependent, in part, on the distribution of fracture fillings and the state of stress ((Gray et al., (1998)

Barnicoat et al., (1997)). This is the determining factor in the emplacement of carbon shown in the above (Figure 5.1).

Flow paths may be erratic and highly localized. Local measurements of geometric and hydraulic properties cannot easily be interpolated between measurement points. In contrast, granular porous media, although also heterogeneous, commonly exhibit smoothly varying flow fields that are amenable to treatment as equivalent continua. Gray et al., (1998) and Barnicoat et al., (1997) all came to the same conclusion that the precipitation of carbon is related to fluid movement along fractures, faults and lithological contacts. This study confirms there results.

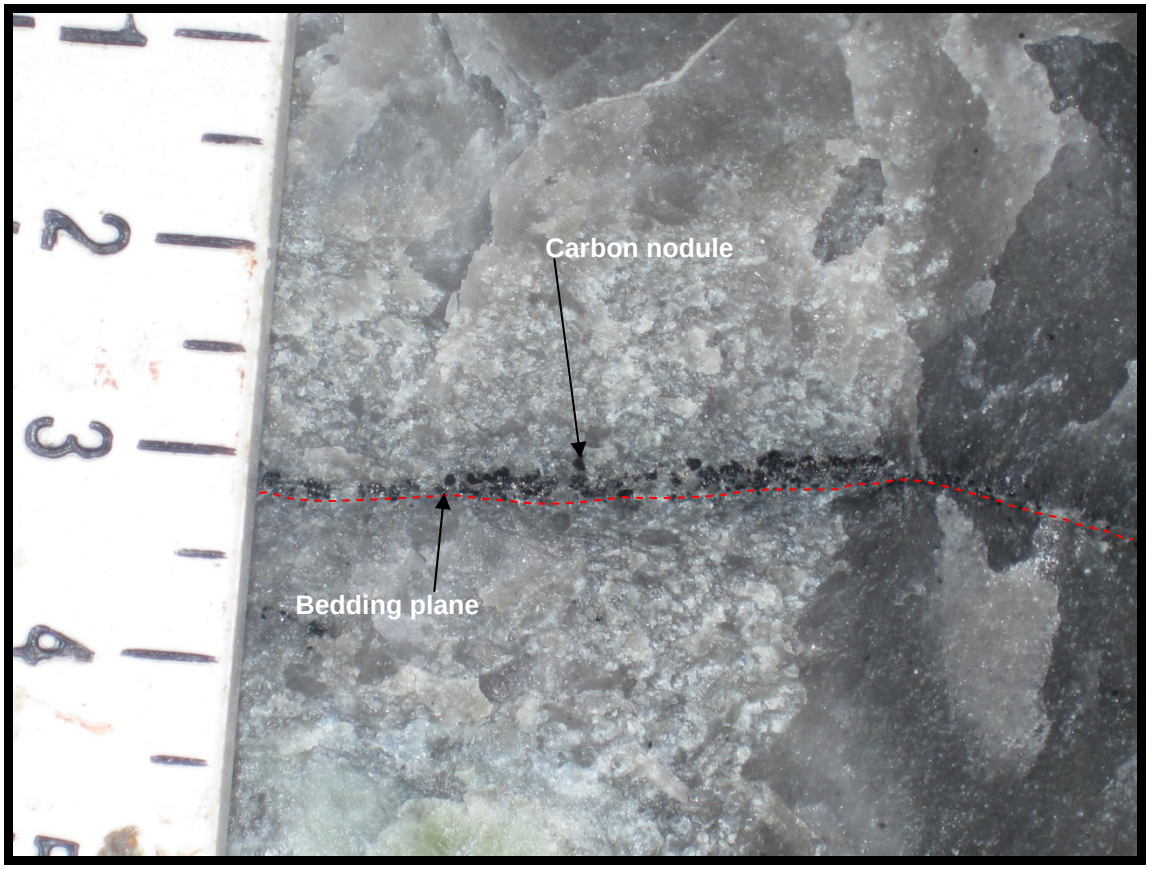

Fig. 5.2 *Carbon nodules on a bedding plane within the Upper Elsburg conglomerate no. 1A.*

In summary carbon occurs along and in association with the following structures.

1. **Contractional faults:** Thrust faults e.g. (Fig. 4.9 and Fig. 4.23). Bedding parallel thrusts/shears e.g. (Fig. 2.7, Fig. 2.14).
2. **Extensional faults:** (Fig. 2.8, Fig. 2.27).
3. **Fractures / veins in association with 1 and 2:** e.g. (Fig. 2.7).
4. **Bedding:** e.g. (Fig. 5.1) Lithological contacts e.g. (Fig. 2.6).
5. **Dykes:** e.g. (Fig. 2.28).

The types of carbon associated with each structure are:

- **Contractional faults:**Type A: Spindle type carbon(Fig.4.9,Fig. 4.23).
- **Extensional faults:** Type A: Spindle (Fig. 2.17, Fig. 2.18) and massive type carbon (Fig. 4.31).
- **Fractures / veins:** Type A: Spindle and filamentous type carbon (Fig. 2.19, Fig. 2.22).
- **Bedding:** Type B: Nodular types (Fig. 5.2), (Fig. 2.21), filamentous (Fig. 2.19) and spindle (Fig. 2.20) type carbon.
- **Dykes:** Type A: Spindle type (Fig.2.28).

A high percentage of carbon along reef contacts is massive and devoid of any fabric (Fig. 4.31). Various examples are described in Chapter 3. Some examples describe the abnormal occurrences of carbon that can be related to the hydrothermal gas/fluid origin of carbon (Figs. 2.18, 4.28 and 4.29). The placer theory does not explain the carbon in above examples.

The observations of various mineral phases within fractures under the scanning electron microscope also point to fluid movement along the fractures. In samples from Western Holdings Gold Mine it is observed that the four minerals namely gold, pyrite, uraninite and carbon, occur in close

association with each other and also along the same fluid pathways. Gold and uraninite is imbedded in pyrophyllite and are associated with carbon or included in the carbon mass within a fluid pathway. This is an indication of the timing which will be discussed below. Fig. 5.3 shows the deformation that took place during the Central Rand compression at 2.8 Ga and before Platberg extension (2.7 Ga). Carbon on all these contacts is post Platberg.

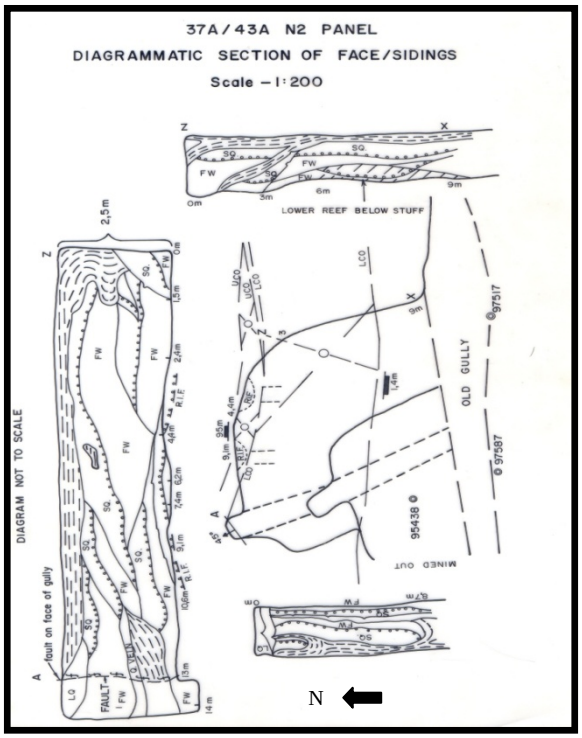

Fig. 5.3 Section of Basal Reef stope faces Western Holdings Mine. Note the multiple reverse faulting towards north and south with all contacts layered with carbon.

According to Hayward (2005) brittle deformation that affects most of the paragenetic sequence of the Central Rand Group late in its post-depositional history is followed by sequences of mineral growth and dissolution that appear throughout the Central Rand Group and have consistent textural relationships with gold.

5.1.2 The stratigraphical control on carbon deposition.

The litho-stratigraphic column (Fig. 1.3) indicates the areas where carbon is the most abundant. The majority of the reefs in this area and their underlying

quartzite are characterised by high degrees of ductile and brittle deformation. Bedding parallel fractures are either present on the contact or within the quartzite or crosscuts the reef or are located within the reef parallel to the contact and within pebbles in the reef.

Carbon layers\lamina occur along and within the conglomerate layers associated with fractures. Secondary permeability (fracture development) is one of the major controls on carbon emplacement.

The lithological layer that hosts the most carbon in the basin is the Basal Reef in the Free State Goldfield, the Carbon Leader Reef in the Carletonville Goldfield or the Central Margin and the Vaal Reef in the Klerksdorp area. The similarity between the former two layers is the type of conglomerate in association with the type of footwall below the conglomerate and the type of layer above the reefs:

1. The Basal and the Leader Reef are a medium to large pebble conglomerate with concordant contacts with the footwall.
2. The yellow argillaceous footwall of the Leader reef and the siliceous grey gritty footwall of the Basal are highly ductile in character. The shale above the Carbon Leader Reef and the Basal Reef acts as aquitards or restricting fluid migration to the layers above the shale. The fluids migrated along and within the shale (where fractured) acting as fluid pathways.
3. The highest percentage of bedding parallel fractures is present in the footwall to the Reefs mentioned.
4. A larger percentage of carbon is present in the Basal Reef when compared to the Carbon Leader Reef and Vaal Reef.
5. The sedimentological characteristic that distinguishes Basal from Carbon Leader Reef and the Vaal Reef is the unconformity between the footwall and the conglomerate of the Basal Reef.

5.1.3 Timing of carbon deposition

The observations in the above section (5.1.1 and 5.1.2) help to clarify the introduction of hydrocarbon fluids to the Central Rand rocks and the timing of their injection. The timing is after major Central Rand compression (2.8 Ga) and Platberg (2.7Ga) extensional phases. Barnicoat et al., (1997) also confirms that the carbon emplacement took place after the major deformation events. The fluid was rich in carbon, iron, sulphide and gold. This is also shown in Fig. 2.2, and is a clear indicator that carbon precipitation is of post Platberg age. However a U-Pb date of 2.3 Ga has been obtained for hydrocarbon migration into the basin by Robb et al., (1989).

Gray et al., (1998) suggest that no major deformation took place after carbon deposition took place; none of the carbon spindles have been fractured or damaged beyond the point of recognising the spindle in its original form. The confusion that is created by various researchers makes it impossible to relate the dates in Table 5.2 nor to correlate them with the logical sequence of events.

5.2 Carbon morphology and contact relationships

The morphology of carbon within the Witwatersrand Basin is discussed in Chapter 2 and in Chapter 3. The classification Type A and Type B carbon, is based on the form and the texture of the carbon refer to Chapter 2 section 2.4.2.

There are two forms of spindles/filaments under the type A carbon classification, being observed on the contact between conglomerate and the quartzite. Filaments with nodules and filaments with no nodule inclusions. The examples below show the form in which the carbon has been observed in various reefs. According to Gray et al., (1998), the carbon was stretched to form these spindles and stopped growing in length with reduction in pressure that kept the contacts apart (Fig. 5.5). Gray et al., (1998) described the carbon

filaments as bedding perpendicular rather than bed parallel, indicating mesophase formation during fracture opening. (Figs.5.4 - 5.9).

In Fig. 5.5 the various stages of carbon stretching are shown in a diagram. The stretching is from the footwall contact to the bottom contact of the conglomerate. Fig. 5.6 shows all three types of carbon that one can observe on the contact of the various reefs.

The shapes vary from cylindrical to planar (filaments) and nodules on planar. The dimensions of these spindles and filaments vary between 1 - 20mm with rare 10cm long spindles in close proximity to thrust faults in Western Holdings 2 shaft. The carbon is at it thickest from the fault up to 10 meters away from fault tapering off to 1mm seam, 20 meters away from fault.

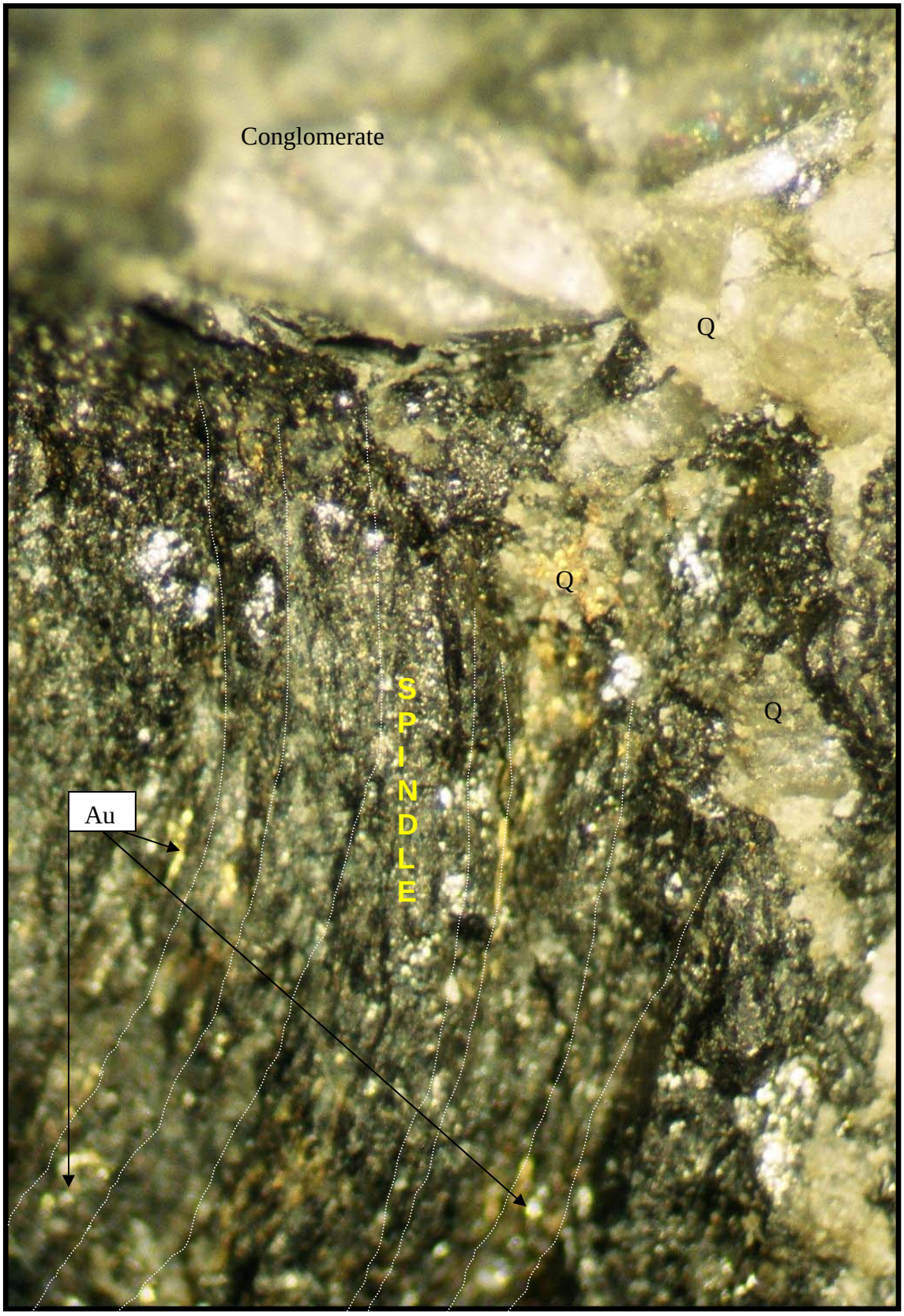

Fig. 5.4 Carbon spindles from Basal Reef Western Holdings Mine. The gold is in between the spindles.

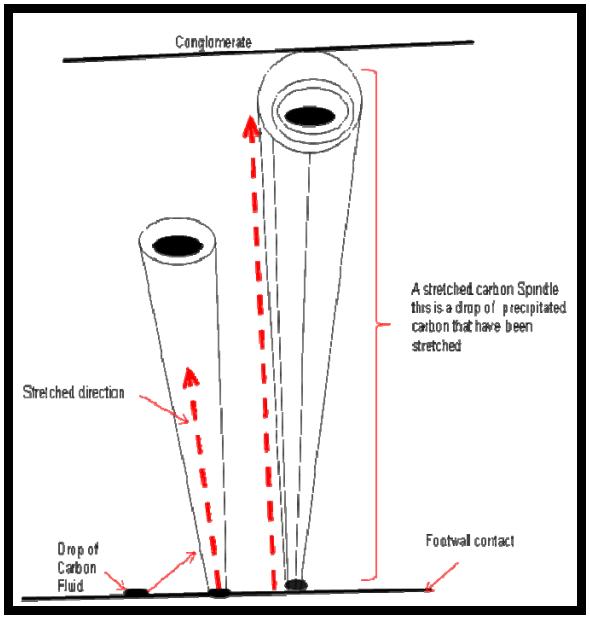

Figure 5.5 The morphology of a carbon spindle.

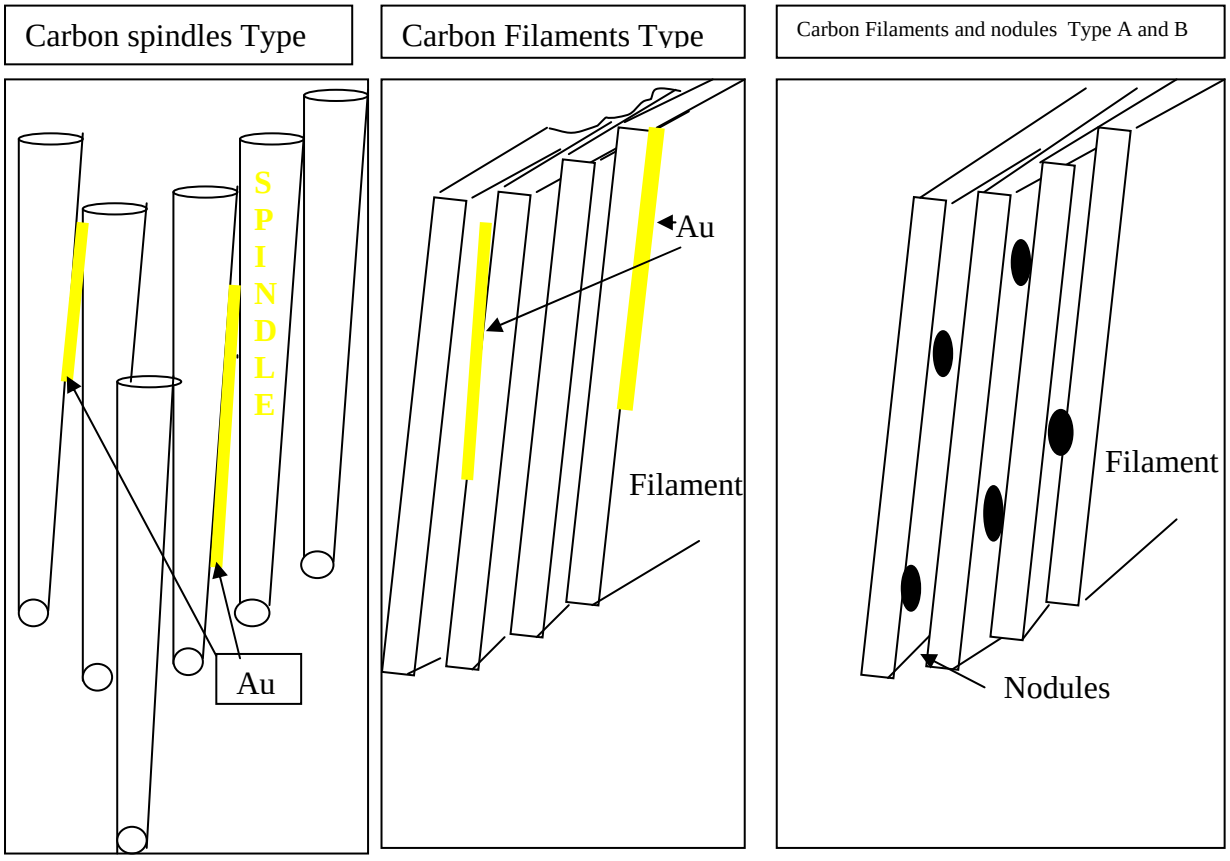

Figure 5.6 The carbon types(spindles and filaments) and the position of gold.

In Fig. 5.4 it is shown that the spindles are slightly rotated showing some movement along the contact.

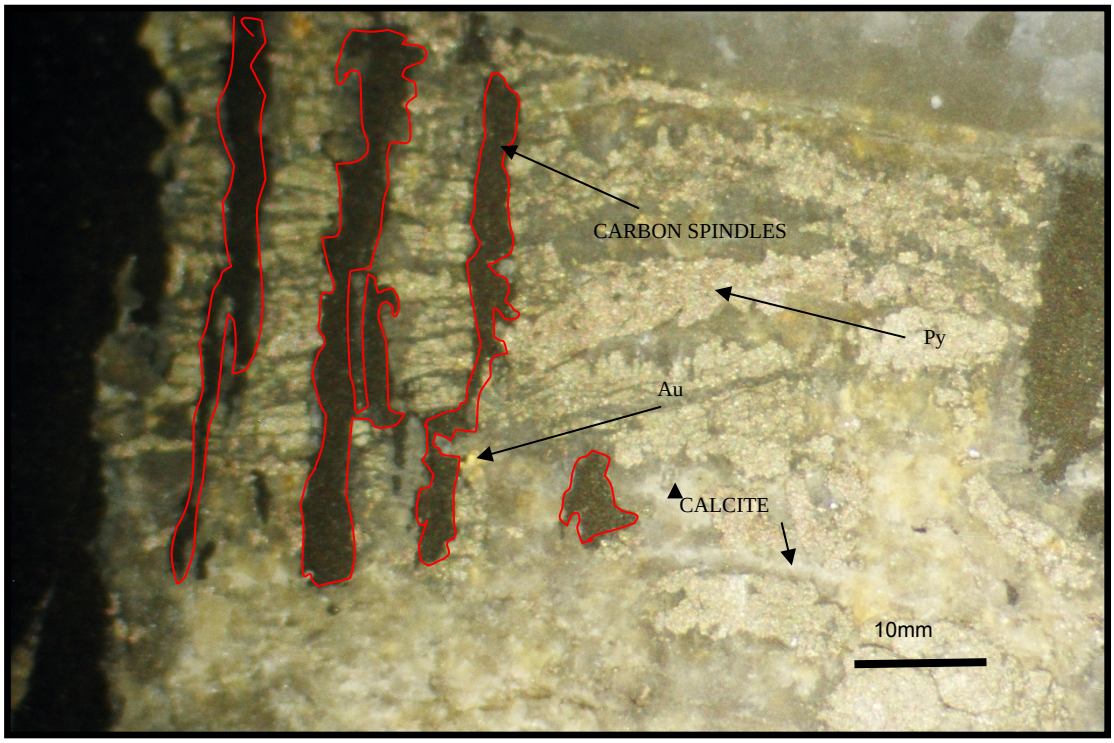

Fig. 5.7 Carbon filling fractures in between pyrite, gold and calcite layers; WHGM Basal Reef.

In Fig. 5.7 carbon indicated by yellow lines, are filling the fractures within the bedding parallel layers of pyrite and calcite. The phases of minerals visible in this view are: Carbon, pyrite, calcite and gold. The first stage is pyrite and calcite, second stage C and Au.

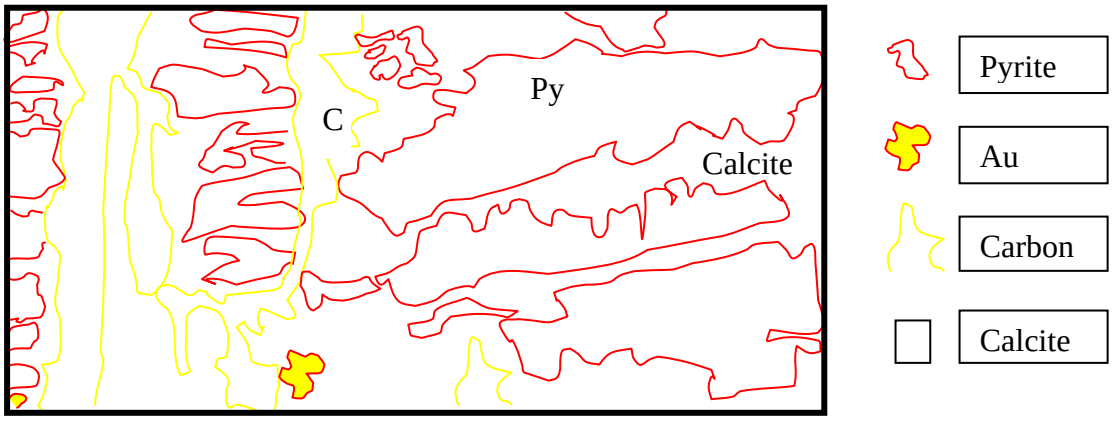

Fig. 5.8 Interpretative sketch of the indicated part of Fig. 5.7 showing the mineral phases and mineral associations.

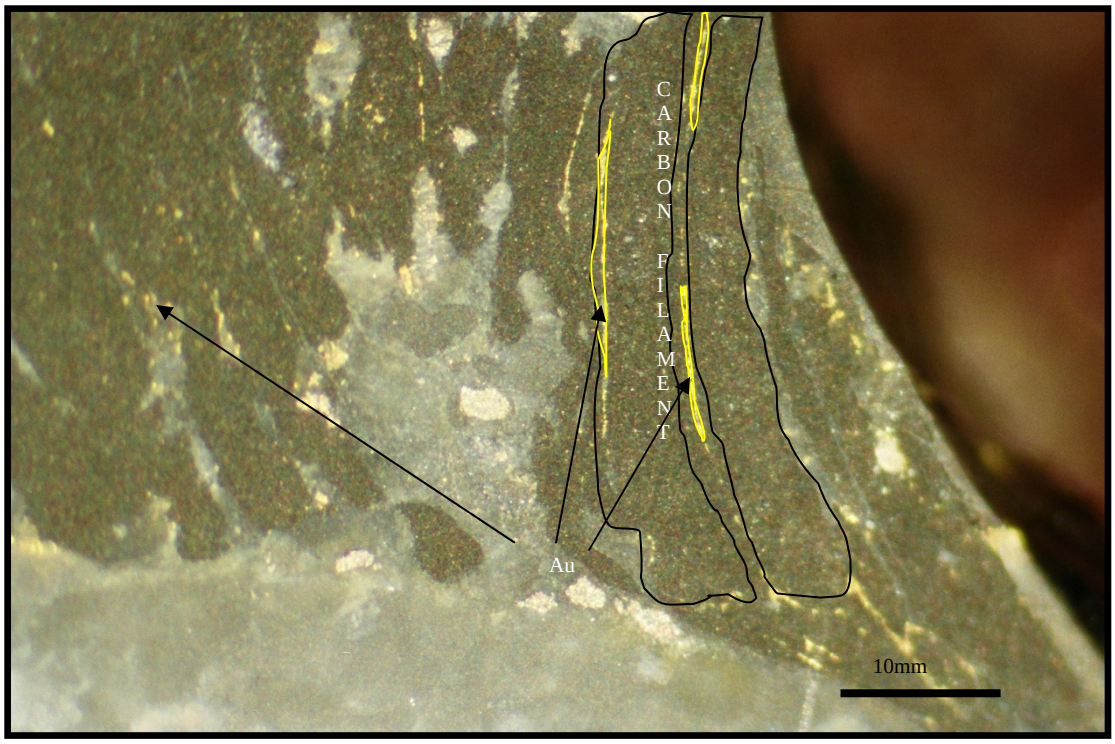

Fig. 5.9 Carbon filaments with gold in between the filaments. B reef Tshepong mine. The gold is situated in between the filaments.

Detailed textural studies done by Barnicoat et al., 1997 indicate that fluid entrapment occurred at a late stage in the evolution of the Witwatersrand Basin. This is corroborated by previous argon chronological information as well as detailed mineralogical analysis of impact-related pseudotachylitic breccias, which also suggests that fluid migration occurred at the time of the 2023 Ma Vredefort impact event (Boer et al., 2006).

According to Frimmel et al., (1999) a largely meteoric source is inferred for the gold-mobilizing fluids in the Witwatersrand reefs because of a lack of Br in the fluid (a composition distinctly different from that of seawater), the presence of organic acids, and $^{18}O_{fluid}$ values around O%.The fluids are ascribed to hydrothermal infiltration triggered by the 2023 Ma Vredefort impact which also created a secondary permeability in the form of a dense network of micro-fractures preferentially in the conglomerate beds of the already metamorphosed Witwatersrand rock sequence. This fluid differs from the

regional metamorphic fluid in the basin by having a considerably higher pH 5.7–7.2. opcit.

5.3 Carbon and associated minerals

1. Carbon is in association with minerals in the fluid pathways quartz (SiO_2), gold (Au), pyrite (Py) and uraninite (U) are all visible under the electron microscope. (Figs. 3.15, 3.18, 3,23). There are more associations that include, calcite, pyrophyllite, lead, thorium, tantalum and sphalerite (Figs. 3.10, 3.11, 3.13, 3.23, and 2.22).

2. Carbon in association with layered mineral phases e.g. the layered pyrite ball in Fig. 5.10. Calcite is associated with gold in the Basal Reef and in the VCR. Calcite is also present with the carbon seam around the pyrite ball (Fig.5.11). It is deduced that the pyrite balls formed within the carbon seam. The carbon and the pyrite ball precipitated out of solution from a hydrocarbon/iron rich gas/fluid. The carbon around the pyrite ball is layered and this resembles the cooling mode as the following minerals precipitated out of solution: pyrite, calcite and carbon (Fig.5.12)

3. The localities in which gold have been found are an indication of the process of deposition (Table 5.1). The interesting fact is that a number of the localities are carbonaceous or the deposition of gold is only possible by hydrothermal fluid movement. The gold at these localities cannot be explained by the sedimentary origin of gold The best example of non-remobilizing of gold is the gold on bedding planes of the Mb5 quartzite, which assayed at 31g/t, 70m below the Vaal Reef. It is too far down from the conglomerate horizon for the gold to be deposited by remobilisation.

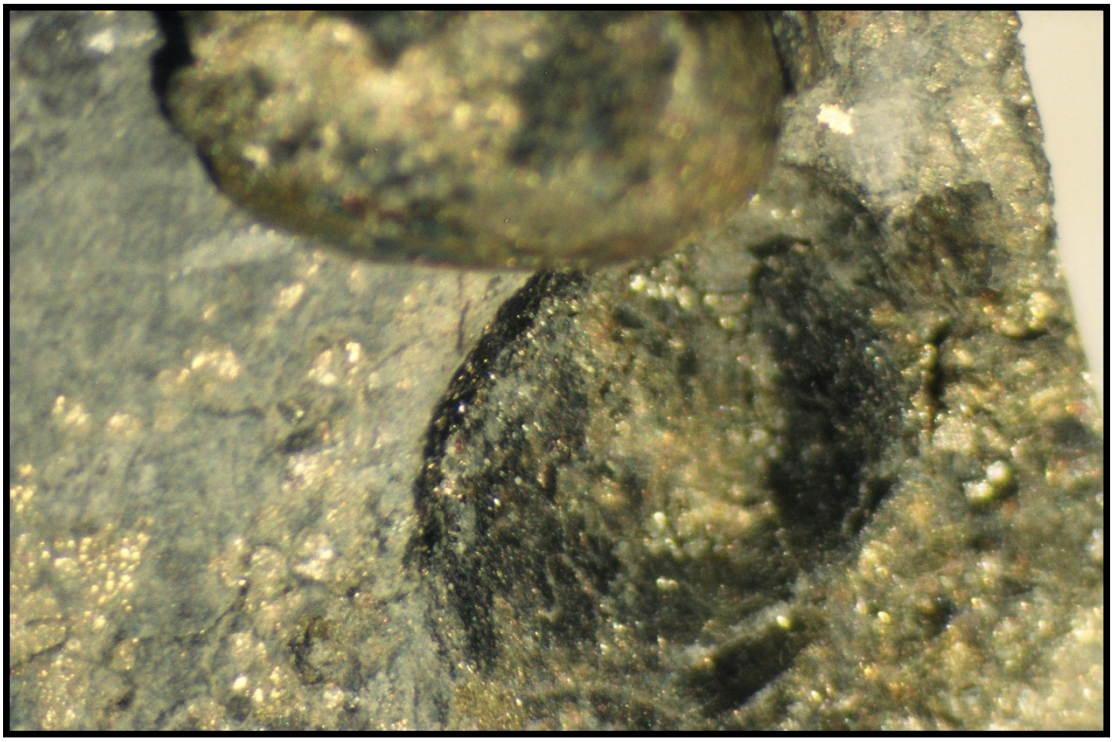

Fig. 5.10 Pyrite ball from carbon seam lying next to the void in the carbon seam from where it has been dislodged. Sample from Basal Reef, WHGM 2#.

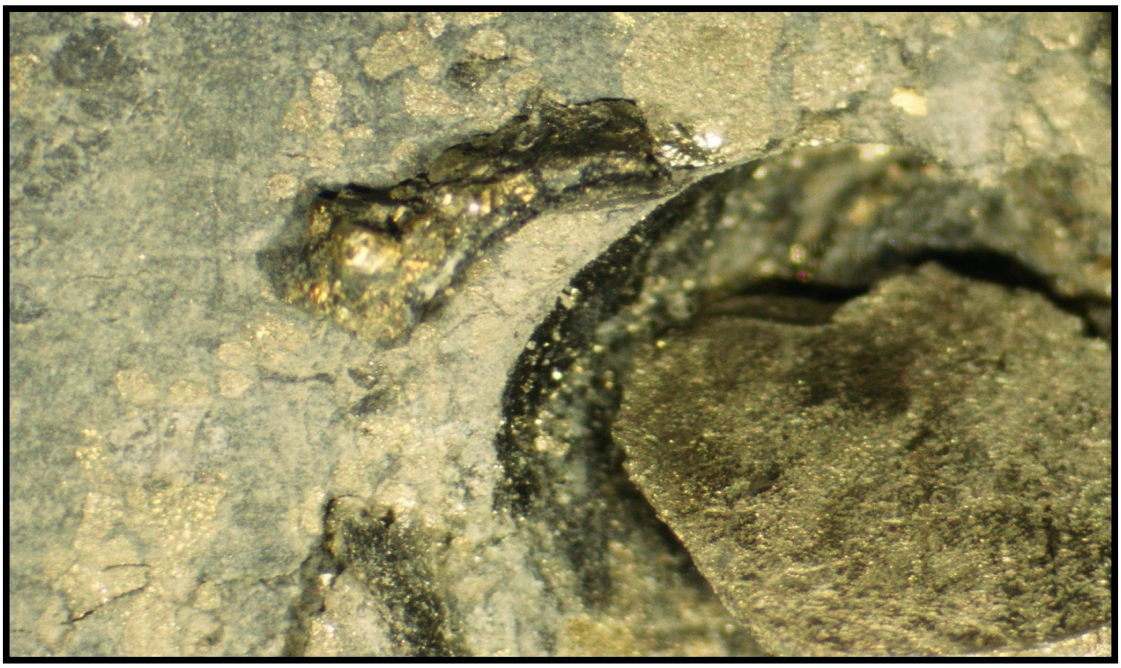

Fig. 5.11 Fragments of the carbon around the pyrite ball show the curved shape of the carbon inside the void. Sample from Basal Reef, WHGM 2#.

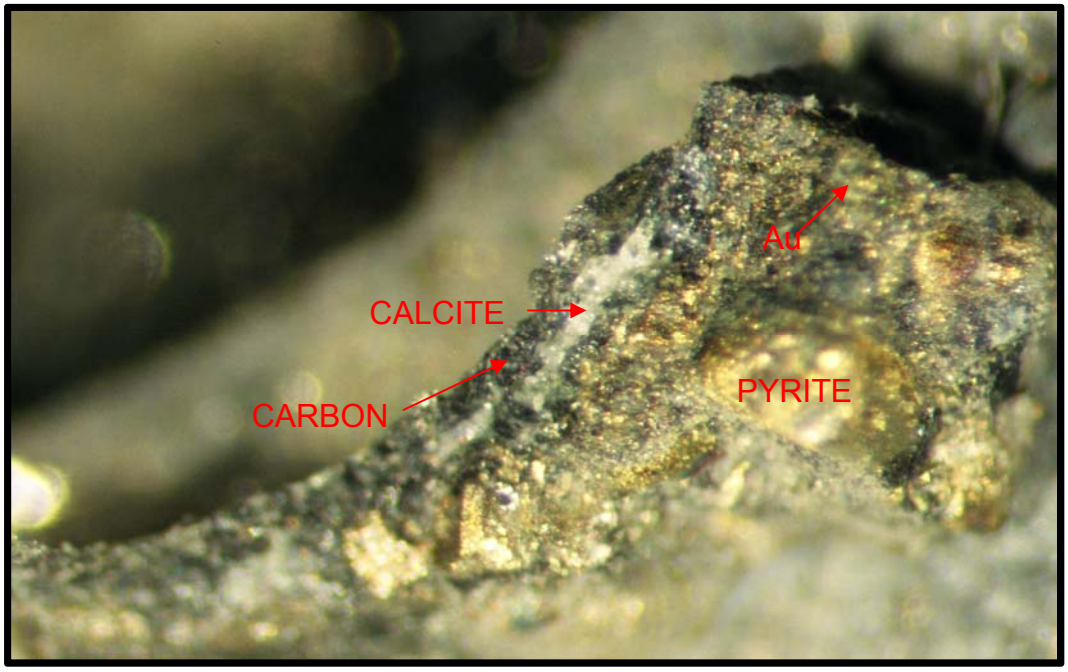

Fig. 5.12 The curved pyrite and carbon outer edge of the void. Sample from Basal Reef, WHGM 2#.

Figure 5.12 suggests that the fluid was rich in Au, Ca, C, Fe, S and CO_2.

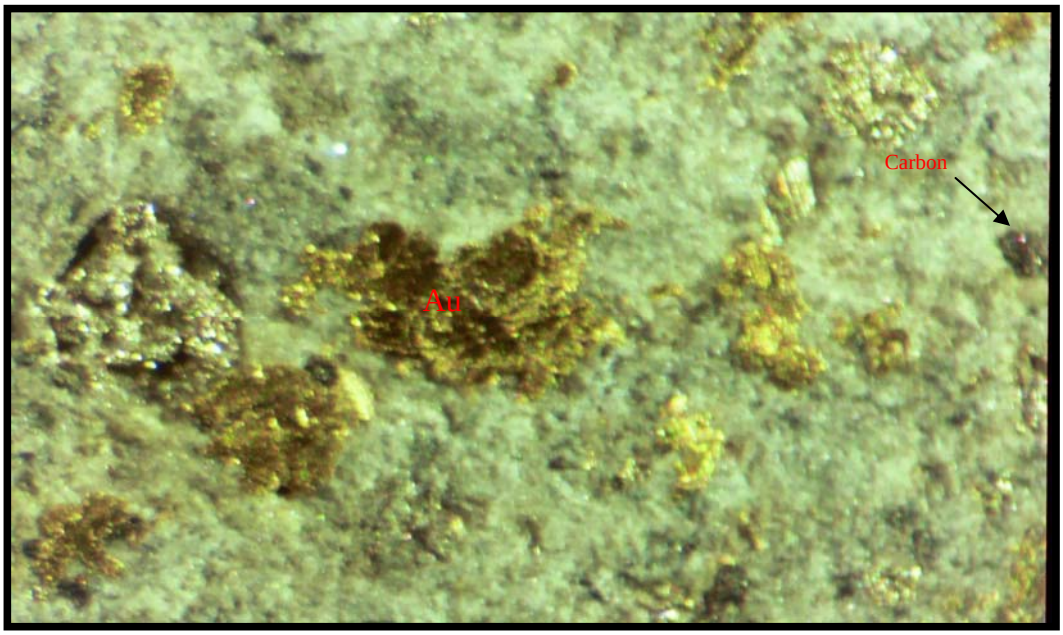

Fig. 5.13 Gold is embedded in chlorite and calcite and pyrophyllite. Sample from VCR, DGM no 2#.

Table 5.1 Gold occurrences related to hydrothermal fluid flow.

Gold occurrences	Description
2.5cm below contact on bedding plane below the Basal Reef	Gold in plate forms
31g.t on bedding plane 71m below Vaal Reef	Gold in fluid pathway nuggets in various shapes
Below Basal Reef	Gold plates of 0.1 mm 2# pillar WHGM
Gold in pyrite	Gold microscopic but in any possible shape
Gold in calcite	Gold in any shape
Gold in quartz vein	Gold is a thick plate precipitated out of solution on top of the pyrite in the same vug.(Fig. 5.20)
Gold in the greenbar	Gold (microscopic)

5.4 Discussion

The gold ore body consists of half a dozen economic conglomerate layers. A total of five reef types do have carbon on the contact or in the conglomerate. Most of these carbon deposits are located on ramps and in bedding parallel fractures. These deposits form part of a later hydrothermal event that post dates the structures associated with the compressional event in the WWR basin at 2.8Ga.

Published information about metamorphic and C-Au-U age relationships, compelled the author to summarize the most recent research results in a table which will highlight the confusion that exists between the researchers from 1990 to 2006. Table 5.2 compares different views on timing of the events and the origin of gold and carbon.

Table 5.2 Comparative summary of 20 researchers

Researcher/s	Publication date	Peak metamorphism Date	Au Date	Uranium Date
BOER	2006	None	None	None
PARNELL	2005	BUSHVELD 2055-2056	Pre 2023Ma	None
LAW & SPENCER	1992	NONE	2.7-2.6 Ga	
PHILLIPS & LAW	2000	2023-2557 Ma	NO DATE	NO DATE
GROVES & FRIMMEL	2003	2250-2350Ma LOWER BASIN 2056Ma HEATING LAVA 2720Ma	3016Ma 3033Ma	3050Ma
LAW	2005	CHLORITE & PYROPHYLLITE	PRE DATE PLATBERG (2709Ma)	DETRITAL
PHILLIPS & MEYER	1989	None	None	None
HAYWARD	2005	None	None	None
BARNICOAT	1997	None	POST DATE HIGH ALTERATION	None
FRIMMEL	1999	None	2,5- 2,0 Ga	None
FRIMMEL	2005	None	None	None
GIBSON	1995	2100-2000	None	None
RASMUSEN	1997	BUSHVELD 2056	None	None
ROBB	1993	None	None	None
KIRK	2001	None	None	None
FRIMMEL & MINTER	2002	BUSHVELD (Sericite age)	DETRITAL 3000Ma	NO DATE

Researcher/s	Carbon date	Au Origin	Carbon Origin	Metamorphic events	Stages
BOER	2023Ma	Pre Vredefort	VREDEFORT IMPACT	None	None
PARNELL	2023Ma	Pre 2023Ma	VREDEFORT IMPACT	BUSHVELD 2055-2056	None
LAW & SPENCER	DETRITAL AGE	GREEN STONE BELT	ORGANIC	NONE	
PHILLIPS & LAW	NO DATE	META FLUIDS	NO DESCRIPTION	1	None
GROVES & FRI,MMEL	2023	DETRITAL	OIL FROM SHALE VREDEFORT IMPACT	Roering date Bif 2480 VREDEFORT Impact 2023Ma PLUTONISM 2078Ma	5
LAW	DETRITAL AGE	META FLUIDS	OIL FROM SHALE	None	None
PHILLIPS & MEYER	None	EPIGENETIC	NO DESCRIPTION	None	None
HAYWARD	None	None	None	WIDESPREAD	1
BARNICOAT	None	HYDROTHERMAL	OIL BOOYSENS	COMPRESIONAL DEFORMATION	None
FRIMMEL	None	METEORITE	None	BUSHVELD 2055-2056	None
FRIMMEL	None	None	None	None	None
GIBSON	None	None	None	Indicating2,1-2,0Ga	None
RASMUSEN	None	None	None	None	None
ROBB	2033	None	None	None	None
KIRK	None	2990Ma	None	None	None
FRIMMEL & MINTER	DETRITAL AGE	DETRITAL	ORGANIC	BUSHVELD	None

5.4.1 Placer theory vs Hydrothermal theory vs Modified Placer theory

It is impressive to note that the oldest hypothesis on the origin of metals within ore bodies via channel ways has postulated as far back as 1556. *Re Metallica* (1556) by Georgious Agricola. To a certain degree all the research done to date suggests fluids and fluid migration as being the origin of carbon.

The carbon distribution in the Witwatersrand Basin is controlled by the structural character of the Basin. The carbon emplacement in the Carletonville goldfields is structurally controlled. Fig. 2.16 is a specimen from the carbon leader reef in the Carletonville goldfield. In this sample, two seams of carbon are structurally emplaced along two bedding parallel fractures which crosscut all of the existing fabrics associated with the 2.8Ga compressional event affecting the WWR basin.

The four theories as mentioned in chapter one are now reviewed below to understand the differences between them concerning the origin of carbon.

1. The Placer theory

   The placer model describes carbon as an algal matt for entrapment of gold. The gold washed in with the sediments and the load was deposited on top of the algal matt and the reefs. Refer to Chapter 2, 2.3. The placerists do not explain origin of carbon in the Wits Basin due the misconception that 10cm algae seam today represents, a prior 7m of algae growth; the algae theory also does not explain carbon on folds or on fault planes.

2. The Hydrothermal theory

   The fluids that formed the carbon seams are ascribed to hydrothermal infiltration triggered by the 2023 Ma Vredefort impact (Frimmel et al., 1997).

3. Modified placer theory

   The modified placer theory combines elements of the detrital ore hypothesis and post-sedimentary thermal overprints. This theory explains carbon as an oil, migrating into the lower lying conglomerates of the middle to lower Central Rand Group. This theory does not explain the carbon on the reef packages above the Booysens shale, e.g. the Ventersdorp Contact Reef (Robb et al. 1997; Frimmel and Gartz 1997; Frimmel and Minter 2002; Gibson and Reimold 1999; Foya 2002), nor carbon associated with the Black Reef.

4. The Volcanic theory

   This theory see all gold originating from overlying volcanic and that the gold permeated into the layers and this theory does not explain the origin of carbon on the contacts of the reefs nor does it explain the existence of carbon on fault planes (Davidson, 1964-65).

Boer et al., (2006) argued inflow of fluids from the Vredefort Impact event. My observations are in agreement with this and my time line for the emplacement of carbon and gold is post Platberg (Chapter 2). According to Zhao et al., (2005) gold appears to have been locally remobilized and possibly derived from pre-existing placer concentrations, which have weathered from greenstone and gneisses from the hinterland. I disagree with this as my basin wide study support a hydrothermal origin.

Minter (1999) summarised the sedimentologic and stratigraphic relationships of the Central Rand Group, arguing that the conglomerates are ancient placers deposited under fluvio-deltaic conditions. Both Bailey et al., (1990) and myself have observed two major changes in the sedimentological history of the Witwatersrand Basin. I have modelled the footwall to the Vaal Reef as a marine environment for the Vaal Reef. Fig. 4.1a and the Kimberley reefs are described as a shallow marine deposit by Bailey et al., (1990).

In his paper, Minter (1990) cited the 1986 abstract of a subsequently published paper by Hutchinson and Viljoen (1988) who also considered many of these aspects and attempted to integrate them all in a broad genetic hypothesis. In addition, they emphasized the additional important problem of determining the source for the Witwatersrand gold. It is therefore important to find the source of the 3.03 Ga year gold of Kirk et al., (2001).

Although this issue was partially addressed by Reimer and Mossman (1990), the question has been generally underemphasized in earlier work and was, therefore, not stressed. My argument based upon this study is that the gold is not from the hinterland but from a hydrothermal source.

The existence of gas within the Witwatersrand Basin, as researched by Boer et al., (2006) is based on a few observations in the fault zones. One of the author's chosen samples is very specific. This example is a hand sample of a quartz vein that contained a vug. In the vug was a small ball of carbonaceous material that was covered with bornite and pyrite. It is inferred that the vug was originally a gas bubble within a very hot fluid high in silica that formed the quartz vein. The gas that filled the bubble was carbonaceous and after cooling the carbon precipitated out of the hot solution. (e.g. Fig. 5.14.) Boer et al., (2006) studied fluid inclusion petrographyc and quadrupole mass spectrometric analyses of the Ventersdorp Contact Reef conglomerate and footwall quartzite samples, as well as Vredefort impact-related pseudotachylitic breccias from the bedding-parallel fault zones at the top and bottom of the Ventersdorp Contact Reef. These analyses by Boer et al, were obtained in an attempt to derive new information on the types of fluids that may have been involved in gold mineralization during the history of this important ore deposit.

Samples from Tau Lekoa Mine, previously known as the Vaal Reefs No. 10 Shaft Mine in the Klerksdorp goldfield, and samples from the western part of Elandskraal Mine, previously known as the Elandsrand Gold Mine in the Carletonville gold-field, were analyzed by Boer (Boer et al., 2006).Three populations of predominantly secondary fluid inclusions are recognized. The earliest one comprises small, wispy-textured inclusions or very small inclusions filled with CH_4. The second involves a moderately saline fluid and the third one a CO_2-rich fluid with variable CO_2/H_2O ratios. Microthermometry indicates fluid entrapment temperatures from 220 to 370 °C at 2 kbar. Tau Lekoa fluid inclusions are enriched in CO_2 compared to the CH_4-enriched inclusions in Elandskraal samples. These differences are explained by comparatively more reducing conditions of fluid entrapment at Elandskraal at 2023Ma.

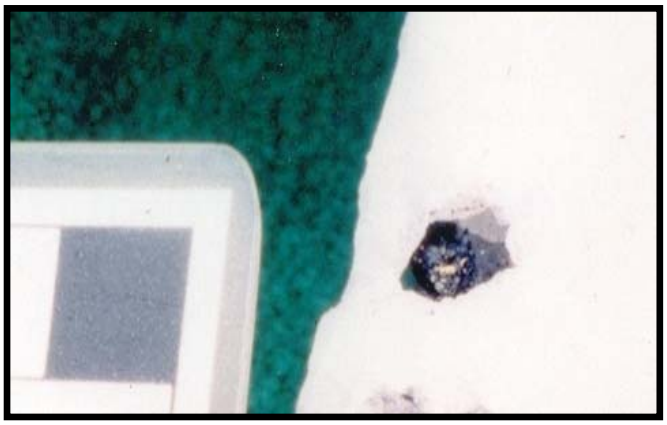

Fig. 5.14 Carbon in vug. Sample from WHGM no 2#

The site specifics of carbon deposits determine the mode of emplacement and gave insight into the emplacement history of carbon. What follows are arguments around the specific sites where carbon is located. Carbon is located along fluid pathways as veins, bedding planes, faults and quartz veins. These are some of the observations that have been made underground. It is deduced that hydrothermal fluids migrated throughout the Central Rand Group part of the basin and that the master bedding plane fault possibly played a significant role in the ingress of fluids into the Central Rand

Group. (e.g. Fig. 5.18 where it is showed that the rutile, pyrite and carbon are all situated in the fluid pathway within the master bedding plane fault.

5.4.2 Metamorphic overprint of the Witwatersrand Basin

Phillips et al,. (1989) studied the coexistence of pyrophyllite-chloritoid-chlorite-muscovite-quartz-rutile-tourmaline-pyrite in shales, arenites and conglomerates within the Central Rand Group showing regional metamorphic conditions over a strike length of 200km. Peak metamorphic temperatures are suggested of between 350º- 400ºC. Coetzee et al., (1995) has seen these isograds truncated by the Black Reef unconformably overlying the Ventersdorp Group. It is therefore deduced that a minimum age for the WWR metamorphic is pre 2.6 Ga and probably reflects the the compressional event at 2.78 Ga in the Witwatersrand Basin (eg. Law and Spencer, 1992).

Zhou et al., (1994) noted that the Witwatersrand goldfields contain abundant assemblages that include pyrophyllite, chloritoid, chlorite, kaolinite and/or kyanite, with quartz. A chemographic analysis done by T. Zhou et al., (1994) of the system Fe (Mg)-Al-Si-O-H involving these minerals, yields 22 potential phase diagrams. Using orientation criteria and thermodynamic calculations as further constraints, this list has been reduced to three possible diagrams. New thermodynamic data favour one of these in particular. This chemographic analysis demonstrates that formation of chloritoid is not restricted to the breakdown reaction of kaolinite plus chlorite in the FMASH system, as stated by previous studies, but could be from pyrophyllite + chlorite → chloritoid + quartz + H_2O.

The metamorphic variation in temperature for various Witwatersrand goldfields fall within the range of 300°C - 400°C, based on chlorite and chloritoid compositions. The lower and upper pressure limits are constrained by the andalusite to kyanite, and the sudoite/chlorite to carpholite boundaries, i.e. 1.5 kbar–2.8 kbar, and 7 kbar, respectively. It is deduced that the main

fabric forming event in the Witwatersrand Group rocks was formed at greenschist metamorphic facies conditions (T:300-400°C; P: 1.5-2.8 Kb)

Under the S.E.M. both pyrite and uraninite are visible in fluid pathways (Fig. 3.14). The association of the pyrite and the uraninite in Fig. 3.15 shows that the fluid pathway is formed in pyrophyllite. The spatial arrangement of gold in the chlorite is evident of late stage intrusion of fluids / gas into the Witwatersrand Basin. The fluid inflow is post tectonic.

Fig. 3.13 shows the uraninite has replaced the pyrophyllite fabric and gold is plated onto the carbon filaments; it also occurs in vug form within a fluid pathway in Fig. 5.14. The gold vein is not plated onto the carbon as seen in the spindles on the reef contact, but it is crystallized in the fractured space Fig.5.15. It is suggested that gold originates with the carbon gas at temperature exceeding 900° C and was transported as a melt from the mantle, cooled down in the crack and crystallized (Fig.5.15).

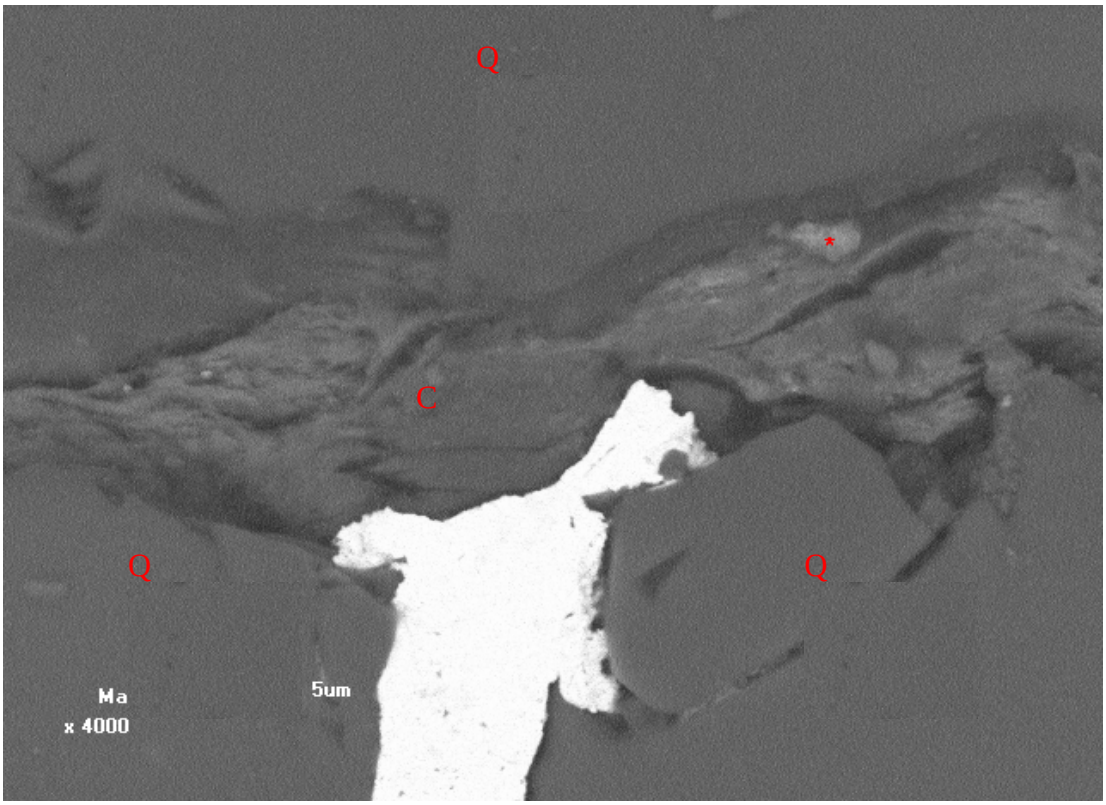

Fig. 5.15 Gold vein in a fluid pathway filled with carbon. Basal Reef, WHGM Western Holdings Gold Mine sample RB 112228.

The fact that the carbon is deposited along the sub outcrops is unique to that particular environment. The fluid migrated along the sub outcrop boundary. The historic structural and sedimentological erosional events had a direct control on the emplacement of carbon in this setting. Carbon within the shale above the basal reef and in the green bar is two deposits which shed light concerning the host to carbon. These shales are considered to be the fluid pathways for the ingress of carbonaceous gas from the mantle to the basal Reef and the Carbon Leader Reef. The reason for this carbon association is that the shale layers are ductile and form thrust zones and these serves as conduits for gas and fluids.

5.4.3 The timeline for gold, carbon and associated minerals in the Witwatersrand Basin

It is observed that the Platberg-age extensional faults (2.7Ga) truncate the mineralized reefs, alteration zones and the host structures (Law and Spencer, 1992). This implies that gold is introduced to the basin at 2700-2600 Ma. The same time as the gold has been introduced to the greenstone belts. On the contrary, this assumption is proven false by the vast amounts of gold discovered along the sub outcrop line between the Ventersdorp Contact Reef and the Middelvlei Reef in the Driefontein ore body at 2 Shaft, as well as along the Ventersdorp Contact Reef and the Carbon leader reef at 4 Shaft. These are zones of mineralization that cover areas on dip for a few kilometers and on strike for a few hundred meters (200m–300m in places).The sub outcrop is an area where erosion took place and not where enrichment took place. These occurrences are interpreted as late stage introduction of gold and proof for hydrothermal fluids transporting the gold into the basin and in particular to the sub outcrop areas.

Detailed textural studies indicate that fluid entrapment occurred at a late stage in the evolution of the Witwatersrand Basin (Post Bushveld Igneous Complex) This is corroborated by previous argon chronological information as well as detailed mineralogical analysis of impact-related pseudotachylitic breccias,

which also suggests that fluid migration occurred at the time of the Vredefort impact event. There was however a deformation event after the gold was deposited which could be described as a relaxation event. (Fig. 5.16). The fracture seen in Fig. 5.16 occurs and post-dates the precipitation of pyrite and Galena within the Carbon Leader Reef at Driefontein Gold Mine. There was a 20km displacement along the Master bedding plane fault which was observed by the author in the Driefontein Gold Mine, which displaced the Black Reef. In the relaxation phase the fault is in a normal sense placing Black Reef shale on top of Ventersdorp lava. The same multistack reef package was observed by the author in the Western Holdings Gold Mine, in the Beatrix Gold Mine and at Vaal Reefs Gold Mine where the author drilled a reactive thrust fault with the top reef displaced in a normal sense on top of the bottom reef. This movement was north over south and may be linked to the sequence of deformities associated with the Vredefort event.

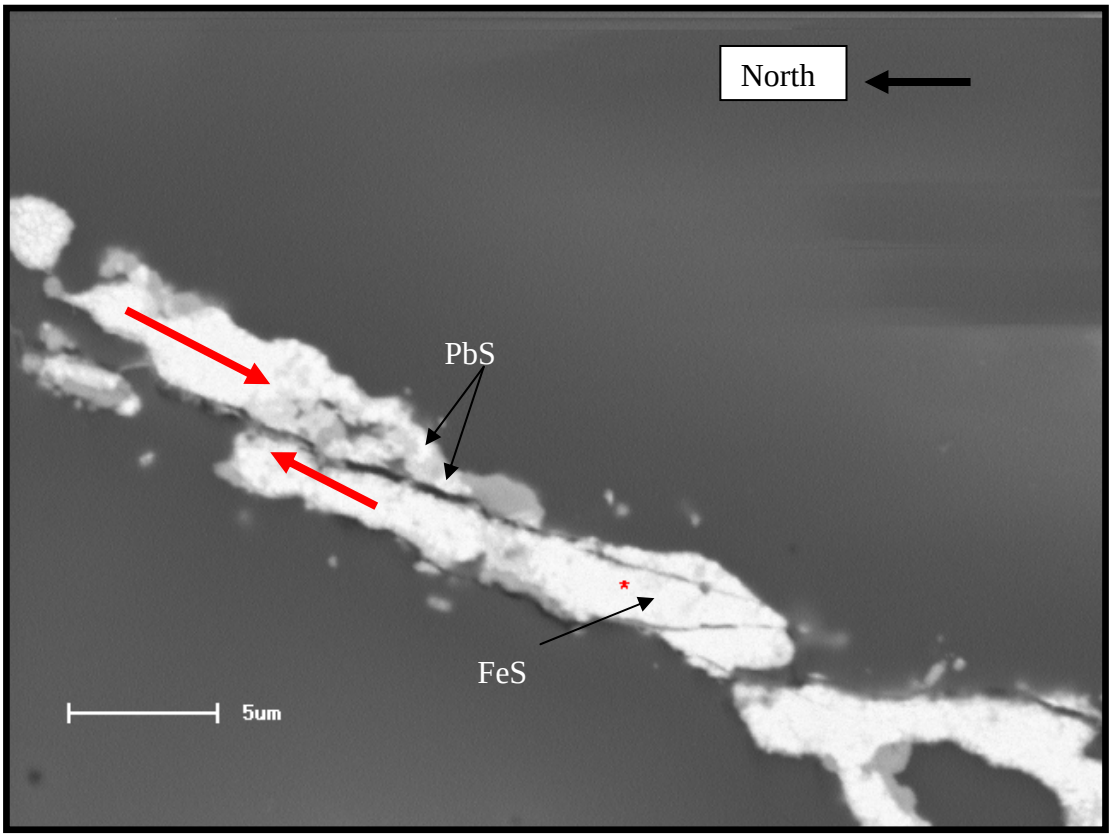

Fig. 5.16 *This is a backscatter image of the pyrite and Galena being displaced in a very fine crack. Driefontein Gold Mine Carbon Leader reef. Sample no. ZW 115. Direction of movement indicated with red arrow*

This small scale micro structure can be interpreted as post Vredefort.

5.4.4 Problems identified with the current models for the nature and origin of gold (Au) and Carbon(C)

The sedimentological explanation for the origin of sediments within the basin was accepted for years but not for the origin of gold. Hence the vast number of contradictory arguments. In attempting to solve this problem with the nature and origin of gold and carbon, attention needs to be given to the following observations: Refer back to Table 5.2

- The osmiridium age for gold is 3030 Ma. Gold is older than the Witwatersrand Supergroup rocks with a deposition age of 2955 Ma.

- The ore body is known for half a dozen economic conglomerate layers.
- The conglomerate layers according to the sedimentologist belief had the same gold mineralization pattern for each layer, which is a bit difficult to model if each layer needs the same sediment source and the same type of gold with an age older than the basin.
- The isotope signature for gold suggests various sources from the mantle; this phenomena has never been addressed.
- The modified placerists need the placer gold to be remobilized for only a few meters.
- The movement of gold along bedding planes, faults and quartz veins are ignored.
- The fact that the gold is deposited along the sub outcrops is ignored.
- Carbon is developed on most of the reefs and its existence renders a biological condition to each reef type and the exposure to the same physic/chemico conditions for each layer according to the sedimentological argument.
- Gold within the green bar is ignored.
- Gold is deposited along fluid pathways (fault planes, bedding planes, unconformities)
- Carbon occurs within crack in quartz pebble.
- Gold is deposited on bedding planes.
- Hydro-carbon migration dated at 2300 Ma. But no carbon observed in the overlying stratigraphic groups except the Black Reef, dated at 2600 Ma.

The nature of gold within carbon is important to understand the timing of both the carbon and the gold. Gray et al., (1998) described carbon mesophase lamellae, as seen in Fig. 5.6. The gold is plated onto the lamellae and the observation suggests that the carbon and gold was transported into the basin at the same time. Fig. 3.17 and Fig. 3.15 indicate that the uraninite, gold and pyrite post dates pyrophyllite fabric formation (Post Witwatersrand contractional and metamorphic event at 2.8 Ga). The three mineral phases

gold, carbon and pyrite occurring together further suggests that they formed at the same time from the same fluid (Fig.5.12).

The order of precipitation in Fig. 3.17and 3.17a is as follows:

Py, U, Pb, C, Au, Ca, Si

The three dimensional diagram shown in Fig.3.17a depicts the order of precipitation in the fluid pathways. The pyrite is emplaced within the pyrophyllite within a fluid pathway and this is indicative of the sequence of mineralization. The uranium replaced the pyrophyllite within a fluid pathway and the pyrite has been crystallized in the fracture within the pyrophyllite and exhibit the shape of the space in the fracture.

The high grade samples and low grade sample differ in mineral content but it is noted the uraninite content is the highest in the high grade samples. The element tantalum is also prominent in one of the high grade samples. The most prominent mineral in defining the fluid pathways within the matrix of the various reefs is pyrophyllite.

5.5 Hypothesis Vredefort Impact model

5.5.1 Why this model

The reason for choosing this model is based upon:

- Post Transvaal age of carbon
- Coexistance of C-Au-U-Py as mineral phases within the same fluid phase
- Vredefort Impact Event has the energy to drive this hydrothermal fluid.

This model includes a diagrammatic view of the impact and a theory for the origin of gold and carbon.

5.5.2 Assumptions

1. All carbon post- dates Platberg extension (2709 Ma).
2. Carbon emplacement post-dates the Witwatersrand metamorphic fabric.
3. It is assumed that the carbon on the Black Reef is of the same emplacement age as that of the Witwatersrand Basin. This implies that the carbon is then younger than 2642 Ma. As carbon is closely associated with gold, it implies that the gold them is also younger than 2642 Ma.
4. A major deformational/thermal event, the Vredefort Impact event is documented at 2023 Ma.
5. The age of carbon is therefore bracketed between 2056 Ma and 2023 Ma.
6. The strong association of gold and carbon suggests that the emplacement of gold and carbonaceous fluids/gasses is also bracketed between the above ages.
7. The controversy (eg. Beach and Smith, 2007) concerning the Re – Os age determination (Kirk et al., 2001) suggesting the isochrons obtained (3030 Ma) preclude the origin of gold mineralization through a hydrothermal process, as these ages predate the deposition of the Central Rand Group host rocks.

The model here proposed to explain carbon and gold in the Witwatersrand Basin is based on an impact model namely the 2.03 Ga Vredefort Impact event.

Carbon that was observed in the phylonitic zones is present due to the gas that has been trapped after the flow of gas was inhibited by either saturation or due to the constraint of porosity due to the saturation of space or the relaxation of pressure from the source (Fig. 2.3). Carbon everywhere in the Precambrian precipitated from a carbonaceous fluid. Gold was transported in the last melt form, from the mantle carrying the isotope signature that reflects the age of gold (3030 Ma)

The catalyst to catalyse this dehydration process is a tantalum silicate. The suggested reaction is where the Carbonaceous gas in the vapour phase gets dehydrated by tantalum silicate. The carbon precipitates out of solution and the gold crystallizes within the carbon.

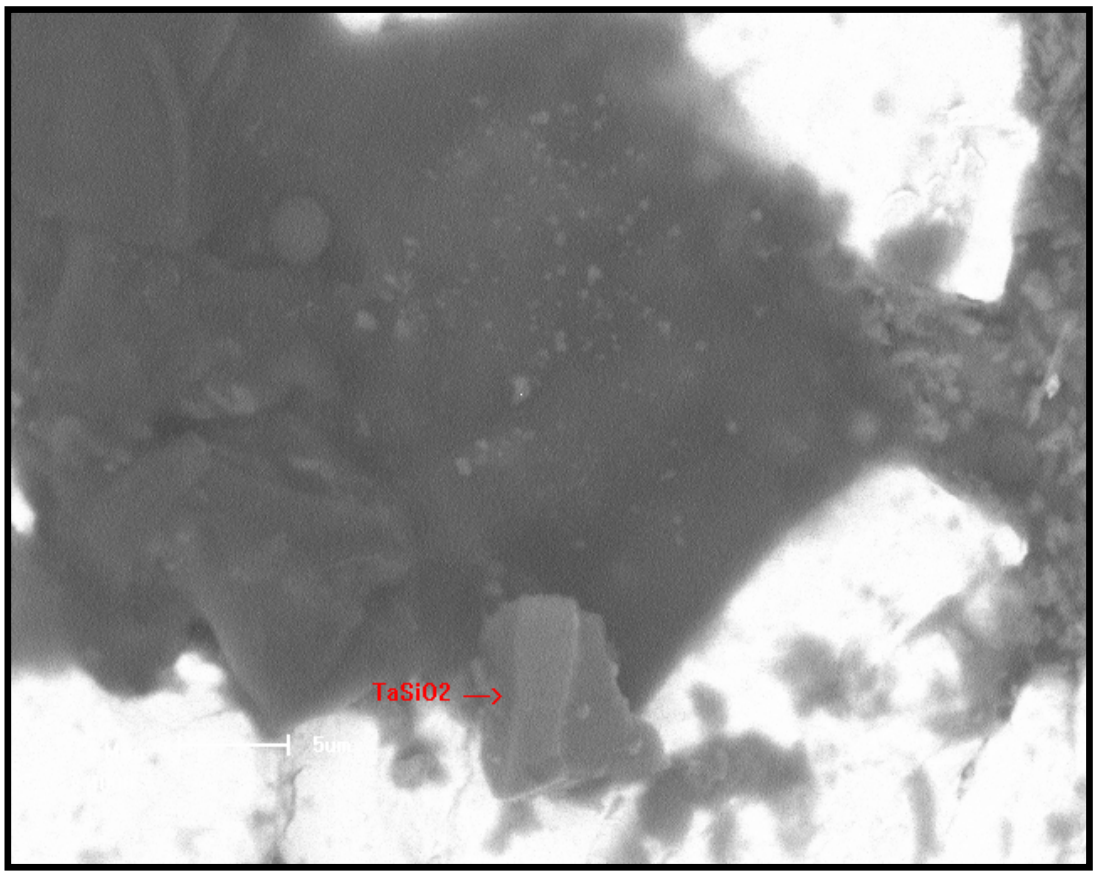

Fig. 5.17 This sample is from the western holdings 2# pillar note the Ta in the centre of the photo.

Considering the deposition of the minerals tantalum, gold, carbon and uraninite within the same fluid pathway. (Fig.5.17), it is strongly suggested that the phases formed at the same time and therefore originate from the same source. The effect of the Vredefort event has been described as being basin- wide on the Kaapvaal Craton. Shockwaves leading to compression and extension structures and re-activation of earlier structures including shock metamorphism was the general effect of the impact on the Witwatersrand Basin.

Thrusting associated with the impact event is best seen along the contact of most reefs as bedding parallel fracturing was studied by Barnicoat et al., (1997). Jolley et al., (2004) studied the gold values along the reefs with high percentage fracturing and noted that the gold values increase as the fracturing intensifies. The fluid transports pyrite, carbon and rutile now crystallized in the fluid pathway. (Fig.5.18). This implies that the Master bedding plane fault is a massive fluid pathway and can dominate the mineralisation of the reefs above the plane; carbon is not present in the reefs below the Master bedding plane fault.

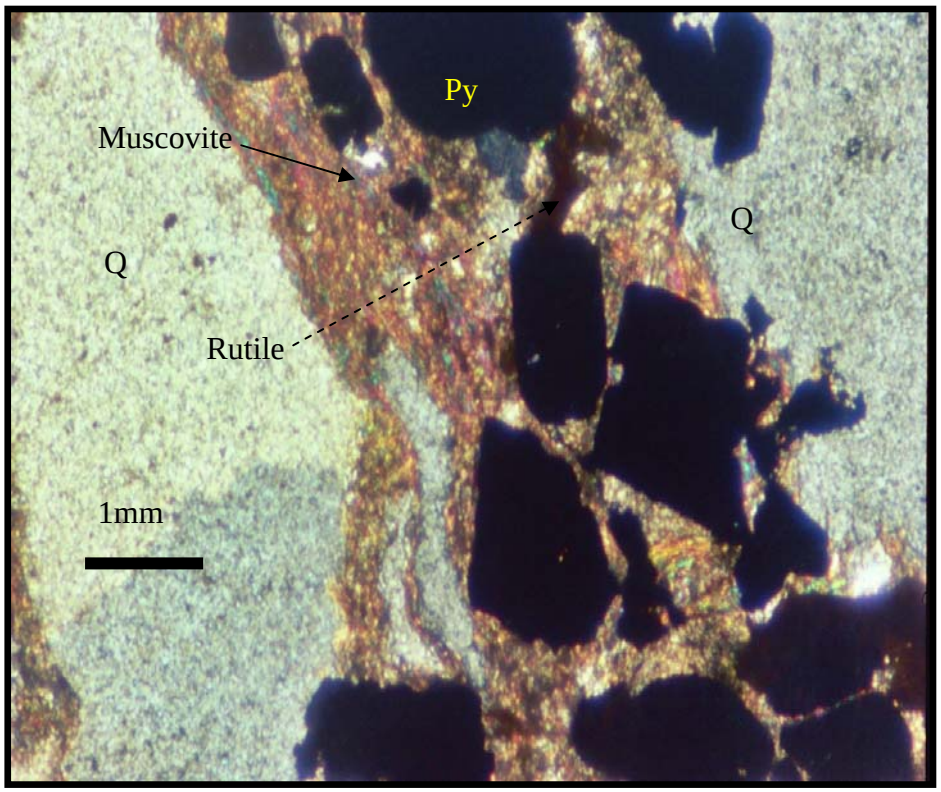

Fig. 5.18 Bh E1s: a fluid pathway in the altered quartzite within the Master bedding plane fault within the footwall quartzite to Carbon Leader Reef. Driefontein Gold mine. Sample no: ZW 747.

5.5.3 The impact process

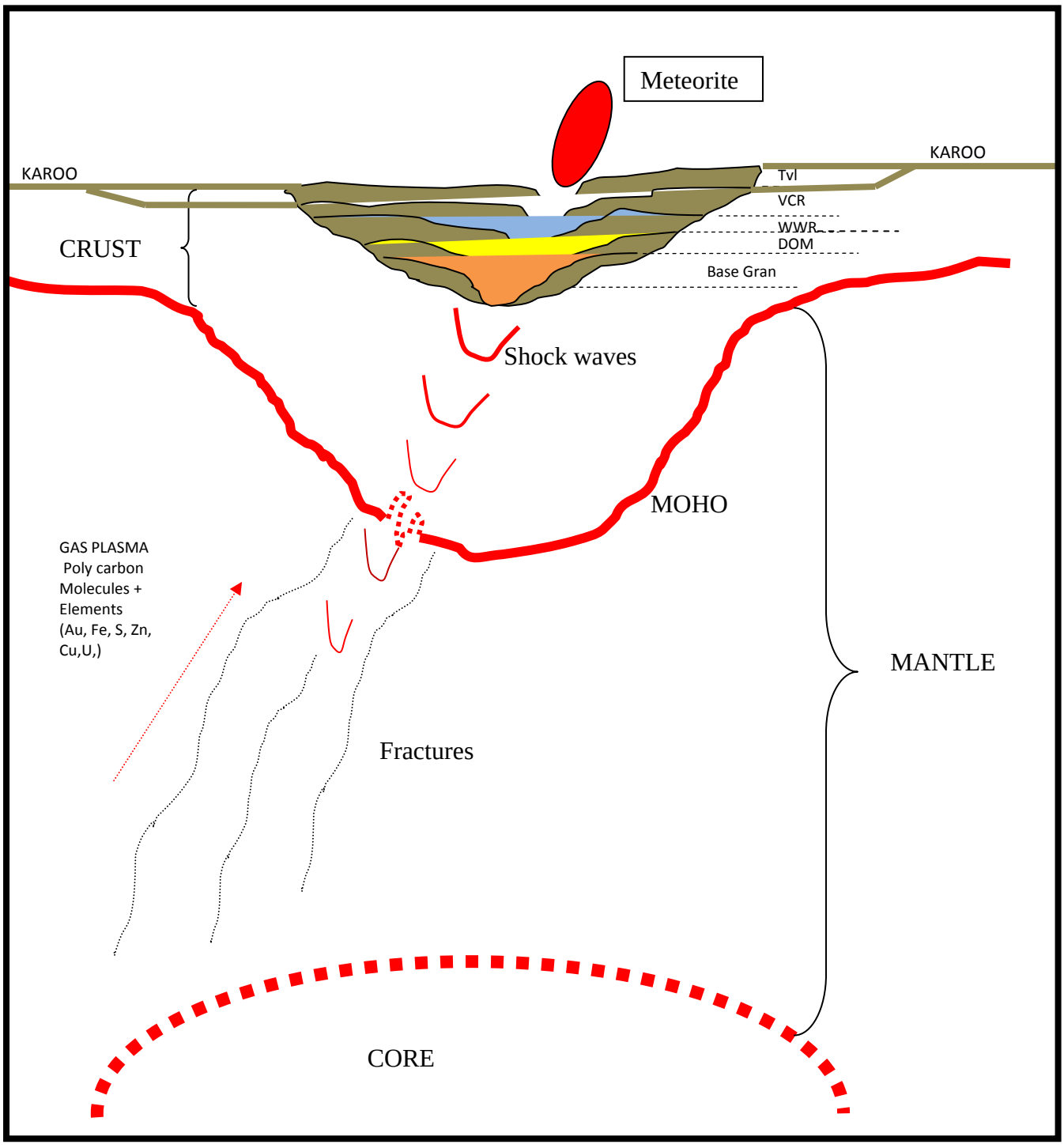

Fig. 5.19 A speculative and schematic diagram of the impact process as hypothesized.

What happened during the first 40 seconds of the impact (Fig. 5.19).

Shock energy dissipates downwards through sedimentary layers in the crustal rock, down into the lower crust and through the Moho and into the mantle, causing fractures all along to a point in the mantle were the energy faded . At this point, Newton's law of "For every action there will be a reaction" is applied and this marks the beginning of the rebound, of which the effect is shown in Fig.5.19.

The three stages along the shockwaves path, starting from stage 1 are discussed below:

Time Zero: energy shock waves start to penetrate the Transvaal sequence into the basement rock: Granites and gneiss.
Stage 1: Shockwaves compress lithosphere and mantle.
Stage 2: Dissipation of shockwaves leads to rebound, marked by the uplift of the lithosphere.
Stage 3: The gas: the excitation of the Mantle plume which contains the plasma. Formation of brittle fractures and the start of the release of plasma into the Witwatersrand Basin. The gold is now being transported by gas/plasma of hydrocarbon molecules and emplaced along pre-existing structures and conglomerates.

The Witwatersrand sediment was hydraulically pumped up by the large amount of gas/fluid that was injected into the permeable layers of the sediment as well as the faults and dykes. This is evident in the form of carbon spindles. The structural events pre 2023 million years ago determined the configuration of the secondary permeability of the reef horizons and the last event determined the vast area of fluid migration.

The master bedding plane fault and the vertical faults that stem from it were the main conduit that fed the polyhydro carbon fluid to the lower reefs of the Central Rand Group. Major thrust faults in Elsburgs as well as the vertical

faults above the thrust faults formed the main conduits for the Elsburgs and the Black Reef.

The meteorite impact event caused major brittle deformation of the reef horizons and determined the deposition of carbon. The dehydrated gas formed the carbon seams and hosted 80 percent of all the gold in the Wits basin.

The carbon rich gas/fluid that was released from the mantle by the impact was injected into the basin. Proof for the occurrence of gas is below:

- Fluid inclusions from a sample from the richest gold mine in the world contain CO_2 and carbon-hydrogen gas.
- Tantalum, gold and carbon in the green bar.
- The solid gold plate within the quartz vein in a Majabeng mine is evidence of hydrocarbon fluid flow with the crystallization in the solid form (Fig.5.20).

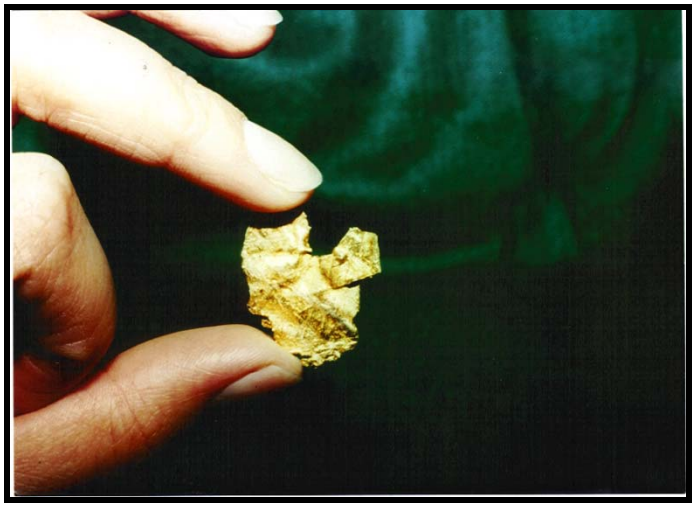

Fig. 5.20 The solid gold Plate from the Majabeng Gold Mine, found within a quartz vein.

5.6 Conclusion

The model proposes to explain the carbon emplacement and the influence that the 2.023 Ga Vredefort Impact Event had on the emplacement thereof. Carbon that was observed in the phylonitic zones is present due to the gas/fluid that has been trapped in the phylonite (fluid pathways) zones after the flow of gas was inhibited by either saturation or due to the constraint of porosity due to the saturation of space or the relaxation of pressure from the source. Gold and uranium are inferred to have been transported by the carbon plasma that originates from the mantle during the Vredefort Impact event.

The associated elements are Ag, As, Ca, Co, Fe, Mg, Mn, Pb, S, Si, Ta, and V. It is concluded that the gas entrapment took place at a late stage in the evolution of the Witwatersrand Basin.

It may be concluded by saying that my observations over the past 30 years of C and Au and their general association with Central Rand Rocks lead me to strongly support a hydrothermal origin for gold, carbon and pyrite. The late stage ingress of these fluids and the pre wits depositional age isotopic results on Au point strongly to a catastrophic origin for the mineralization.

Table 5.3 below summarizes the history of events linked to the lithostratigraphic units within the basin. These events suggest the need for further research.

TABLE 5.3 Summary of events and Stratigraphy after Coward et al., (1995), Amstrong et al., (1991),Robb et al., (1993), Kositcin et al., (2003).

Time (Ma)	STRAT IGRAPHY	EVENTS	COMMENTS
	Basement to Dominion		
3074±5	Dominion		
3030 ±5		Au isotopic age	
2985±14[2]	WWR Supergroup		
	(base) West Rand Group		
2914±8	Jeppestown Lava (Crown)		
2902±13	Central Rand Group		
2780±3		Met event WWR Compressional event WWR Basin	See Fig.3. 3 Bedding parallel thrust deforming met. fabric (chlorite); association with Master-bedding plane fault.
2714±8	VCR		
2714±9	Ventersdorp Supergroup:	Extensional event /reactivation of WWR. compressional structure in WWR Supergroup	
2709±4	Kliprivierberg		
2714±9	Platberg		
2557±49	Transvaal Supergroup		
	Black Reef		
2300			Carbon and gold migration interaction with U into WWR Basin
2054		BIC intrusion	
2023		Vredefort event	

References

Armstrong, R.A., Compston, W., Retief, E.A., William, L.S. and Welke, H.J. (1991). Zircon ion microprobe studies bearing on the age and evolution of the Witwatersrand triad: Precambrian Research, v. 53, p. 243-266.

Bailey, A.C., Law, J.D.M., Cadle, A.B. and Phillips, G.N. (1990). The Zandfontein Quartzite Formation; a marine deposit in the Central Rand Group, Witwatersrand Supergroup. S. Afr. J. Geol., 93, 135-146.

Barnicoat, A.C., Henderson, I.H.C., Knipe, R.J., Yardley, B.W.D., Napier, R.W., Fox, N.P.C., Kenyon, A.K., Muntingh, D.J., Strydom, D., Winkler, K.S., Lawrence, S.R. and Cornford, C. (1997). Hydrothermal gold mineralization in the Witwatersrand basin: Nature, v. 386, p. 820-824.

Beach, A. and Smith, R. (2007). Structural geometry and development of the Witwatersrand Basin, South Africa. In: Deformation of the continental crust: the legacy of Mike Coward. Ed. by A.C. Ries, R.W.H. Butler, R.H. Graham., Geological Society, London, Special Publications, Vol. 272, p. 533-542.

Boer, R. and Reimold, W.U. (2006). Conditions of gold remobilization in the Ventersdorp Contact Reef, Witwatersrand Basin, South Africa Geological Society of America Special Papers, 2006, 405, p. 387-402.

Coetzee, D.S., Van Reenen, D.D. and Roering, C. (1995). Quartz vein formation, metamorphism, and fluid inclusions associated with thrusting and bedding-parallel shear in Witwatersrand quartzites, South Africa: South African Journal of Geology, v. 98, p. 371-199.

Coward, M.P., Spencer, R.M., Spencer, C.E. (1995). Development of the Witwatersrand Basin, South Africa. In: Coward, M.P., Ries, A.C. (Eds.), Early Precambrian Processes. Special Publication Geological Society London, 95, 243-269.

Davidson C.F. (1953) The gold uranium ores of Witwatersrand, Mining Metal London 88(2): 73-85.

Davidson, C.F. (1957). The occurrence of uranium in ancient conglomerates. Econ Geol: 668-693.

Davidson, C.F. (1964-65) The mode of banket orebodies. Inst. Mining Metal London, Trans. 74, 319-338, 844-847.

Davidson C.F, Bowie S.H.U. (1951) On thucholite and related hydrocarbon-uraninite complexes, with a note on the origin of the Witwatersrand gold ores.Geol. Surv. Gt. Brit. Bull3, pp1-19.

De Wit, J. M., Roering, C., Hart, R. J., Armstrong, R.A., De Ronde, C.E.J., Green, R.W.E., Tredoux, M., Peberdy, E., Hart, R.A. (1992). Formation of an Archaean continent, Nature, 357, 553-562.

England, G.L., Rasmussen, B., Krapez, B., and Groves, D.I. (2001). The origin of uraninite, bitumen nodules and carbon seams in Witwatersrand gold-uranium-pyrite ore deposits, based on a Permo-Triassic analogue: Economic Geology, v. 96, p. 1907-1920.

Foya, SN. (2002). Post Impact Ore Mineralization in the Vredefort Structure.

Frimmel, H.E. (2005). Archaean atmospheric evolution: Evidence from the Witwatersrand gold fields, South Africa: Earth-Science Reviews, v. 70, 1-46.

Frimmel, H.E. and Minter, W.E.L. (2002). Recent developments concerning the geological history and genesis of the Witwatersrand gold deposits, South Africa: Society of Economic Geologists Special Publication 9, p. 17-45.

Frimmel, H.E. Hallbauer,D.K. Gartz,V.H. (1998). Gold mobilizing fluids in the Witwatersrand Basin: composition and possible sources. Mineralogy and Petrology 66: p. 55-81

Frimmel, H.E. and Gartz,V.H. (1997). Witwatersrand gold particle chemistry matches model Mineralium Deposita 32, 523-530.

Gartz VH, Frimmel HE (1999) Complex metasomatism of an Archean placer in the Witwatersrand Basin, South Africa: the Ventersdorp contact reef a hydrothermal aquifer?

Gibson, R.L. and Reimold, W.U. (1999). The significance of the Vredefort dome for the thermal and structural evolution of the Witwatersrand basin, South Africa: Mineralogy and Petrology, v. 66, p. 5-23.

Gibson, R.L., and Wallmach, T. (1995). Low pressure-high temperature metamorphism in the Vredefort Dome, South Africa-anticlockwise pressure-temperature path followed by rapid decompression. Geological Journal 30, 121-135.

Graton, L.C, (1930) *Hydrothermal origin of Rand gold deposits. Econ Geol.25 (supp.to no 3) pp1-185).*

Gray, G.J., Lawrence, S.R., Kenyon, K., Cornford, C. (1998). Nature and origin of 'carbon' in the Archaean Witwatersrand Basin, South Africa Journal of the Geological Society,London, v 155, p 39 - 59

Groves, D.I., Rasmussen, B., Krapez, B. (2003). A comparison between the Witwatersrand and orogenic gold systems: a test of the hydrothermal Witwatersrand model. In: Eliopoulos, D.G., et al., (Eds.), Mineral Exploration and Sustainable Development. Proceedings of the 7th Biennial SGA Meeting, 24-28 August 2003. Millpress, Rotterdam, pp. 727-730.

Hallbauer D.K, and Utter T. (1977). Geochemical and morphological characteristics of gold particles from Recent river deposits and the fossil placers of the Witwatersrand. Minerallium Deposita, 12, 293-306.

Hallbauer, D.K. (1975). The plant origin of Witwatersrand carbon: Minerals Science and Engineering, v. 7, p. 111-131.

Hargraves, R.B. (1960). A Bibliography Of The Geology Of The Witwatersrand System, Univ. Witwatersrand econ.geol.Res.Unit inform.Circ.1

Hatch F. H, Corstorphine, (1909) The geology of South Africa.London: Mcmillian, pp 146-41.

Hayward C.L,. Reimold, W.U Gibson R.L. Robb L. J. (2005).Gold mineralization within the Witwatersrand Basin, South Africa: evidence for a modified placer origin, and the role of the Vredefort impact event Geological Society, London, Special Publications 2005, v. 248, p. 31-58.

James, D.E., Fouch, M.J., Van Decar, J.C., van der Lee, S., (2001) Tectospheric structure beneath Southern Africa. Geophys. Res. Lett. 28, 2485– 2488.

Jolley, S.J., Freeman, S.R., Barnicoat, A.C., Phillips, G.M., Knipe, R.J., Pather, A., Fox, N.P.C., Strydom, D., Birch, M.T.G., Henderson, I.H.C. and Rowland, T.W. (2004). Structural controls on Witwatersrand gold mineralisation: Journal of Structural Geology, v. 26, p. 1067-1086.

Kirk, J., Ruiz J., Chesley, J., Walshe, J., England, G. (2002). Sept. 13 issue of Science. Scientists Discover That 40 Percent Of The World's Gold Is 3 Billion Years Old. American Scientist

Kirk, J., Ruiz, J., Chesley, J., Spencer, T., Walshe, J. (2001). A detrital model for the origin of gold and sulfides in the Witwatersrand basin based on Re-Os isotopes. Science. v .297, p. 1856 -1858

Koen, G.M., (1961). The genetic and size distribution of uraninite in the Witwatersrand bankets: Geol Soc v. 64, p. 24-54.

Koppel, V.H., Saager, R. (1974). Lead Isotope Evidence on the Detrital Origin of Witwatersrand Pyrites and its Bearing on the Provenance of the Witwatersrand Gold. Economic Geology, v. 69, p. 318-331.

Kositcin, N. (2003). Critical tests of models for basin evolution and gold-uranium mineralisation for the Witwatersrand basin through geochronology and geochemistry of detrital zircons and detrital and authigenic xenotime: Unpublished Ph.D. thesis, Perth, University of Western Australia, 347 p.

Law, J.D.M. and Phillips, G.N. (2000). Basin evolution and hydrothermal gold mineralization in the Witwatersrand: Implications for exploration in other basins: Geological Association of Canada and the Mineralogical Association of Canada. The Millenium Gesocience Summit: GacMac 2000, Calgary, Alberta, May 29 June 1, 2000, Abstract 616, 4 p.

Law, J.D.M. and Spencer, R.M. (1992). A detailed study of the Kimberley Reef on portions of Kinross and Winkelhaak mines: Unpublished geological research report, Johannesburg, Gencor Ltd., Mineral Resources Division, 94 p.

Leube, A. (1962). Grundzuge der geotektonischen Entwiklung Sudafrikas. Geol.Rundisch. 52, 721-744.

Leube, A. and Cissarz,A. (1966) Formation of mineral deposits in relation to structural developments of the Kaapvaal Craton. Mineralium Deposit. p 201 – 225.

Liebenberg, W.R. (1955) The occurrence and origin of gold and radioactive minerals in the Witwatersrand system, the Dominion reef, the Ventersdorop contact reef and the Black Reef. Geol Soc.South Africa Trans , vol 58, p. 101-223.

Miholic S. (1954). Genesis of the Witwatersrand gold-uranium deposits. Econ. Geol. 49, 537-540.

Minter, W.E.L. (1999). Irrefutable detrital origin of Witwatersrand gold and evidence of eolian signatures: Economic Geology, v.94, no 5, p. 665-670.

Maclare, J.M, (1908)Gold: Its geological Occurences and geographical distribution,London:The mining Journal, pp 95-98.

Palmer, J.A. (1986). Palaeoweathering in the Witwatersrand and Ventersdorp Supergroups: Unpublished M.Sc. thesis, University of the Witwatersrand, Johannesburg, South Africa, p. 166.

Park and MacDiarmid 3rd Edition. (1975). Ore Deposits, Pages 434, 502 p. 4-6.

Parnell, J. (2004). Petrographic evidence for emplacement of carbon into Witwatersrand conglomerates under high fluid pressure. Journal of Sedimentary Research, v. 69, p. 164-170.

Parnell, J. (1996). Phanerozoic analogus for carbonaceous matter in the Witwatersrand ore deposits, Economic Geology, v 91.

Penning, W.H. (1888). The South African Gold fields. J. Soc. Arts 36, 433-44.

Phillips, G.N., Law, D.M. (2000). Witwatersrand gold fields: geology, gneiss and exploration. SEG review. Vol 13 p.439-500.

Phillips, G.N., Law, D.M. (1994). Metamorphism of the Witwatersrand goldfields. A review. Ore Geol. Rev 9,1-31.

Phillips, G. N. (1987). Metamorphism of the Witwatersrand goldfields: conditions during peak metamorphism. J. Metam. Geol. 5, p 307-322.

Phillips, G.N., Myers, R.E., Law, J.D.M., Bailey, A.C., Cadle, A.B., Beneke, S.D. and Giusti, L. (1989). The Witwatersrand goldfields, I: Post-depositional history, syn-sedimentary processes, and gold distribution: Economic Geology Monograph, p. 585-597.

Pretorius D.A. (1964). The geology of the Central Rand goldfield. In: Haughton, S.H.(Ed.), The Geology of Some Ore Deposits in Southern Africa, Geol.Soc.S.Afr.,64

Ramdohr, P. (1958). New observations on the ores of the Witwatersrand in South Africa and their genetic significance, Geol. Soc. S. Afr. Trans., 61 (annex) :1-51.

Rasmussen, S.E. and Fesq, H.W. (1973). Neutro activation analysis of samples from the Kimberley reef conglomerate: Johannesburg, National Institute for Metallurgy, p. 241.

Reimer, T.O. and Mossman, D.J. (1990). Sulfidization of Witwatersrand black sands: From enigma to myth: Geology, v. 18, p. 426-429.

Robb, L.J., Meyer, F.M. (1994). Geological environment and mineralisation processes during the formation of the Witwatersrand Au-U deposits.XVth CMMI Congress,Johannesburg ,SAIMM 1994, vol.3, p 3-18

Robb, L.J., Davis, D.W. and Kamo, S. (1989). U-Pb ages on single detrital zircon grains from the Witwatersrand basin: Constraints on the age of sedimentation and on the evolution of granites adjacent to the depository. University of the Witwatersrand, Johannesburg, Economic Geology Research Unit Information Circular, 208.

Robb, L.J., Landais, P., Meyer, F.M. and Davis, D.W. (1993). Nodular kerogen in granites: Implications for the origin of carbonaceous matter in the Witwatersrand Basin, South Africa. In: Parnell, J., Ruffell, A.H. and Moles, N.R. (eds.) Geofluids '93, Torquay 4-7 May 1993, 446-449.

Stanistreet, I.J., McCarthy, T.S. (1991). Changing tectono-sedimantary scenarious relevant to the development of the Late Archean Witwatersrand basin: Journal of African Earth Sciences, v 13, p. 65-82.

Tainton, S. (1994). A Review Of The Witwatersrand Basin and The Trends In Exploration. XVth CMMI Congress,Johannesburg ,SAIMM 1994, vol.3, p 19-45

Von Rahden,H.V.R, (1965) Aparrent fineness of gold from two Witwatersrand gold mines. Econ Geol. 60:980-997.

Wallmach T. and Meyer F. M.(1990) A petrogenetic grid for metamorphosed aluminous Witwatersrand shales. *South African Journal of Geology, v. 93, p. 93-102.*

Yardley, B.W.D. (1997). The evolution of fluids through the metamorphic cycle. In: Jamtveit, B. Yardley, B.W.D. (eds.). Fluid flow and transport in rocks. Chapman & Hall, London, pp. 99-121.

Zhao, B., Robb, L.J., Harris, C and Jordaan, L.J. (2005). Origin of hydrothermal fluids and gold mineralization associated with the Ventersdorp Contact Reef, Witwatersrand Basin, South Africa: Constraints from S, O, and H isotopes.

Zhou, T., Dong, G. and Phillips, G.N. (1994). Chemographic analysis of assemblages involving pyrophyllite, chloritoid, chlorite, koalinite, kyanite, quartz: An application to metapelites in the Witwatersrand Goldfields: Journal of Metamorphic Geology, v. 12, p. 655-666.

APPENDICES

1. Discussion on the historical work done

Meaningful arguments are few but one has to take the latest scientific evidence into context to build a model and compare the structure and sedimentology data collected underground to get to the hard evidence.

Let's look at the following arguments for both origins. And I quote as follows:

"Although the thucholite is in rounded grains that appear to be detrital, similar shapes can be found in veins of undoubted hydrothermal origin (Davidson and Bowie, 1951). It has been suggested that the thucholite was formed by the polymerization of hydrocarbon gases under the influence of radioactive bombardmen" (Park and MacDiarmaid, 1975).

"Methane is abundant in the mine areas, and the association of hydrocarbons with uranium may mean that the thucholite is a secondary product formed where these gases encounter uraninite (Park and MacDiarmaid, 1975). Thus the association between gold and carbon may actually be an association between uranium and hydro gold and carbon may actually be an association between uranium and hydrocarbons, and in turn between uraninite and gold" (Davidson and Bowie, 1951).

"The hydrothermal theory explains the restriction of gold to conglomerates as a function of permeability; the most permeable channels for epigenetic fluids would reasonably be the conglomerate beds, where the interstitial openings are larger than in the quartzites and where the clay is at a minimum" (Graton, 1930).

Hargraves (1960, 1963) studied many assays of Witwatersrand ore; his reports were based upon random mill samples. He concluded that gold increased in fineness at depth, and that the average silver content of the bullion in individual reefs varies as a function of the relative elevation of the reef. There is general agreement that the conglomerates were laid down by southeasterly flowing streams, so that, as in other placers, the fineness of the gold increases downstream.

Von Rahden (1965) was unable to confirm Hargraves' results by direct sampling of the Ventersdorp Contact Reef and the underlying Witwatersrand Reefs. Von Rahden explained the variations in fineness shown by the ores as a redistribution of silver during the metamorphism of placer gold. His evidence apparently contradicted that obtained by Hargraves.

Geologists are so united in their defense of a placer origin for the ores that this hypothesis has been referred to as "a national article of faith" by a member of the opposing school (Davidson, 1953). The placerists do not deny the action of hydrothermal fluids on the Witwatersrand sediments, but they ascribe these effects to regional metamorphism rather than to the infiltration of ore-bearing solutions. They point out that the Witwatersrand sediments were derived from the basement, which was known to contain numerous small, gold bearing quartz veins. The richer ores are concentrated in gravels - generally in the coarser, cleaner gravels – but the quartzites, many of which are also clean and permeable, are essentially gold free.

Several of the hydrothermalist's objections to a placer origin can be attributed to metamorphism brought about by temperatures as high as 300 degrees Celsius (Ramdohr, 1953). The replacement textures and shredded appearance of the gold may result from mobilization and recrystallization during metamorphism. The lack of magnetite and ilmenite may be due to a diagenetic reaction

(Ramdohr, 1958) or to a metamorphic reaction involving the iron and sulfur, the latter being abundantly supplied by the black shales.

Breakdown of the ilmenite by these processes would explain why rutile is associated with the deposits. Careful sampling has shown neither enrichment nor increased gold values of the reefs near dikes, though small amounts of gold have been reworked in the igneous metamorphic aureole, leaving mineralization along cross-cutting dikes and gash veins (Park and MacDiarmaid, 1975).

Hydrothermal effects can be observed, but they are related to fissures. Although alteration may be shown to grade laterally from the fractures, the gold content does not vary with the degree of hydrothermal alteration. The placerists also point out that no known igneous source for the gold has been found, and at no place does the ore fill strong, persistent, crosscutting fissures.

The presence of uranium minerals with the gold seemed at first to support the epigenetic hypothesis, but recent studies have arrived at the opposite conclusion. The original objection to a placer origin for the uranium was based upon the supposition that uraninite and pitchblende were unstable under surface condition; for example, Davidson and Bowie (1951) noted that the uranium is leached from the mine dumps by meteoric water.

The placerists argue that the mine waters are abnormally acidic and that the presence of detrital pyrite grains with the uraninite presupposes a low redox environment that might favor the chemical stability of urininite (Ramdohr, 1958). Laboratory studies have shown that uraninite is physically resistant to the abrasive action of stream transport and should be as persistent in a placer deposit as monazite and other common detrital minerals (Koen, 1958).

Similar uranium concentrations in the Blind River district of Ontario seem to be of

detrital origin (Robertson and Steenland, 1960). In both districts, the uraninite is in rounded grains that show all the signs of attrition and none of the signs of collidal deposition. Some thucholite grains in the Witwatersrand ores exhibit the relict octahedral cleavage of crystalline uraninite, and in places they have been shattered cataclastically by compaction; it is unlikely that these features would be shown by colloidally deposited, epigenetic pitchblende (Ramdohr, 1958).

It has also been pointed out that the gold-"carbon" association may be a product of the metamorphic redistribution of gold. Accordingly, a precipitant for gold mobilized during metamorphism. Paragenetic studies corroborate this interpretation (Liebenberg, 1955).

A recent – and devastating – argument against the hydrothermal origin of the uranium minerals is based upon radiometric age determinations of radiogenic lead in galena and detrital monazite. The parent uraninite for the radiogenic lead in galena samples and the detrital grains of monazite are among the oldest materials known (about 3,000 million years old) and match the age of granites in the basement rock. The age of the Witwatersrand Series is not known, but it is thought to be about 2.200 million years old.

Whatever the origin of the gold and uranium ores, their localization is a function of sedimentary textures. The ore concentrations are directly related to the conglomerate beds and do not depend upon superimposed structures. Until the advocates of a hydrothermal origin provide unequivocal evidence, the South African geologists will continue to direct exploration according to a placer theory because this approach has proved highly successful in the past (Park and MacDiarmaid, 1975).

2. Table: Tantalum emissions from three carbon samples.

Element	KA	KB	MA	MB	LA	KA	KB	MA	MB	LA	KA	KB	MA	MB	LA
Ag															375
2Ag					3968					204					
As					2477										
Au					25								1291	868	218
Ca	417					294									
Co					370										
F	367														
Fe	2279	613													154
Mg	2243	1117													
Mn	70														
Pb		196	731												
S	3850										53				
Si	1921					3394					4388				
2Si						806					2050				
Ta				4866					4648					22232	
Te															56
U				143										118	
V		179										98			

3. Table of Carbon Classification

APPENDICES

Discussion on the historical work done

Meaningful arguments are few but one has to take the latest scientific evidence into context to build a model and compare the structure and sedimentology data collected underground to get to the hard evidence.

Let's look at the following arguments for both origins. And I quote as follows:

"Although the thucholite is in rounded grains that appear to be detrital, similar shapes can be found in veins of undoubted hydrothermal origin (Davidson and Bowie, 1951). It has been suggested that the thucholite was formed by the polymerization of hydrocarbon gases under the influence of radioactive bombardment."(Park and MacDiarmaid, 1975).

"Methane is abundant in the mine areas, and the association of hydrocarbons with uranium may mean that the thucholite is a secondary product formed where these gases encounter uraninite (Park and MacDiarmaid, 1975). Thus the association between gold and carbon may actually be an association between uranium and hydro gold and carbon may actually be an association between uranium and hydrocarbons, and in turn between uraninite and gold" (Davidson and Bowie, 1951).

"The hydrothermal theory explains the restriction of gold to conglomerates as a function of permeability; the most permeable channels for epigenetic fluids would reasonably be the conglomerate beds, where the interstitial openings are larger than in the quartzites and where the clay is at a minimum" (Graton, 1930).

Hargraves (1960, 1963) studied many assays of Witwatersrand ore; his reports were based upon random mill samples. He concluded that gold increased in fineness at depth, and that the average silver content of the bullion in individual reefs varies as a function of the relative elevation of the reef. There is general agreement that the

conglomerates were laid down by southeasterly flowing streams, so that, as in other places, the fineness of the gold increases downstream.

Von Rahden (1965) was unable to confirm Hargraves' results by direct sampling of the Ventersdorp Contact Reef and the underlying Witwatersrand Reefs. Von Rahden explained the variations in fineness shown by the ores as a redistribution of silver during the metamorphism of placer gold. His evidence apparently contradicted that obtained by Hargraves.

Geologists are so united in their defense of a placer origin for the ores that this hypothesis has been referred to as "a national article of faith" by a member of the opposing school (Davidson, 1953). The placerists do not deny the action of hydrothermal fluids on the Witwatersrand sediments, but they ascribe these effects to regional metamorphism rather than to the infiltration of ore-bearing solutions. They point out that the Witwatersrand sediments were derived from the basement, which was known to contain numerous small, gold bearing quartz veins. The richer ores are concentrated in gravels - generally in the coarser, cleaner gravels – but the quartzites, many of which are also clean and permeable, are essentially gold free.

Several of the hydrothermalist's objections to a placer origin can be attributed to metamorphism brought about by temperatures as high as 300 degrees Celsius (Ramdohr, 1953). The replacement textures and shredded appearance of the gold may result from mobilization and recrystallization during metamorphism. The lack of magnetite and ilmenite may be due to a diagenetic reaction (Ramdohr, 1958) or to a metamorphic reaction involving the iron and sulfur, the latter being abundantly supplied by the black shales.

Breakdown of the ilmenite by these processes would explain why rutile is associated with the deposits. Careful sampling has shown neither enrichment, nor increased gold values of the reefs near dikes, though small amounts of gold have been

reworked in the igneous metamorphic aureole, leaving mineralization along cross-cutting dikes and gash veins (Park and MacDiarmaid, 1975).

Hydrothermal effects can be observed, but they are related to fissures. Although alteration may be shown to grade laterally from the fractures, the gold content does not vary with the degree of hydrothermal alteration. The placerists also point out that no known igneous source for the gold has been found, and at no place does the ore fill strong, persistent, crosscutting fissures.

The presence of uranium minerals with the gold seemed at first to support the epigenetic hypothesis, but recent studies have arrived at the opposite conclusion. The original objection to a placer origin for the uranium was based upon the supposition that uraninite and pitchblende were unstable under surface condition; for example, Davidson and Bowie (1951) noted that the uranium is leached from the mine dumps by meteoric water.

The placerists argue that the mine waters are abnormally acidic and that the presence of detrital pyrite grains with the uraninite presupposes a low redox environment that might favor the chemical stability of urininite (Ramdohr, 1958). Laboratory studies have shown that uraninite is physically resistant to the abrasive action of stream transport and should be as persistent in a placer deposit as monazite and other common detrital minerals (Koen, 1958).

Similar uranium concentrations in the Blind River district of Ontario seem to be of detrital origin (Robertson and Steenland, 1960). In both districts, the uraninite is in rounded grains that show all the signs of attrition and none of the signs of collidal deposition. Some thucholite grains in the Witwatersrand ores exhibit the relict octahedral cleavage of crystalline uraninite, and in places they have been shattered cataclastically by compaction; it is unlikely that these features would be shown by colloidally deposited, epigenetic pitchblende (Ramdohr, 1958).

It has also been pointed out that the gold-"carbon" association may be a product of the metamorphic redistribution of gold. Accordingly, a precipitant for gold mobilized during metamorphism. Paragenetic studies corroborate this interpretation (Liebenberg, 1955).

A recent – and devastating – argument against the hydrothermal origin of the uranium minerals is based upon radiometric age determinations of radiogenic lead in galena and detrital monazite. The parent uraninite for the radiogenic lead in galena samples and the detrital grains of monazite are among the oldest materials known (about 3,000 million years old) and match the age of granites in the basement rock. The age of the Witwatersrand Series is not known, but it is thought to be about 2.200 million years old.

Whatever the origin of the gold and uranium ores, their localization is a function of sedimentary textures. The ore concentrations are directly related to the conglomerate beds and do not depend upon superimposed structures. Until the advocates of a hydrothermal origin provide unequivocal evidence, the South African geologists will continue to direct exploration according to a placer theory because this approach has proved highly successful in the past (Park and MacDiarmaid, 1975).

CLASSIFICATION OF CARBON TYPES

TYPE OF CARBON	PHOTO	PHOTO	BP	UNCONFO	CH	CHAMAR	CAV	CONGLOM-	FUALT
Type A: SPINDLE CARBON	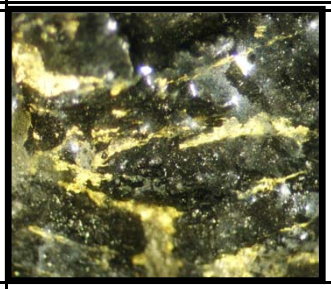	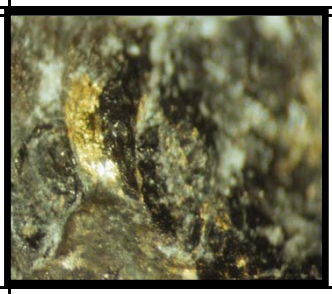	Y	Y	Y	Y		Y	Y
Type A: SPINDLE WITH NODULE		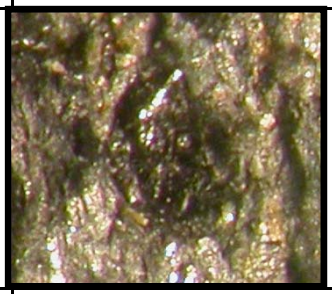	Y	Y	Y	Y		Y	
Type B: CARBON IN CRACKS		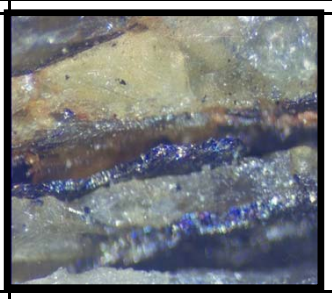					Y		
Type A&B : CARBON ALONG FAULTS							Y		Y
Type B :CARBON IN VUGS							Y		

Type A: MASSIVE CARBON NO GOLD			Y	Y	Y	Y			